



**Diana Catarina José Pinheiro de Castro**

Licenciada em Biologia Humana

## **Characterization of autophagy induced by linoleic acid**

Dissertação para obtenção do Grau de Mestre em Genética  
Molecular e Biomedicina

Orientador: Doutor José Manuel Fuentes Rodríguez

Co-orientador: Doutora Mireia Niso Santano

Centro de Investigación Biomédica en Red de Enfermedades Neurodegenerativas  
(CIBERNED),  
Universidad de Extremadura, Espanha



FACULDADE DE  
CIÊNCIAS E TECNOLOGIA  
UNIVERSIDADE NOVA DE LISBOA

Julho de 2016





**Diana Catarina José Pinheiro de Castro**

Licenciada em Biologia Humana

## **Characterization of autophagy induced by linoleic acid**

Dissertação para obtenção do Grau de Mestre em Genética  
Molecular e Biomedicina

**Dissertação apresentada na Faculdade de Ciências e  
Tecnologia da Universidade Nova de Lisboa para obtenção  
do Grau de Mestre em Genética Molecular e Biomedicina.  
A presente dissertação foi desenvolvida em colaboração  
com o Centro de Investigación Biomédica en Red de  
Enfermedades Neurodegenerativas (CIBERNED),  
Universidad de Extremadura, Espanha**

Orientador: Doutor José Manuel Fuentes Rodríguez

Co-orientador: Doutora Mireia Niso Santano



FACULDADE DE  
CIÊNCIAS E TECNOLOGIA  
UNIVERSIDADE NOVA DE LISBOA

Julho de 2016



Characterization of autophagy induced by linoleic acid

Copyright Diana Catarina José Pinheiro de Castro, FCT/UNL, UNL

A Faculdade de Ciências e Tecnologia e a Universidade Nova de Lisboa têm o direito, perpétuo e sem limites geográficos, de arquivar e publicar esta dissertação através de exemplares impressos reproduzidos em papel ou de forma digital, ou por qualquer outro meio conhecido ou que venha a ser inventado, e de a divulgar através de repositórios científicos e de admitir a sua cópia e distribuição com objectivos educacionais ou de investigação, não comerciais, desde que seja dado crédito ao autor e editor.



## Agradecimentos

---

Ao longo de todos os caminhos é muito importante o apoio dos que nos são chegados, pois não se chega a lado nenhum sozinho.

Em primeiro lugar, quero agradecer aos meus avós Jorge e Mimi por todo o apoio que me deram e continuam a dar. Por estarem sempre presentes em todos os momentos e pelo ser humano fantástico que são. Espero que vos orgulhe, como vocês me orgulham a mim.

Aos meus pais por me fazerem acreditar que eu posso ser o que eu quiser e nunca me deixarem desistir. Por me aturarem mesmo quando sou insuportável. Um muito obrigado!!

Ao meu Zé, por todas as provas de carinho e de paciência, pelas quais tem passado. Por seres aquela pessoa que nem é preciso abrir a boca, para saberes qual o meu estado de espírito. Por estares sempre perto, mesmo estando longe.

Ao Jorginho, peço desculpas pelas ausências demoradas e agradeço-te por seres o meu eterno companheiro das jogatanas.

À Vitória, pelos seus mimos e ron-rons super reconfortantes.

Ao Professor Doutor José Manuel Fuentes, pela sua simpatía e disponibilidade imediata. Por ter sido sempre tao rápido nas respostas e esclarecimentos de dúvidas que tive ao longo do ano.

À Doutora Mireia Niso Santano, por ser a melhor co-orientadora que podia ter tido. A forma como ensina é fenomenal, porque consegue explicar coisas complexas, como se fossem muito simples, e isso é algo que nem todos somos capazes de fazer.

À Sokhna por me obrigar a desenvolver o castelhano à força, quer nos almoços, quer nos experiências. Muito obrigado por partilhares o teu conhecimento (fosse em que língua fosse!), e me ajudares a desenvolver espirito crítico em relação a tudo. És uma excelente pessoa e mereces tudo de bom pela tua vida fora. Boa sorte!

Ao Mário, por ser a pessoa mais prestável que conheço, sempre pronto a ajudar os colegas, mesmo que isso lhe atrasasse o seu próprio trabalho. Sucesso em Nova York!

À Rosana, pela sua boa disposição e estar sempre preocupada pelos outros.

À Guadalupe por me ensinar todas as técnicas, no inicio, e pela paciência com o meu “portunhol”.

À Puri e a Eli, pela ótima companhia que proporcionam.

À Filipa, palavras não chegam para te agradecer todos os momentos que passámos desde a entrada na Universidade até aqui. És a minha companheira dos estudos e das festas. Desejo-te toda a sorte e sei que vais chegar até onde queres.

À Rosélia, que é sem dúvida das melhores pessoas que conheci. Obrigado pelas nossas conversas, pelos devaneios, pelos trabalhos e pelo convívio. Que saudades tuas, riquinha!

À Catarina e à Margarida, pela excelente companhia que são.

À Joana, pelas palavras de apoio e positivismo que sempre que falamos me dás, és a melhor madrinha académica!

Ao Andrey, pela convivência e amizade que ficam depois de alguns anos, agora já estamos mais perto de abrir o meu laboratório, com os teus sistemas operativos!

A todos os meus outros familiares, amigos ou conhecidos que de uma forma ou de outra, estiveram presentes em alguns momentos do meu percurso académico e me deram ânimo para continuar.



## Abstract

---

Parkinson's disease is one of the most common neurodegenerative disorder that is slowly progressive and manifested by muscle rigidity, tremor, decreased mobility and postural instability. The disease is caused by a combination of genetic and environmental factors.

The most prominent pathological features are the severe loss of dopaminergic neurons in the substantia nigra *pars compacta* and the presence of cytoplasmic protein inclusions called Lewy bodies, primarily composed of fibrillar  $\alpha$ -synuclein and ubiquitinated proteins within some remaining nigral neurons.

Autophagy is a catabolic process that maintain cellular homeostasis, through the selection of misfolded proteins, damaged organelles, and even pathogenic organisms to be degraded by lysosomes. Autophagy can mediate cytoprotection (for instance neuroprotection and cardioprotection in the context of ischemic preconditioning) and delay the pathogenic manifestations of aging.

Dysregulation of autophagy has been observed in the brain tissues from Parkinson's disease patients and animal models. In recent years, some reports have shown a new relationship between macroautophagy and lipid metabolism.

In this work, we used the most consumed polyunsaturated fatty acid in our diet, linoleic acid, to evaluate if it induces autophagy and if there is a possible relationship between linoleic acid-induced autophagy and the neuroprotective/toxic mechanisms triggered by this compound. We found that linoleic acid induces autophagy at concentrations equal or higher than 200  $\mu$ M, and we describe its activation pathway, using Western blotting and immunofluorescence assays. Our results suggest that linoleic acid-activated autophagy process is mammalian target of rapamycin-independent, class III phosphatidylinositol 3-kinase/Beclin1-independent and AMP-activated protein kinase-dependent. As for the neuroprotective capacity of linoleic acid, we observed that alone it shows some toxicity. However, if co-administered with an inducer of reactive oxygen species (such as paraquat), linoleic acid does not increase paraquat toxicity. On the other hand, when linoleic acid is co-administered with puromycin (protein aggregates generator) it has a neuroprotective effect.

Keywords: Parkinson's disease (PD), autophagy, polyunsaturated fatty acid (PUFA), linoleic acid (LA), microtubule-associated protein 1 light chain 3 (LC3)



## Resumo

---

A doença de Parkinson é uma das doenças neurodegenerativas mais comuns, progressiva e que se manifesta por rigidez muscular, tremores, instabilidade postural e diminuição da mobilidade. A doença é causada por uma combinação de fatores genéticos e ambientais.

Os fatores patológicos mais proeminentes são a perda severa de neurónios dopaminérgicos, na região da substância nigra *pars compacta*, e a presença de agregados proteicos denominados Corpos de Lewis, compostos por  $\alpha$ -sinucleína e proteínas ubiquitinadas, com diminuição dos neurónios nigroestriatais.

A autofagia é um processo essencial das nossas células para manter a homeostase celular, seleccionando proteínas alteradas, organelos, ou até mesmo organismos patogénicos para serem degradados pelos lisossomas. Ao nível do organismo, a autofagia pode mediar citoprotecção (por exemplo neuroprotecção e cardioprotecção no contexto de pré-condicionamento isquémico) e retardar as manifestações do envelhecimento patogénicos.

A desregulação da autofagia tem sido observada nos tecidos de cérebro de pacientes e de modelos animais, com PD. Nos últimos anos alguns estudos têm mostrado uma nova relação entre a macroautofagia e o metabolismo lipídico.

Usando o ácido gordo poli-insaturado mais consumido na nossa dieta, o ácido linoleico, queremos saber se este induz a autofagia e se há uma relação entre a possível autofagia induzida por ácido linoleico e a neuroprotecção/toxicidade. Verificamos que o ácido linoleico induz autofagia a concentrações iguais ou superiores a 200  $\mu$ M, e descrevemos a sua via de activação, usando para tal, a técnica de Western blot e de Imunofluorescência. Relativamente às vias de activação de autofagia por LA, os nossos resultados sugerem que é mammalian target of rapamycin-independent, class III phosphatidylinositol 3-kinase/Beclin1-independent e AMP-activated protein kinase -dependent. Quanto à sua capacidade neuroprotectora, os resultados sugerem que apesar de o ácido linoleico sozinho apresentar alguma toxicidade, se for incubado com um indutor de espécies reactivas de oxigénio (como paraquat), não aumenta a toxidade e se for incubado com puromicina (gerador de agregados proteicos) tem efeito neuroprotector.

Palavras-chave: Doença de Parkinson (PD), autofagia, ácidos gordos poli-insaturados (PUFA), ácido linoleico (LA), microtubule-associated protein 1 light chain 3 (LC3)

“If you want to reach where most of people don't reach, do what most don't do.”

Bill Gates

# Table of contents

---

Agradecimientos .....	VII
Abstract .....	IX
Resumo.....	XI
Table of contents.....	XIII
Abreviation list .....	XV
List of figures .....	XVII
List of tables .....	XIX
1. Introduction.....	1
1.1 Physiopathology of Parkinson’s Disease .....	2
1.2 Risk factors .....	4
1.2.1 Environmental factors .....	5
1.2.2 Genetic factors .....	5
1.3 Glial cells and Parkinson’s Disease .....	6
1.3.1 Microglia.....	7
1.3.2 Astrocytes.....	7
1.4 Ubiquitin-proteasome system.....	8
1.5 Autophagy .....	9
1.5.1 Signaling Pathway.....	13
1.5.2 Autophagy and Parkinson’s Disease.....	15
1.5.3 Non-canonical autophagy .....	16
1.5.4 Lipid droplets in autophagy.....	18
1.5.5 Lipid role in autophagy .....	20
1.6 Diet .....	20
1.6.1 PUFA .....	22
1.6.2 Linoleic Acid.....	23
2. Rational and aims .....	25
3. Materials and methods .....	27
3.1 Appliances .....	27
3.2 Reagents.....	28
3.3 Antibodies .....	30
3.4 Cell lines.....	31
3.5 Cell maintenance.....	31
3.6 Defrosting/freezing .....	31

3.7	Cell culture.....	31
3.8	Treatments .....	32
3.9	Linoleic acid .....	34
3.10	Western Blot.....	34
3.11	MTT assay .....	35
3.12	Flow Cytometry .....	35
3.13	Trypan Blue.....	36
3.14	Immunofluorescence.....	36
3.14.1	Lipid droplets.....	36
3.14.2	small interfering RNA (siRNA).....	37
3.15	Plasmid transfection.....	37
3.16	Data analysis.....	38
4.	Results .....	39
4.1	Effect of LA in cell viability.....	39
4.2	LA induces autophagy .....	41
4.3	LA promotes autophagy flux .....	43
4.4	LA-induced autophagy is Atg5-dependent.....	46
4.5	LA induces mTOR-independent autophagy.....	46
4.6	LA enhances the phosphorylation of AMPK $\alpha$ .....	47
4.7	LA -induced autophagy is BECN1-independent.....	50
4.8	Effect of LA in different organelles .....	53
4.8.1	LA does not alter organelle structures .....	53
4.8.2	LA induces autophagy even with lysosome and mitochondria damage .....	56
4.9	LA has neuroprotector role in neuronal cell lines .....	58
4.9.1	LA does not protect neurons against cell death.....	58
4.9.2	LA protects neurons from protein aggregates .....	59
5.	Discussion .....	64
6.	Conclusions.....	68
7.	References.....	70

## Abreviation list

---

**AMBRA1** Activating molecule in Beclin1-regulated autophagy 1  
**AMP** Adenosin monophosphate  
**AMPK** AMP-activated protein kinase  
**Atg** Autophagy-related genes  
**BCA** Bicinchonic acid  
**BFA** Brefeldin A  
**BSA** Bovine serum albumin  
**BECN1** Beclin 1  
**BECN/PI3K** Beclin/phosphatidylinositol-3-phosphate  
**Co** Control  
**CC** Compound C  
**CMA** Chaperone-mediated autophagy  
**CoA** Coenzyme A  
**CQ** Chloroquine  
**Cyt C** Cytochrome C  
**DA** Dopamine  
**DMEM** Dulbecco's Modified Eagle Medium  
**DMSO** Dimethyl sulfoxide  
**DNA** Desoxyribonucleic acid  
**ER** Endoplasmic reticulum  
**FASN** Fatty acid synthase  
**FBS** Fetal bovine serum  
**IF** Immunofluorescence  
**LA** Linoleic acid  
**LAP** LC3-associated phagocytosis pathway  
**LB** Lewy Bodies  
**LC3** Microtubule-associated protein 1 light chain 3  
**L-DOPA** L-3,4-dihydroxyphenylalanine  
**LP** Lipid droplets  
**MAO-B** Monoamine oxidase B  
**MAP4K3** Mitogen-activated protein kinase kinase kinase kinase 3  
**MeDi** Mediterranean diet  
**MEF** Mouse embryonic fibroblast  
**MPP<sup>+</sup>** 1-methyl 4-phenylpyridine

**MPTP** 1-methyl-4-phenyl-1,2,3,6-tetrahydropyridine  
**mTOR** Mammalian target of rapamycin complex 1  
**mTORC1** Mammalian target of rapamycin complex 1  
**NAD<sup>+</sup>** Nicotinamide adenine dinucleotide  
**NADPH** Nicotinamide adenine dinucleotide phosphate  
**NP-40** Nonidet P-40  
**p-AMPK** Phospho-AMPK  
**PBS** Phosphate buffered saline  
**PD** Parkinson's Disease  
**PFA** Paraformaldehyde  
**PI3K/AKT** Phosphatidylinositol 3-kinase/serine-threonine kinase  
**PI(3)P** Phosphatidylinositol 3-phosphate  
**PINK1** PTEN-induced putative kinase 1  
**PKA** Protein kinase A  
**p-mTOR** Phospho-mTOR  
**PQ<sup>2+</sup>** Paraquat  
**PUFA** Polyunsaturated fatty acid  
**RNA** Ribonucleic acid  
**ROS** Reactive oxygen species  
**siRNA** Small interfering ribonucleic acid  
**UPS** Ubiquitin-proteasome System  
**TTBS** Tris buffered saline with tween 20  
**ULK1** Uncoordinated-51-like protein kinase  
**WB** Western Blot  
**WT** Wild type



## List of figures

Figure 1.1 A brain with parkinson's disease with the substantia nigra and Lewy body labeled.....	3
Figure 1.2 Biochemical senescence and pathogenetic pathways to cell death in Parkinson disease..	4
Figure 1.3 The ubiquitin–proteasome pathway of protein degradation.....	9
Figure 1.4 Autophagy and neurodegenerative disorders.....	10
Figure 1.5 Model of ULK1 regulation by AMPK and mTORC1 in response to glucose signals .....	14
Figure 1.6 Regulation of VPS34 complex formation in response to nutrients.....	15
Figure 1.7 Canonical and non-canonical autophagy pathways. ....	18
Figure 1.8 Projection of a confocal stack of an abdominal adipocyte isolated from an Akt (PKB) <i>Drosophila melanogaster</i> mutant.....	19
Figure 1.9 Structure of the main PUFAs present in the human diet.....	22
Figure 1.10 Structure of linoleic acid.....	23
Figure 4.1 Effect of LA in cell proliferation, by MTT assay..	40
Figure 4.2 Effect of LA in cell viability. ....	40
Figure 4.3 LA induces autophagy. .	42
Figure 4.4 Autophagic flux induced by LA.....	43
Figure 4.5 Determination of autophagy flux by fluorescence microscopy. ....	44
Figure 4.6 LA promotes autophagy flux. ....	45
Figure 4.7 LA-induced autophagy is <i>Atg5</i> -dependent.....	46
Figure 4.8 LA-induced autophagy is mTOR-independent.....	47
Figure 4.9 LA enhances the phosphorylation of AMPK $\alpha$ .....	48
Figure 4.10 Compound C induces autophagy. ....	49
Figure 4.11 LA-induced autophagy is AMPK-dependent.....	50
Figure 4.12 Autophagy induced by LA is BECN1 independent.....	51
Figure 4.13 3-MA does not inhibit the autophagy induced by LA.....	51
Figure 4.14 LA-induced autophagy is BECN1-independent. ....	52
Figure 4.15 Implication of BECN1 in LA-induced autophagy. ....	52
Figure 4.16 LA does not impair lysosomes.....	54
Figure 4.17 Effect of LA treatment in organelle structures .....	55
Figure 4.18 LA-induced autophagy is organelles-independent.....	56
Figure 4.19 LA-induced autophagy is Golgi-apparatus-independent.....	57
Figure 4.20 LA-induced autophagy is ER-independent .....	57
Figure 4.21 LA induces lipid droplets biogenesis.....	58
Figure 4.22 LA does not protect cells against cell death induced by PQ.....	59
Figure 4.23 LA does not reduce %PI <sup>+</sup> cells induced by PQ.....	59
Figure 4.24 LA protect cells against cell death induces by puromycin.....	60
Figure 4.25 LA reduce %PI <sup>+</sup> cells, with puromycin.....	60
Figure 4.26 LA enhances p62 degradation.....	61



## List of tables

---

Table 1.1 Monogenic forms of Parkinson’s disease, by gene. Adapted from ((Kalia and Lang 2015). ..	6
Table 3.1 Primary antibodies.....	30
Table 3.2 Compounds used to block different signaling pathways.....	32
Table 3.3 Plasmids used for overexpression .....	38

## 1. Introduction

---

Parkinson disease (PD) is a neurodegenerative disorder that affects the nervous system in the area that coordinate the activity, muscle tone and movement. It results from a combination of genetic and environmental factors, and manifests with a broad range of symptoms (**Appukuttan, Ali et al. 2013**). There are motor and non-motor symptoms.

The first symptoms of the disease usually appear around 60 years, reaching disability in the course of 5 or 15 years. The incidence of this neurodegenerative disorder increases with age affecting more than 3% of the population over 65 years, although in the last 40 years, the age of onset has been anticipated being as frequent from 50 (**Rodriguez, Rodriguez-Sabate et al. 2015**).

The parkinsonian motor symptoms include bradykinesia, muscular rigidity, tremor at rest, postural and gait impairment. (**Kalia and Lang 2015**). Non-motor features include olfactory dysfunction, cognitive impairment, psychiatric symptoms, sleep disorders, autonomic dysfunction, pain and fatigue. They are also frequently present before the onset of the classical motor symptoms (**Kalia and Lang 2015**).

Symptoms of PD clinically appear when almost 50 % of neurons are lost. This neuronal loss is located in the area between the brain and spinal cord, brainstem, particularly those neurons that are in a black substance called core. The portion of this core is called the *substantia nigra pars compacta* (SN). It is so named because some neurons in this area are pigmented in black color due to the presence of the neuromelanin pigment. (**Rodriguez, Rodriguez-Sabate et al. 2015**).

As pigmented neurons of the SN disappear, they fail to produce dopamine (DA). DA is an organic chemical of the catecholamine and phenethylamine families that plays several important roles in the brain and body and acts as a neurotransmitter, and is capable of transporting information from one neuron to another group through chemical and electrical mechanisms. DA is responsible for transmitting information from the SN to other areas of the brain forming circuit connections. Because of the degeneration of dopaminergic neurons in the SN, DA levels decrease characteristic disorders of the disease appear progressively (**Segura-Aguilar, Paris et al. 2014**).

The mainstay of PD management is symptomatic treatment with drugs that increase DA concentrations or directly stimulate DA receptors. These drugs include levodopa (L-DOPA), DA agonists, monoamine oxidase type B inhibitors (MAO-B), and, less commonly, amantadine. Since none of these drugs have proven to be neuroprotective or disease-modifying, therapy does not need to be

started at time of diagnosis for all patients. However, treatment should be initiated when symptoms cause the patient disability or discomfort, for improving function and quality of life.

Bradykinesia and rigidity reliably respond to early dopaminergic treatments in the disease. At best, MAO-B inhibitors are only moderately beneficial. DA agonists or L-DOPA are needed for more severe symptoms and progressive disability. In contrast to bradykinesia and rigidity, tremor is inconsistently responsive to DA replacement therapy, especially in lower doses. Anticholinergic drugs, such as trihexyphenidyl or clozapine can be effective for tremor (**Appukuttan, Ali et al. 2013**).

Available therapies for PD only treat symptoms of the disease. The major goal of PD research is the development of disease-modifying drugs that slow or stop the underlying neurodegenerative process. Potential pharmacological targets for disease modification in PD include neuroinflammation, mitochondrial dysfunction and oxidative stress, calcium channel activity, LRRK2 (Leucine-rich repeat kinase 2) kinase activity, as well as  $\alpha$ -synuclein accumulation, aggregation, and cell-to-cell transmission (including immunotherapy techniques) (**Luo, Hoffer et al. 2015**).

### ***1.1 Physiopathology of Parkinson's Disease***

Besides the loss of dopaminergic neurons, there are the presence of protein inclusions called Lewy bodies (LB) primarily composed of fibrillar  $\alpha$ -synuclein and ubiquitinated proteins within some remaining nigral neurons (**Figure 1.1**). The redox imbalance in DA metabolism upon aging, inflammation, and exposure to environmental toxins that likely act in concert with genetic predisposition are supposedly the causes of PD. During these processes, different reactive oxygen or nitrogen species (ROS/RNS) are formed in excess causing damage to organelles and macromolecules (**Aranda, Sequedo et al. 2013**).

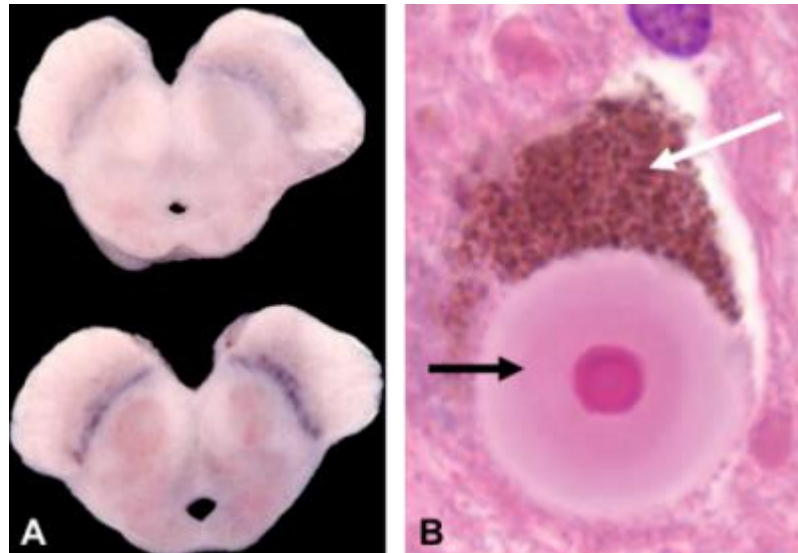


**Figure 1.1** A brain with PD with the substantia nigra and LB labeled. (A) Cross section of the midbrain showing the pigmented substantia nigra in a normal brain (bottom) and depigmented nigra in a brain with PD (upper). (B) Microscopic section of a substantia nigra pigmented neuron containing neuromelanin (white arrow) and a LB (black arrow) within the cytoplasm of the neuron. The LB has a dense core and a lighter halo. <http://medicaliaorg.ning.com/group/neurosciences/forum/topics/parkinson-s-disease-and-other-movement-disorders>.

ROS represent a link between exposure to environmental factors (e.g., pesticides, herbicides, and heavy metals) and genetic risk factors of PD. It is important to note that protein aggregation may be not only an increase in ROS generation, but also can be caused by a dysfunction in degradative systems. The cells maintain a state of constant renewal through continuous synthesis and degradation of all intracellular components including soluble proteins and organelles. The two most important mechanisms regulating the cellular quality control are the ubiquitin-proteasome system (UPS) and autophagy (Shen, Tang et al. 2013).

One of the most important characteristic hallmarks of PD is mitochondrial dysfunction (Figure 1.2). It has been postulated that the accumulation of mitochondrial ROS in different tissues during the years can result in alterations in mtDNA, and subsequently cell death, leading to a decrease in tissue function associated with age (Rubinsztein, Codogno et al. 2012).

Mitochondria are the primary source of potentially damaging endogenous ROS, which have been linked to neurodegeneration too, and can induce protein carbonyls, lipid peroxidation and DNA damage. Importantly, release of cytochrome c (Cyt C) from mitochondria triggers apoptosis, and so the clearance of damaged mitochondria is vital for cell survival. ROS are also able to increase the release of Cyt C and induce the mitochondrial permeability transition pore (mPTP), both activate apoptosis (Luo, Hoffer et al. 2015).

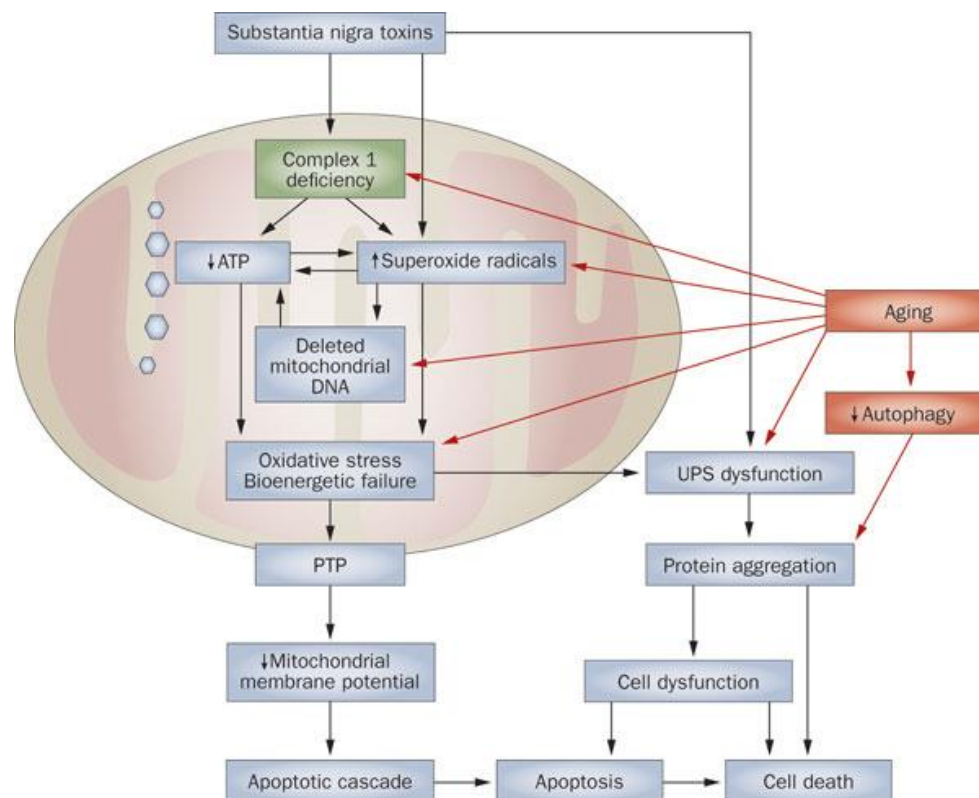


**Figure 1.2** Biochemical senescence and pathogenetic pathways to cell death in Parkinson disease. (Schapira and Schrag 2011).

To prevent cellular damage from faulty mitochondria a number of protective mechanisms have involved; for example, mitochondria have an endogenous proteolytic mechanism to degrade misfolded proteins, proteins located on the inner and outer membranes can be degraded in the cytosol by the UPS and also specific mitochondrial components can be sequestered and directed to lysosomes for degradation by autophagy. Furthermore, electron microscopy analysis has revealed that entire mitochondria are detectable in both yeast vacuoles and mammalian lysosomes. It is the selective degradation of mitochondria by autophagy that is now termed mitophagy (Wager and Russell 2013).

## 1.2 Risk factors

Gender is an established risk factor, with the male-to-female ratio being approximately 3:2. Ethnicity is also a risk factor for the disease. The prevalence is highest in people of Hispanic ethnic origin, followed by non-Hispanic caucasians, Asians, and Africans. Age is the greatest risk factor for the development of PD. The prevalence and incidence increase exponentially with aging and peak after 80 years of age (Kalia and Lang 2015). However, age by itself is not a risk factor, only that arise in old

age can be to increase the risk of disrupting cellular regulation, being longer exposed to harmful environmental effects and/or the combination of genetic susceptibility.

### 1.2.1 Environmental factors

Today a lot of pesticides, herbicides and industrial chemicals have been linked to the development of the disease. Among the most studied compounds found to participate extensively in neurodegeneration, there are rotenone (a substance of plant origin used as an insecticide and acts as a potent inhibitor of complex I of the mitochondrial respiratory chain), the 6-hydroxydopamine (6-OHDA) (a neurotoxin that induces oxidative stress), or bipyridinics such as 1-methyl-4-phenylpyridine (MPP<sup>+</sup>) (a MPTP (1-methyl-4-phenyl-1,2,3,6-tetrahydropyridine) derivative) and the herbicide paraquat (PQ<sup>2+</sup>).

MPTP crosses the blood brain barrier and is taken up by dopaminergic neurons through DA transporter after oxidation to MPP<sup>+</sup> by MAO-B. This cation is very reactive and inhibits complex I (NADH ubiquinone oxidoreductase) of the electron transport chain. That is why, today, MPTP/MPP<sup>+</sup> and other inhibitors of this complex, including rotenone and PQ<sup>2+</sup>, are used as PD models in *in vivo* and *in vitro*. (Padman, Bach et al. 2013)

PQ<sup>2+</sup> (N,N'-dimethyl-4,4'-bipyridinium dichloride) is the organic compound with the chemical formula [(C<sub>6</sub>H<sub>7</sub>N)<sub>2</sub>]Cl<sub>2</sub>. It is classified as a viologen, a family of redox-active heterocycles of similar structure. This salt is one of the most widely used herbicides. It is quick-acting and non selective, killing green plant tissue on contact, but it is also toxic to human being and animals (Filograna, Godena et al. 2016).

### 1.2.2 Genetic factors

Beyond gender, race, age and environmental factors, there are familiar mutations of PD. The most convincing evidence came with the discovery of monogenic forms of PD. *SNCA*, which encodes the protein  $\alpha$ -synuclein, was the first gene to be associated with inherited PD. Mutations in *LRRK2* and *parkin* are the most common causes of dominantly and recessively inherited PD, respectively (Wirdefeldt, Adami et al. 2011).

Mutations of at least six genes have been linked with hereditary PD:  $\alpha$ -synuclein (*SNCA* or *PARK1*), Parkin (*PARK2*), ubiquitin carboxyhydroxylase L1 (*UCH-L1* or *PARK5*), PTEN-induced putative kinase 1 (*PINK-1* or *PARK6*), DJ-1 (*PARK7*), and *LRRK2* (*PARK8*) (Table 1.1). First line of



evidence is given by  $\alpha$ -synuclein, the principal component of LB. Missense mutations in the gene encoding  $\alpha$ -synuclein (PARK1) and multiplications of the  $\alpha$ -synuclein gene locus (PARK4) lead to familial cases of PD (**Gan-Or, Dion et al. 2015**). Large studies determined that the hereditary component of PD is at least 27%, and in some populations, single genetic factors are responsible for more than 33% of PD patients. Interestingly, many of these genetic factors, such as *LRRK2*, *GBA*, *SMPD1*, *SNCA*, *PARK2*, *PINK1*, *PARK7*, *SCARB2* and others, are involved in the autophagy-lysosome pathway (ALP). Some of these genes encode lysosomal enzymes, whereas others correspond to proteins that are involved in transport to the lysosome, mitophagy, or other autophagic-related functions.

**Table 1.1** Monogenic forms of Parkinson's disease, by gene. Adapted from ((**Kalia and Lang 2015**)).

<b>Autosomal dominant</b>	<b>Protein</b>
<i>SNCA</i>	$\alpha$ -synuclein
<i>LRRK2</i>	Leucine-rich repeat kinase 2
<i>VPS35</i>	Vacuolar protein sorting 35
<i>EIF4GI</i>	Eukaryotic translation initiation factor 4- $\gamma$ 1
<i>DNAJC13</i>	Receptor-mediated endocytosis 8 (REM-8)
<i>CHCH2</i>	Coiled-coil-helix-coiler-coil-helix domain containing 2
<b>Autosomal recessive</b>	
<i>Parkin</i>	Parkin
<i>PINK1</i>	PTEN-induced putative kinase 1
<i>DJ-1</i>	DJ-1

### ***1.3 Glial cells and Parkinson's Disease***

Glial cells, sometimes called neuroglia or simply glia, are non-neuronal cells that maintain homeostasis, form myelin, and provide support and protection for neurons in the central and peripheral nervous systems. In the central nervous system, glial cells include oligodendrocytes, astrocytes, ependymal cells and microglia, and in the peripheral nervous system glial cells include Schwann cells and satellite cells. To study the mechanisms of neurodegeneration in PD, researchers have focused their attention primarily on the affected nigral dopaminergic neurons. However, it is now known that the neighboring glial cells play a significant role in the degenerescence of these neurons (**Su, Zhang et al. 2016**).

### 1.3.1 Microglia

Microglia is a type of glial cell located throughout the brain and spinal cord. Microglia account for 10–15% of all cells found within the brain. As the resident macrophage cells, they act as the first and main form of active immune defense in the central nervous system (CNS).

Microglia also has a role in neurodegenerative disorders. Many of the normal trophic functions of glia may be lost or overwhelmed when the cells become chronically activated in progressive neurodegenerative disorders. In such disorders, there is abundant evidence that activated glia play destructive roles by direct and indirect inflammatory attack (**Sanchez-Guajardo, Tentillier et al. 2015**).

Recent research suggests a complex role for microglia not only in PD but in other disorders involving  $\alpha$ -synuclein aggregation, such as multiple system atrophy. In these neurodegenerative processes, the activation of microglia is a common pathological finding, which disturbs the homeostasis of the neuronal environment. The term activation comprises any deviation from what otherwise is considered normal microglia status, including cellular abundance, morphology or protein expression. The microglial response during disease will sustain survival or promote cell degeneration (**Finkbeiner, Cuervo et al. 2006**).

### 1.3.2 Astrocytes

Astrocytes, the most numerous of glial cells, constitute a major class of cells in the mammalian brain and outnumber neurons by several folds in the human brain.

Astrocytes can release and supply neurons with neurotrophic factors such as nerve growth factor (NGF), neurotrophin-3, and basic fibroblast growth factor (bFGF) as well as metabolic substrates such as lactate and the antioxidant glutathione for the survival and proper functioning of neurons. On the other hand, when astrocytes undergo a state of gliosis in response to neuronal injury or toxic insults, together with microglia, they release cytokines and chemokines that are deleterious to neurons (**Rappold and Tieu 2010**).

The presence of an active inflammatory response in the brain mediated primarily by resident astrocytes and microglia has been long recognised, but somewhat overlooked, in PD. Both reactive gliosis resulting from activated astrocytes and microgliosis resulting from microglial activation occur within areas of neurodegeneration in PD. However, Astrocytes and microglia are both involved in

clearance of extracellular debris, which might aid in the survival of neurons (**Janda, Lascala et al. 2015**).

#### **1.4 Ubiquitin-proteasome system**

The UPS is a highly conserved and tightly regulated pathway for the coordinated degradation of a wide variety of proteins with half-lives ranging from minutes to several days. UPS curates proteome stability in various subcellular sites including the nucleus, the cytosol, the endoplasmic reticulum (ER), the mitochondria, and even the extracellular space (**McKinnon and Tabrizi 2014**). Therefore, UPS is the main site of protein synthesis quality control and it is also involved in the recycling of both normal short-lived proteins and of nonrepairable misfolded or unfolded proteins (**Figure 1.3**). The expression levels and activity of the UPS constituent components are tightly regulated, at both the transcriptional and posttranslational level, either under basal conditions or at conditions of increased oxidative and/or proteotoxic stress (**Tsakiri and Trougakos 2015**).

Impairment of the UPS has been implicated in the pathogenesis of a wide variety of neurodegenerative disorders including Alzheimer's, Parkinson's and Huntington's diseases (**Le 2014**). The most significant risk factor for the development of these disorders is aging, which is associated with a progressive decline in UPS activity and the accumulation of oxidatively modified proteins. Nevertheless, the gradual accumulation of stressors during aging along with the (mostly lifestyle-related) unbalanced redox homeostasis or high glucose levels eventually result in increasingly damaged proteome. This outcome may then increase genomic instability due to reduced fidelity in processes like DNA replication and repair, which then results in higher levels of proteome instability and so forth. To date, no therapies have been developed which can specifically upregulate this system (**Bang, Kang et al. 2014**).

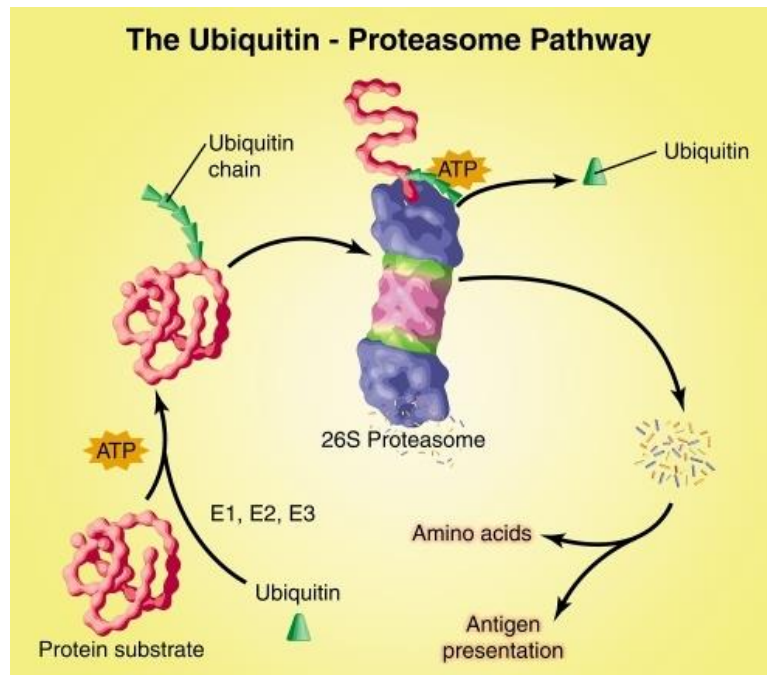


**Figure 1.3** The ubiquitin–proteasome pathway of protein degradation. Ubiquitin (Ub) is conjugated to proteins destined for degradation by an ATP-dependent process that involves three enzymes (E1–E3). A chain of five Ub molecules attached to the protein substrate is recognized by the 26S proteasome, which removes Ub and digests the protein into peptides. The peptides are degraded to amino acids by peptidases in the cytoplasm or used in antigen presentation. (Rajan and Mitch 2008)

## 1.5 Autophagy

Autophagy is an intracellular catabolic mechanism which is responsible for the degradation of cellular components such as proteins or organelles, by the action of lysosomal enzymes (Mizushima, Yoshimori et al. 2010). Proteins involved in this process are called ATG proteins. There are three types of autophagy: chaperone-mediated autophagy (CMA), microautofagia and macroautophagy (Figure 1.4) (Glick, Barth et al. 2010).

CMA involves direct translocation of unfolded proteins across the lysosome membrane. Chaperone proteins mediate this process by binding to cytosolic substrates that enter the lysosome through interaction with a receptor/channel on the lysosomal membrane. For a protein to be a CMA substrate, it must have in its amino acid sequence a pentapeptide motif biochemically related to KFERQ. This substrate protein-chaperone complex binds to lysosome-associated membrane protein type 2A (LAMP-2A), which acts as the receptor for this pathway. LAMP-2A, a single span membrane protein, is one of the three spliced variants of a single gene *lamp2*.

Microautophagy describes the process of direct uptake of cytoplasmic materials at the lysosome surface by invagination of the lysosome membrane. After vesicles containing the cytosolic substrates

pinch off into the lysosomal lumen, they are rapidly degraded (Mizushima, Yoshimori et al. 2010). Microautophagic pathway is especially important for survival of cells under starvation, nitrogen deprivation or after treatment with rapamycin.

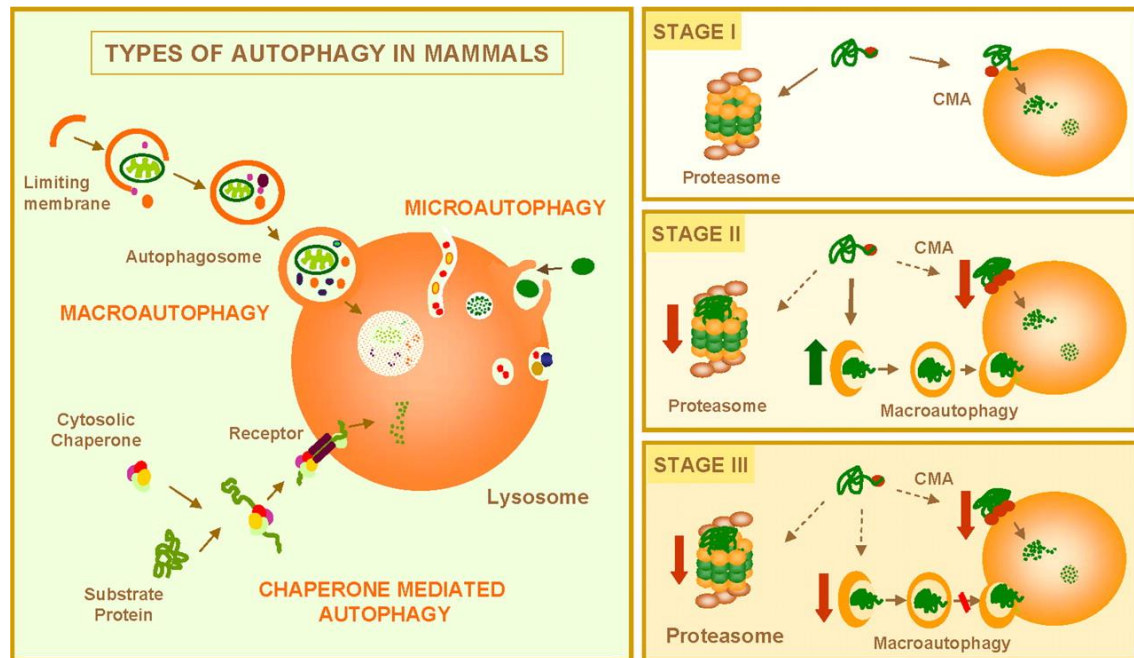


**Figure 1.4 Autophagy and neurodegenerative disorders.** Left, Mammalian cells use three types of autophagy. Microautophagy and macroautophagy involve the sequestration of complete cytosolic regions directly by the lysosomes or in an intermediate compartment, the autophagic vacuole, which is then delivered to lysosomes. In chaperone-mediated autophagy, single soluble proteins are recognized by a cytosolic chaperone and a receptor at the lysosomal membrane that mediates their translocation across the membrane into the lysosomal lumen. Right, Misfolded or altered proteins are selectively degraded by the ubiquitin/ proteasome system or by chaperone-mediated autophagy (STAGE I). However, when these altered proteins organize in toxic multimeric complexes, they often alter the proteolytic activity of these two pathways. Upregulation of macroautophagy can compensate for this deficit (STAGE II). Aggravating factors, such as oxidative stress and aging, can precipitate the failure of macroautophagy with the consequent detrimental effect on cell functioning, often resulting in cellular death (STAGE III). (Finkbeiner, Cuervo et al. 2006).

Macroautophagy (therefore referred as autophagy) involves the engulfment of the cargo into double-membrane autophagosomes, which subsequently fuse with endosomes and lysosomes for cargo degradation (Chen, Khambu et al. 2014). Autophagosome formation is a complex and highly regulated process that requires more than 30 autophagy-related proteins (Atg) that have been identified by molecular dissection of autophagic process through genetic screening of yeast. These proteins form functional complexes Atg mediating macroautophagy individual stages: initiation or induction, nucleation, membrane elongation, load detection and autophagosomes fusion with lysosomes. Macroautophagy induction occurs after cell conditions such as, stress or nutrient deficiency.

The corresponding Atg proteins can be divided into four major groups: the Atg1/unc-51-like kinase (ULK) complex, two ubiquitin-like protein (Atg12 and Atg8/LC3) conjugation systems, the class

III phosphatidylinositol 3-kinase (PI3K)/Vps34 complex I, and the Atg9/mATG9 transmembrane protein system.

The process starts upon activation of cell-specific signaling pathways that suppress mammalian target of rapamycin (mTOR) signaling complex (mTORC1) (**Cheng, Ren et al. 2013**). This is followed by vesicle nucleation at the isolation membrane, most likely at ER level. It involves the recruitment and assembly of several proteins including Vps34, Beclin-1, and UVRAG among others. Vps34 has a PI3K activity and produces phosphatidylinositol 3-phosphate, which is needed for the targeting of Atg family proteins involved in subsequent vesicle elongation. First, ULK1/2-mAtg13-FIP200 (equivalent to Atg1-Atg13-Atg17 in yeast) complex is build and then two ubiquitin-like conjugation systems (involving Atg12-Atg5-Atg16) are recruited and mediate the lipid conjugation of Atg8/LC3, among other reactions involved in the vesicle elongation step (**Rubinsztein, Codogno et al. 2012**).

Among known Atg-encoded proteins, only microtubule-associated protein 1 light chain 3 (LC3), a mammalian orthologue of yeast Atg8, can localize to all types of autophagic membranes, including the phagophore (the immature autophagosome, also known as the isolation membrane), the autophagosome, and the autolysosome (a hybrid organelle formed by fusion of the autophagosome and lysosome). Nascent LC3 (pro-LC3) is processed by Atg4-family proteins, which are cysteine proteases, into LC3-I immediately after synthesis. During autophagy, cytosolic LC3-I is conjugated to phosphatidylethanolamine (PE) to become LC3-II by the activating enzyme Atg7 and the conjugating enzyme Atg3. The conjugation of LC3 to PE is also facilitated by the Atg12–Atg5 conjugate along with Atg16L1. LC3-II is then recruited to autophagosomal membranes (**Ge and Schekman 2014**).

Finally, LC3 is released from LC3-PE by a second Atg4-dependent cleavage, while LC3-II in the autolysosomal lumen is degraded by autophagy. Thus, LC3 conversion (LC3-I to LC3-II) and lysosomal degradation of LC3-II reflect the progression of autophagy, and detecting LC3 by immunoblot analysis is often used to monitor autophagic activity. However, the number of autophagic organelles at a given moment is regulated by both the on-rate (autophagosome formation) and off-rate (degradation upon fusion with lysosomes). Thus, although the amount of LC3-II correlates with the number of autophagosomes, its amount at a certain time point does not necessarily indicate the degree of autophagic flux, a term used to indicate overall autophagic degradation (i.e., delivery of autophagic cargo to the lysosome) rather than autophagosome formation. Furthermore, not all LC3-II is present on autophagic membranes (**Gomez-Sanchez, Yakhine-Diop et al. 2016**). A significant amount of LC3-II can still be detected in cells deficient in some of the upstream Atg factors (e.g., FIP200, Atg13, Atg9, Vps34, Beclin-1, Atg14, and Atg2), suggesting that some population of LC3-II may be ectopically generated in an autophagy-independent manner. LC3 can also be recruited directly to bacteria-containing phagosome membranes in a process termed LC3-associated phagocytosis. Thus, it is important to measure the amount of LC3-II delivered to the lysosomes by comparing LC3-II amounts

in the presence and absence of bafilomycin A1 (a vacuolar H<sup>+</sup>-ATPase inhibitor), lysosomal protease inhibitors (e.g., E64d and pepstatin A), or lysosomotropic agents (e.g., chloroquine - CQ) to inhibit lysosomal degradation of LC3-II (**Hoyer-Hansen, Bastholm et al. 2007**).

Another widely used autophagy marker, p62, also called sequestosome 1 (SQSTM1), binds directly to LC3 and GABARAP (Atg8 orthologues) family proteins via a short LC3 interaction region (LIR) (**Ichimura and Komatsu 2010**). This may serve as a mechanism to deliver selective autophagic cargo for degradation by autophagy. The p62 protein is itself degraded by autophagy and serves as a marker to study autophagic flux. When autophagy is inhibited, p62 accumulates, while when autophagy is induced, p62 quantities decrease (**Jiang and Mizushima 2015**).

Increasing evidences suggest that autophagic deregulation causes accumulation of abnormal proteins or damaged organelles, which is a characteristic of chronic neurodegenerative conditions, such as PD, a multifactorial disorder, which is neuropathologically characterized by age-dependent neurodegeneration of dopaminergic neurons in the midbrain. Indeed, promoting the clearance of aggregate proteins via pharmacological induction of autophagy has proved to be an useful mechanism for protecting cells against the toxic effects of these proteins in the context of neurodegenerative diseases and protecting neurons from apoptosis (**Segura-Aguilar, Paris et al. 2014**).

In some cases, autophagy displays substrate specificity, even though autophagy is often considered to be a nonselective pathway for the degradation of bulk cytoplasmic components. Indeed, the unique feature of the autophagy process where the initial sequestering compartment expands into an autophagosome allows for flexible cargo selection. In addition, superfluous or damaged organelles and misfolded or aggregated proteins are selectively targeted for degradation by autophagy (**Svenning and Johansen 2013**).

Selective autophagy is based on the recognition and degradation of a specific cargo, in a process depending on receptor proteins that bind Atg8/LC3 to facilitate enrichment of cargoes sequestered for degradation (**Pimentel-Muinos and Boada-Romero 2014**). Among them, mitophagy has been increasingly implicated in the pathogenesis of PD through the PINK1-PARKIN-mediated pathway. Selective autophagy can be classified according to the cargoes involved (**Wager and Russell 2013**). We can cite aggrephagy (protein aggregates), pexophagy (peroxisomes) and xenophagy (bacteria, virus and protozoans).

### 1.5.1 Signaling Pathway

- mTOR pathway

Autophagy is inhibited by the mammalian target of rapamycin (mTOR), mTOR is a highly conserved serine/threonine kinase that is capable of integrating signals from many stimuli including amino acids, energy levels, oxygen, growth factors, and stress to coordinate cell growth and maintain metabolic homeostasis. Under nutrient sufficiency, high mTOR activity prevents ULK1 activation by phosphorylating the Ser 757 residue and disrupting the interaction between ULK1 and AMPK (**Figure 1.5**). Activation of pathways that stimulate mTOR activity is considered to inhibit autophagy. mTOR forms two functionally distinct complexes in mammals, mTORC1 (mTOR complex 1) and mTORC2 (mTOR complex 2) (**Marlin and Li 2015**). mTORC1 is sensitive to both growth factors and nutrients, and the presence of amino acids has been shown to be essential for activation of the mTORC1 kinase. Proteins including Ste-20-related kinase (mitogen-activated protein kinase kinase kinase 3) MAP4K3 and Vps34 have been described to play a role in amino acid signaling possibly through regulation of phosphatases and endocytic trafficking upstream of mTORC1 (**Kim, Kundu et al. 2011**).

- AMPK pathway

Autophagy is promoted by AMP activated protein kinase (AMPK), which is a key energy sensor and regulates cellular metabolism to maintain energy homeostasis (**Mihaylova and Shaw 2011**). Under glucose starvation, AMPK promotes autophagy by directly activating ULK1 through phosphorylation of Ser 317 and Ser 777. Importantly, AMPK is an established negative regulator of the mTOR signaling cascade (**Gwinn, Shackelford et al. 2008**). This can be accomplished by AMPK-mediated phosphorylation of the TSC complex which is a negative regulator of mTORC1 activation at the lysosome (**Chen, Zhao et al. 2015**). Alternatively, AMPK can directly phosphorylate the Raptor subunit of mTORC1, which induces 14-3-3 binding and inhibits mTORC1 target phosphorylation. Through these both mechanisms, AMPK is able to relieve mTOR-mediated autophagy repression (**Choudhury, Yang et al. 2014**).



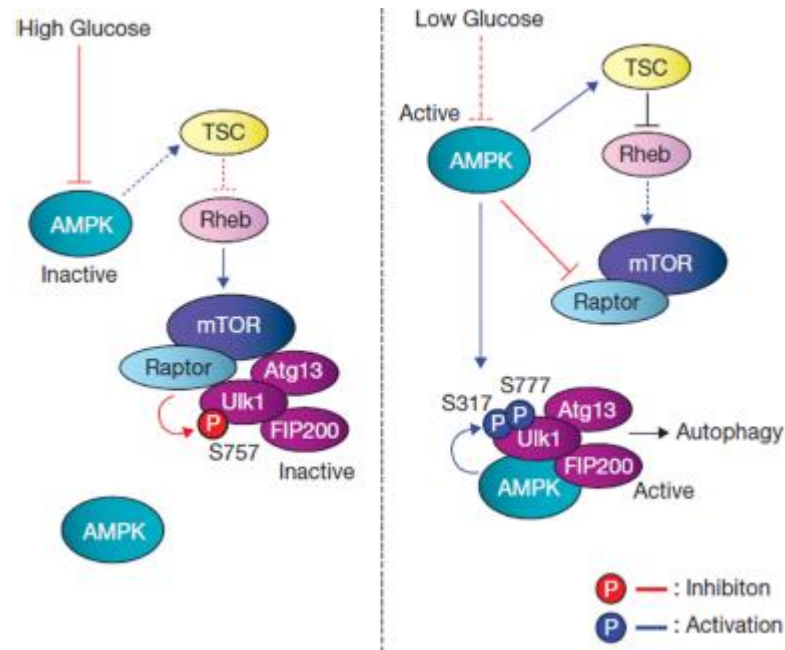


**Figure 1.5 Model of ULK1 regulation by AMPK and mTORC1 in response to glucose signals.** Left: when glucose is sufficient, AMPK is inactive and mTORC1 is active. The active mTORC1 phosphorylates ULK1 on Ser 757 to prevent ULK1 interaction with and activation by AMPK. Right: when cellular energy level is limited, AMPK is activated and mTORC1 is inhibited by AMPK through the phosphorylation of TSC2 and Raptor. Phosphorylation of Ser 757 is decreased, and subsequently ULK1 can interact with and be phosphorylated by AMPK on Ser317 and Ser 777. The AMPK-phosphorylated ULK1 is active and then initiates autophagy. (Kim, Kundu et al. 2011).

- Beclin1/PI3K

Beclin-1 (BECN1) is a mammalian ortholog of the yeast Atg6 and BEC-1. This protein interacts with either Bcl-2 or PI3K class III, playing a critical role in the regulation of both autophagy (**Figure 1.6**) and cell death. A BECN1 binding partner, AMBRA1 (activating molecule in Beclin1-regulated autophagy 1), has also been identified as a target for ULK1-mediated phosphorylation. Under nutrient-rich conditions, AMBRA1 binds BECN1 and Vps34 at the cytoskeleton through an interaction with dynein. However, it is unclear if BECN1 binds Atg14 and AMBRA1 in the same complex at the site of the phagophore. Interestingly, AMBRA1 was shown to act in an mTORC1-sensitive positive-feedback loop to promote K63-linked ubiquitination of ULK1 through recruitment of the E3-ubiquitin ligase, TNF receptor associated factor 6 (TRAF6). This pathway of autophagy was not associated with LC3 processing but appeared to involve autophagosome formation from late endosomes and the trans-Golgi (**Kang, Zeh et al. 2011**).

Above basal level, autophagy is further induced upon activation of the hVps34/BECN1 complex, that generates phosphatidylinositol 3-phosphate (PI(3)P). The generation of PI(3)P is considered to be required for canonical induction of autophagy (**Grotemeier, Alers et al. 2010**).

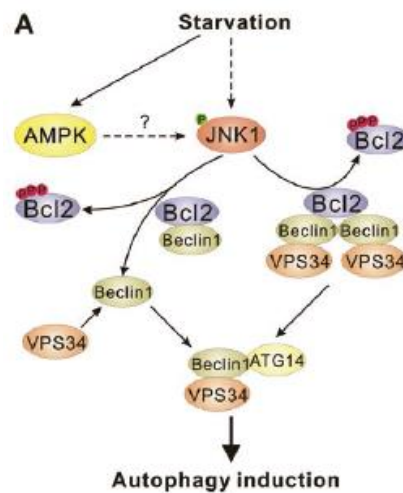


**Figure 1.6 Regulation of VPS34 complex formation in response to nutrients.** Starvation activates JNK1 kinase, possibly through direct phosphorylation by AMPK. JNK1 phosphorylates Bcl-2, relieving Bcl-2-mediated repression of Beclin-1-VPS34 complexes. Bcl-2 may inhibit VPS34 complexes by disrupting Beclin-1-VPS34 interaction (left arrow) or by stabilizing an inactive Beclin-1 homodimeric complex (right arrow). (Russell, Yuan et al. 2014).

### 1.5.2 Autophagy and Parkinson's Disease

Aggregated and ubiquitinated proteins cause synaptic impairment, damage to organelles, and cell death in the central nervous system. Many types of neurodegenerative diseases are accompanied by the accumulation of aggregated and ubiquitinated proteins. Autophagy is involved in the degradation and removal of aggregated proteins, and the inhibition of constitutive autophagy leads to neurodegeneration in the central nervous system. Autophagy helps to clear damaged organelles and protein aggregates or lipid droplets (LP), which represent unwanted and usually toxic cargo that may lead to cellular dysfunction (Lynch-Day, Mao et al. 2012).

Even sporadic PD cases are genetically linked to  $\alpha$ -synuclein polymorphisms, which may modulate  $\alpha$ -synuclein transcription. Misfolded  $\alpha$ -synuclein oligomers can be degraded by different catabolic pathways including CMA and macroautophagy, and it accumulates in different pathological situations underlying PD pathology. Importantly, abnormal expression of  $\alpha$ -synuclein can interfere with different types of autophagy. In fact, upregulation of wild-type (WT)  $\alpha$ -synuclein leads to significant inhibition of macroautophagy and mutant forms of  $\alpha$ -synuclein A30P and A53T have been shown to inhibit CMA. Such variants of  $\alpha$ -synuclein not only are poorly degraded by CMA but also block degradation of other substrates by this pathway. This mechanism suggests an important point of interplay between autophagy and oxidative stress (Gonzalez-Polo, Fuentes et al. 2013).

Another important breakthrough has been the demonstration that Parkin, mutated in autosomal recessive forms of PD, is recruited to damaged mitochondria to facilitate the mitochondria-selective autophagy, mitophagy (**Egan, Shackelford et al. 2011**). Mitophagy is the process by which mitochondria are selectively degraded by the highly conserved autophagic machinery. It occurs during developmental processes in specialized cells such as erythrocytes, while in other cell types damaged mitochondria are removed in order to maintain a functional mitochondrial population. They are also the primary source of potentially damaging endogenous ROS, which have been linked to neurodegeneration, and can induce protein carbonyls, lipid peroxidation, and DNA damage. Importantly, release of Cyt C from mitochondria triggers apoptosis. Then, the clearance of damaged mitochondria is vital for cell survival (**Janda, Isidoro et al. 2012**).

ROS are also able to increase the release of Cyt c and induce the mitochondrial permeability transition pore (mPTP), both of which activate apoptosis. Accumulating evidence from epidemiological studies and toxin-induced animal models of PD strongly point to environmental toxins as possible triggers of nigrostriatal dopaminergic neurons degeneration. Almost all of these toxic substances have been shown to deregulate macroautophagy by pathologically enhancing or interfering with autophagic flux (**Giuliano, Cormerais et al. 2015**). Low levels of ROS and RNS play an increasingly recognized role in signal transduction and regulation of physiological processes, including autophagy (**Son, Shim et al. 2012**).

The parkinsonian pro-oxidants produce high levels of ROS and RNS that act both positively and negatively on signaling pathways and lipid-protein complexes regulating autophagy. The relationship between autophagy and oxidative stress in PD and other pathologies is very complex and cannot be summarized in one phrase “defective autophagy induces oxidative stress and oxidative stress induces autophagy,” mainly because the effects of excessive ROS and RNS on the autophagic machinery can be either activating or inhibiting (**Tavakkoli, Miri et al. 2014**). The balance between positive and negative signals will tune the autophagic process in cell type and oxidant-specific manner and can turn on induced autophagy, as well as turn off the basal autophagy.

### **1.5.3 Non-canonical autophagy**

The canonical autophagy pathway is characterized by a complex series of membrane biogenetic steps that result in formation of the autophagosome (i.e. the structure that engulfs and sequesters the cytoplasmic cargo marked for degradation). The Beclin/phosphatidylinositol-3-phosphate (BECN/PI3K) complex is recruited to the nascent autophagosome where it produces a pool of phosphatidylinositol-3-phosphate, thereby marking the forming membrane for targeting to lysosomes.

This phosphoinositide pool also organizes the events that culminate in lipidation of the autophagy protein LC3 in preparation for fusion of the double-membrane autophagosome to lysosomes (**Bankaitis 2015**).

The ability of autophagy to sequester and clear large particles from the cytoplasm has broader implications as evidenced by the discovery of non-canonical autophagy pathways. This pathway counters the strategies used by intracellular pathogens to encourage their entry into cells and to subsequently inhibit maturation of conventional phagolysosomes so that these organelles are co-opted as suitable microenvironments for pathogen propagation. These immune response applications are classified as non-canonical autophagy pathways because the action is initiated at the plasma membrane, and the operant autophagosomes are systems enclosed by a single membrane (**Figure 1.7**).

While the pathway remains dependent on the BECN1/PI3K complex, it is neither dependent on components of the canonical autophagy pre-initiation complex nor is it subject to control by the TOR nutrient sensor kinase. Such a noncanonical LC3-associated phagocytosis pathway (LAP) more generally promotes immune responses by facilitating antigen presentation, by regulating interferon production, and by dampening inflammation potential by clearing cell corpses (**Niso-Santano, Malik et al. 2015**).

The non-canonical pathway described by (**Niso-Santano, Malik et al. 2015**) shares some features with LAP in that it too does not require the canonical pre-initiation machinery for autophagosome formation. It is fundamentally distinct from the LAP pathways, however, as it demands a functional Golgi system, and is independent of any BECN1/PI3K requirement.

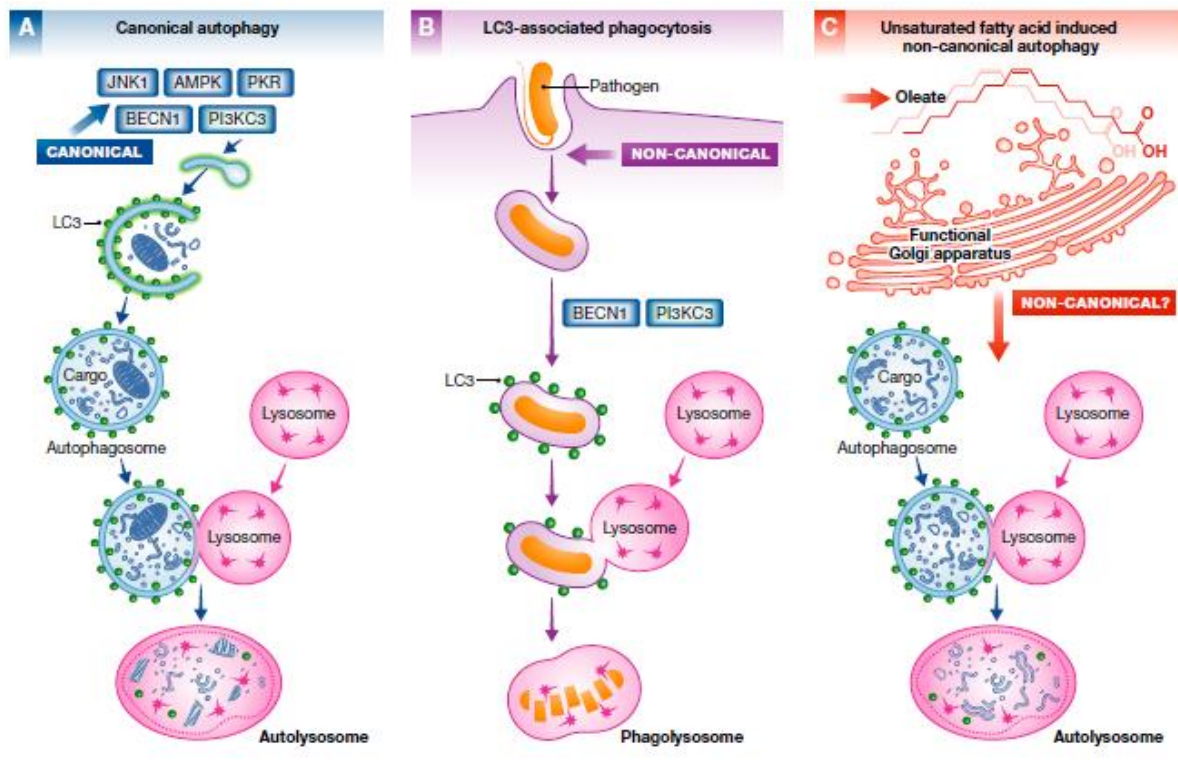


**Figure 1.7 Canonical and non-canonical autophagy pathways.** Canonical autophagic pathway (A) involves different components than the LC3-associated phagocytosis pathway (B) and the oleate-induced non-canonical autophagic pathway (C). (Bankaitis 2015).

#### 1.5.4 Lipid droplets in autophagy

LDs are storage organelles for the neutral lipids (**Figure 1.8**) present in most cell types. The LDs core consists mainly of triacylglycerols (TAGs) and steryl esters (STEs). Evidence points to the ER as the site of formation of the LDs, being the main source of the autophagosomal membrane. LDs serve important functions in the cell by providing lipids and energy as well as by storing free fatty acids that may otherwise become cytotoxic. Deletion of biosynthetic enzymes of STEs and TAGs has opposite effects on the lipidation state of Atg8, suggesting novel and complementary roles for these neutral lipids in regulation of the autophagic process (Shpilka, Welter et al. 2015).

A complex relationship between autophagy and LDs is described: on one hand autophagy is implicated in lipophagy, a process of LD degradation, while on the other hand LDs are linked to autophagy regulation. When autophagy is inhibited by fatty acid synthase (FASN) there are an amount of LDs, so we believe that LDs are essential to the autophagic process.

Indeed, FASN is a cytosolic multienzyme complex that catalyzes the synthesis of long chain fatty acids using malonyl-CoA, acetyl-CoA and NADPH as substrates (Wang, Ma et al. 2015).

Physiologically, FASN is expressed in liver cells and lipogenic tissue and is regulated by insulin, glucocorticoids, and glucagon as well as by nutrients. The NADPH-dependent process plays a central role in energy homeostasis by converting excess carbon intake into FAs for storage (**Tao, He et al. 2013**).

FASN is expressed at relatively low levels in normal cells (except liver, brain, lung and adipose tissue), whereas it is highly expressed in a wide variety of cancers, including cancer of the prostate, breast, brain, lung, ovary, endometrium, colon, thyroid, bladder, kidney, liver, pancreas, stomach, oesophagus, eye, mesothelium and skin (**Grube, Dunisch et al. 2014**).

Several natural and synthetic FASN inhibitors such as the antifungal agent cerulenin and its synthetic derivative C75, the  $\beta$ -lactone orlistat as well as the bactericide triclosan have been shown to inhibit cancer cell growth, by inducing cell death. Nuclear fragmentation assay and Western blotting (WB) analysis after targeting FASN with those inhibitors demonstrated autophagy and apoptosis (**Sadowski, Pouwer et al. 2014**).

In a related, LDs have recently emerged as organelles that participate in aggregate clearance. The involvement of LDs in autophagosome biogenesis and the ability of autophagosomes to deliver LDs to the vacuole/lysosome may be a key mechanism by which cells eliminate aggregated proteins (**Shpilka and Elazar 2015**).

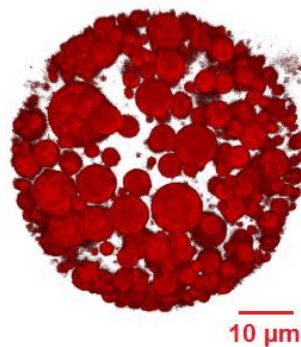


**Figure 1.8** Projection of a confocal stack of an abdominal adipocyte isolated from an Akt (PKB) *Drosophila melanogaster* mutant. The adipocyte was stained with Nile Red to image neutral lipids in order to evidence and quantify LD within the cell. (**Reyes-DelaTorre, Alejandro et al, 2012**).

### 1.5.5 Lipid role in autophagy

The macroautophagy within hepatocytes function is the degradation of intracellular lipid reserves. Although the lipolytic function of lysosomes was known previously, the mechanism of lipid delivery to the lysosome was unclear. They contain numerous lysosomal hydrolases and lipases operating in an acidic environment (pH <5.2) to degrade the charge delivered. Studies in cultured hepatocytes lacking autophagy by pharmacological inhibition with 3-methyladenine (3-MA) or using RNA interference against ATG5 and ATG7 have shown that inhibition of macroautophagy results in an increase in the accumulation of triglyceride (TG) hepatocellular, when compared to controls. Increased TG accumulation occurs under both basal conditions and when hepatocytes receive a lipogenic stimulus such as treatment with physiological concentrations of oleic or after culturing in a medium lipogenic, methionine, and choline deficient medium (**Brenner, Galluzzi et al. 2013**).

Electron microscopy studies demonstrate that inhibition of macroautophagy in hepatocytes and liver leads to a marked increase in the number and size of LD, showing that lipid accumulation occurs in the form of LD. Interestingly, the increase in hepatocellular reserves TG resulting from a decrease in lipolysis lipid reserves is due to a decrease in the delivery of lipid load to lysosomes, and not an increase in hepatocellular TG synthesis or reduced secretion in the form of very low density lipoproteins (VLDL). Immunofluorescence colocalization experiments between a neutral lipid dye (BODIPY 493/503) and autophagosome marker (LC3) or lysosomal marker (LAMP1) have revealed the localization of cellular lipid components autophagosome and lysosomal system under conditions which macroautophagy is activated with rapamycin (a TOR inhibitor) or a lipid providing stimulus. Additionally, pharmacological or genetic ablation of autophagy reduces bodipy-LC3 and bodipy-LAMP1 colocalization observed (**Wrighton 2015**).

## 1.6 Diet

Nutritional epidemiological studies in PD have focused on groups of food items, macronutrients (such as protein, fat, and carbohydrates), or other specific nutrients. Several dietary habits have been shown to modify the risk of developing PD.

Intake of coffee and tea in relation to PD has been studied extensively. Caffeine acts as an adenosine receptor antagonist and experimental evidence suggests that it may exert a neuroprotective effect. Of the 7 case-control studies that investigated tea intake for a possible association with PD, three reported an inverse association, three found no association, and one reported an increased risk (**Agim and Cannon 2015**).

Calcium and vitamin D intake were associated with PD risk when the source was dairy products, but not when the source was non-dairy products suggesting that a compound in dairy products other than calcium or vitamin D was responsible for the association (**Agim and Cannon 2015**).

The role of antioxidants in PD has been studied based on the hypothesis that oxidative stress is involved in the pathogenesis of the disease. A meta-analysis of 7 case-control and one cohort study that assessed intake of antioxidants in relation to PD risk reported an inverse association with moderately high vitamin E intake and PD, whereas high intake of vitamin E (defined as fourth quartile or fifth quintile of intake) was not associated with further reduction in PD risk (**Albarracin, Stab et al. 2012**).

Total dietary fat intake is supplied in three categories: saturated fatty acids, unsaturated fatty acids, and cholesterol. MUFAs (mono-unsaturated fatty acids) and PUFAs (poly-unsaturated fatty acids) have been shown to have antiinflammatory and neuroprotective properties by reducing the oxidative stress and inhibiting neuronal apoptosis. PUFAs help regulation of dopamine activity in basal ganglia, controlling movement. Supplementation or higher intake of unsaturated fatty acids was shown to alleviate neurotoxin-induced PD-like syndrome (**de Lau, Bornebroek et al. 2005**). As the neuroprotective effect of PUFA has been repeatedly shown, both *in vivo* and *in vitro*, high fat diet has been shown to be associated with increased risk of PD. In a small case-control study, higher Mediterranean diet (MeDi) score was significantly associated with lower risk of PD (**Dong, Beard et al. 2014**).

The MeDi has received attention in recent years because of growing evidence associating MeDi with lower risk for AD, cardiovascular disease, several forms of cancer, and overall mortality. The MeDi is characterized by high intake of vegetables, legumes, fruits, and cereals; high intake of unsaturated fatty acids (mostly in the form of olive oil) compared to saturated fatty acids; a moderately high intake of fish; a low-to-moderate intake of dairy products, meat and poultry; and a regular but moderate consumption of ethanol, primarily in the form of wine and generally during meals (**Alcalay, Gu et al. 2012**).

Overall, dietary factors do not seem to play a major role in PD. There is strong evidence, however, for caffeine as a protective agent in PD. Intake of dairy products, in particular milk, may be a risk factor, but underlying mechanisms are unknown. There is finally some evidence that intake of vitamin E may be protective in PD, but results are not consistent (**Russell, Yuan et al. 2014**).



### 1.6.1 PUFA

PUFA are basic components involved in the architecture and function of cellular membranes, being endogenous mediators for cell signaling and involved in the regulation of gene expression. They are precursors of eicosanoids, such as prostaglandins and leukotrienes, and docosanoids such as protectins or resolvins (**Igarashi, Kim et al. 2012**). They can act as transcription factors modulating protein synthesis, as ligands in signal transduction, and as membrane components able to regulate the fluidity, permeability and dynamics of cell membranes (**Johansson, Monsen et al. 2015**). Unsaturated FAs can induce non-canonical BECN1-independent autophagy in vitro and in vivo through a phylogenetically conserved mechanism that requires an intact Golgi apparatus (**Enot, Niso-Santano et al. 2015**).

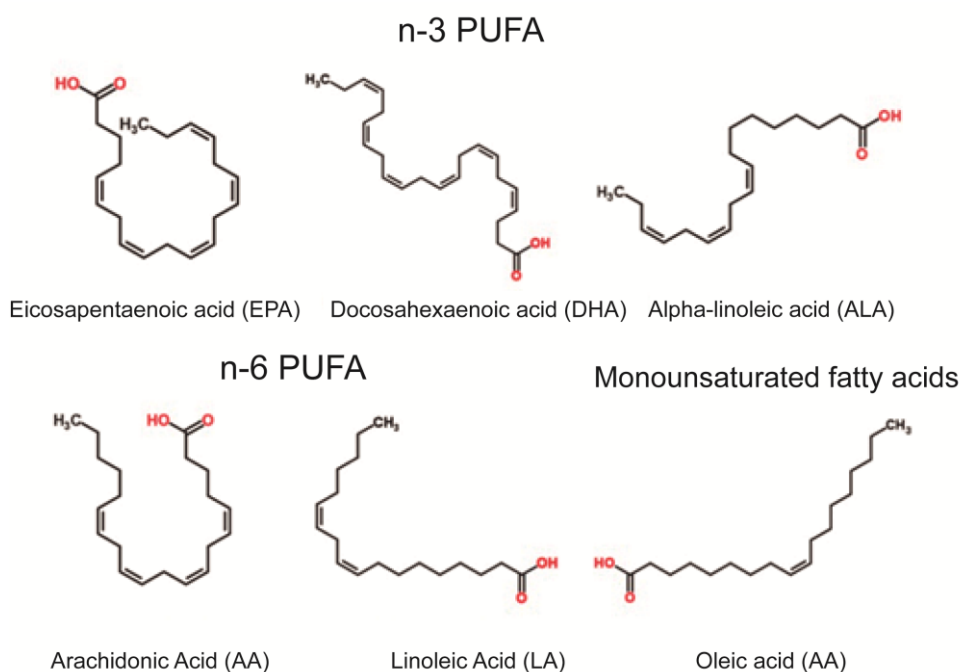


**Figure 1.9** Structure of the main PUFAs present in the human diet. n- 3 (EPA, DHA, and ALA), n- 6 (AA and LA) and monounsaturated (OA). (**Moreno, Macias et al. 2012**)

This type of fat helps to increase the rates of high-density lipoprotein cholesterol (HDL) and maintain low rates of low-density lipoprotein cholesterol (LDL). Excess involves the production of toxic compounds (**Cetrullo, Tantini et al. 2012**). They can be obtained in blue fish and vegetables such as corn, soybean, sunflower, pumpkin, nuts etc.

In relation to their structure, PUFA are fatty acids that contain more than one double bond in their backbone and they can be divided in two types: Omega-3 (n-3) and Omega-6 (n-6) (**Figure 1.9**). The nutritional dietary recommendations of n-3 PUFA are clearly defined and consensual (amounts and types), but the recommendations of the n-6 PUFA are more controversial (**Chen, Zhang et al. 2014**). Existing reports suggest that omega-6 essential fatty acids are typically proinflammatory and are linked with initiation and progression of carcinogenesis and others reports that suggest n-3 PUFA supplementation is a potential neurogenic and oligodendrogenic treatment to naturally improve post-stroke brain repair and long-term functional recovery (**Rovito, Giordano et al. 2013**) (**Hu, Zhang et al. 2013**). Studies using animal models of PD show that, in addition to its essential role in protecting dopaminergic neurons, maternal n-3 PUFAs supplementation played an important role in maintaining the cognitive integrity in inflammation-induced neurotoxicity (**Delattre, Carabelli et al. 2016**).

Further, PUFAs are essential components of neuronal and glial cell membranes. They regulate the production of pro/anti-inflammatory cytokines that may also contribute to neurodegenerative diseases such as PD (**Lopez-Vicario, Alcaraz-Quiles et al. 2015**).

### 1.6.2 Linoleic Acid

Linoleic acid (LA) is an omega-6 PUFA. It is a carboxylic acid with an 18-carbon chain and two cis double bonds, with the first double bond located at the sixth carbon from the methyl end (**Figure 1.10**).

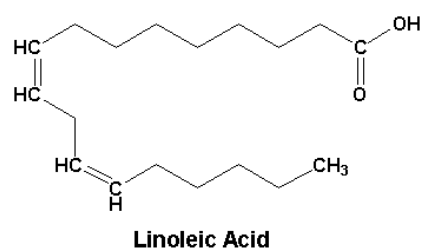


**Figure 1.10** Structure of linoleic acid. <http://conjugatedlinoleicacid.co.uk>

LA belongs to one of the two families of essential fatty acids, which means that the human body cannot synthesize it. LA comes from other food components and it is used in the biosynthesis of arachidonic acid and thus some prostaglandins, leukotrienes, and thromboxane. It is found in the lipids of cell membranes (**Choque, Catheline et al. 2014**).

In fact, LA is abundant in nuts, fatty seeds (flax seeds, hemp seeds, poppy seeds, sesame seeds, etc.) and their derived vegetable oils: poppy seed, safflower, sunflower, corn, and soybean oils.

LA, in several studies, shows that a deficient diet in linoleate (the salt form of the acid) causes mild skin scaling, hair loss and poor wound healing in rats, though others studies shows that linoleic acid can promote inflammation and metabolic disease.

## 2. Rational and aims

---

One of important cellular dysfunction in PD pathogenesis is autophagy desregulation. As it has been described the importance of PUFAs in autophagy modulation, it would be interesting to study their potential neuroprotective effects in PD models. Linoleic acid is a PUFA and it is the most present in our diet. If it possesses a neuroprotective effect, it would be a cheap and accessible compound..

In order to achieve our objective, we emphasize the following specific topics:

- Perform a dose-response of linoleic acid to determine the non cytotoxic concentrations that induce autophagy.
- Characterization of autophagy by linoleic acid to prove the implication of different signaling pathways.
- Find out the relation between LA-induced autophagy and various organelles.
- Find out if the LA-induced autophagy induces neuroprotection.



### 3. Materials and methods

---

#### 3.1 Appliances

- Rocker - Labnet Rocker 25 model
- Tube shaker - Bunsen
- Analog Magnetic shuffler - Bunsen serie MC-8
- Autoclave - Raypa Steam Sterilizer
- Analytical balance - ADAM PW 124 model
- Electronic balance - AND GF 300 model
- Thermostatic bath - Bunsen serie BA
- Camera Hammamatsu Orca-ER (adapted inverted optical microscope fluorescence Olympus IX81 model)
- Camera Olympus model DP70 (adapted inverted optical microscope fluorescence Olympus IX51 model)
- Chemiluminescence imager – Amersham Imagen 600, GE Healthcare
- Olympus IX51 model)
- Laminar flow hood - TELSTAR model AV-100
- Fume hood - Flores Valles
- Refrigerated centrifuge table Heraeus Megafuge 1.0R model
- Refrigerated centrifuge table Hermle Z 36 HK model
- Freezer -20°C Edesa Práctica model
- Freezer -80°C Heraeus HERA freeze model
- Freezer -80°C Thermo Scientific Forma 994 model
- Automatic cell counter - Bio-Rad TC10™ Automated Cell Counter model
- Electrophoresis equipment Bio-Rad Mini-Protean® III Cell model
- Transfer equipment Bio-Rad Trans-Blot SD Semi-Dry Transfer Cell model
- Spectrophotometer Thermo Scientific NanoDrop 2000 model
- Refrigerator 4°C and -20°C Edesa Style model
- Power Supplies - Bio-Rad POWER PAC 200 and POWER PAC 300 models
- Automatic homogenizern Accumet AB150 Fischer Scientific
- CO<sub>2</sub> incubator with temperature control - Thermo Scientific HEPA Class 100 model
- Plate reader - ELISA TECAN Sunrise model
- Shaved ice machine - Scotsman AF 80 model
- Microcentrifuge - Qualitron DW 41 model
- Optical microscope - Olympus CK model

- Inverted optical microscope fluorescence Nikon Eclipse Ti
- Inverted optical microscope fluorescence Olympus modelo IX51 and IX81
- pH-metro CRISON GLP 21 model
- Metal block thermostat - Bunsen serie TMR

### 3.2 Reagents

#### Ambion Laboratories

- BLOCK-iT™ Alexa Fluor® Red Fluorescent Oligo

#### Applied Biosystems Laboratories

- Negative control to *siRNA* (Silencer ® Negative Control #1 *siRNA*) (scrambled)

#### Bio-Rad Laboratories

- Coomassie® Brilliant Blue R-250
- Sodium dodecyl sulfate (SDS)
- Polyacrylamide gel 12% Mini-PROTEAN® TGX™ Precast Gel
- Molecular weight marker for protein electrophoresis (Precision Plus Protein™ Dual Color Standars)
- Buffer Tris/glycine 10X
- Buffer Tris/glycine/SDS (Laemmli) 10X

#### Fluka Chemika Laboratories

- Paraformaldehyde (PFA)

#### GIBCO Laboratories

- Medium DMEM
- Medium Opti-MEM® I Reduced Serum Medium
- Trypsin EDTA 10X 2,5 %
- Versene 1X

#### GE Healthcare Laboratories

- PVDF Hybond-P membranes
- Photographic paper HyperFilm™ ECL

#### HyClone Laboratories

- Streptomycin / Penicillin (10 mg/mL of streptomycin and 10.000 U/mL of penicillin)
- Fetal Bovine Serum (FBS)

Invitrogen Laboratories

- Lipofectamine® 2000 Transfection Reagent

KODAK Laboratories

- Fixative solution for photographic film
- Developing solution for photographic film

Molecular Probes Laboratories

- Alexa Fluor® 488 anti-rabbit IgG antibody
- Alexa Fluor® 568 anti-mouse IgG antibody

Panreac Laboratories

- Glacial acetic acid
- Hydrochloric acid (HCl) 37%
- Calcium chloride (CaCl<sub>2</sub>)
- Magnesium chloride (MgCl<sub>2</sub>)
- Potassium chloride (KCl)
- Sodium chloride (NaCl)
- Absolute ethanol
- sodium fluoride (NaF)
- Disodium phosphate (Na<sub>2</sub>HPO<sub>4</sub>)
- Potassium phosphate (KH<sub>2</sub>PO<sub>4</sub>)
- Glycerin
- Glycine
- Methanol

Pierce Laboratories

- ECL Plus Western Blotting Substrate

QIAGEN Laboratories

- HiPerfect Transfection Reagent (HiP)

Roche Laboratories

- Nonidet (NP40)

Sigma-Aldrich Laboratories

- Bicinchoninic acid (BCA)
- Linoleic acid (LA)
- Bovine serum albumin (BSA)
- β – mercaptoethanol
- Bromophenol Blue Solution
- Dimethylsulfoxide (DMSO)



- 2- [4- (2-hydroxyethyl) -1-piperazinyl (1)] - ethanesulfonic (HEPES)
- Hoechst 33342
- m-chloro carbonylcyanide phenylhydrazone (CCCP)
- Nile red
- Oxaloacetate
- sodium pyruvate
- Red ponceau
- Sucrose
- Copper sulfate (II)
- Thapsigargin
- Triclosan
- Triton X-100
- Trizma® (Tris) base
- Trypan blue solución (0,4 %)
- Tween 20
- Propidium Iodide (PI)

#### Southern Biotech Laboratories

- Glue Fluoromount G

#### Thermofisher Laboratories

- Black plate 96-well polystyrene Cat. No.:437869/437958
- Silencer negative control #1 AM4611

### 3.3 Antibodies

The following primary antibodies were used:

**Table 3.1 Primary antibodies.**

Antibody	Distributor	Host and Molecular weight
Atg5	Cell signaling 2630	Rabbit, 55 KDa
Cytochromo C	Santa Cruz sc-7159	Rabbit, 14 KDa
GAPDH	Milipore NG1740950	Mouse, 37 KDa
LC3	Cell Signaling 2775	Rabbit, 16 and 18 KDa
p62 (SQSTM1) (2C11)	Abnova H00008878-M01	Mouse, 62 KDa
pAMPK(Thr172) /AMPK	Cell Signaling 2535	Rabbit, 62 KDa
pmTOR (Ser2448) /mTOR	Cell Signaling 2971/2972	Rabbit, 289 KDa
pS6K (ser235/236) /S6K (54D2)	Cell Signaling 4858/2317	Rabbit, 32 KDa
β-actin	Abcam ab8227	Rabbit, 42 KDa

### **3.4 Cell lines**

SH-SY5Y (human neuroblastoma derived cell line);

H4 WT, H4 ATG5 KO (human neuroglioma derived cell line);

MEF WT and ATG5 KO (mouse embryon fibroblast);

U251 (human glioma derived cell line).

### **3.5 Cell maintenance**

Maintenance is a vital process when working with cell cultures. It allows us throughout our experiments, thawing vials of cells to amplify, seed, treat and freeze new road that will ensure our work in the future.

### **3.6 Defrosting/freezing**

Cells are frozen in a solution of 10% dimethylsulfoxide (DMSO) in FBS (10ml DMSO in 90 ml FBS). Although toxic at room temperature, DMSO is a cryoprotectant which protects cells from ice crystals, preventing cell death, at extreme temperatures. However, DMSO is not always appropriate because it can induce differentiation into certain cell lines, in which case it is better to go to glycerol. Generally, we freeze a cell density of approximately 1 million in 1 mL of FBS / DMSO, in a dry cryotube and store it in a freezer of -80°C. The ideal of a freeze is that it is slow and progressive.

### **3.7 Cell culture**

Human cell lines and mouse cell lines were obtained as described: H4 cells stably expressing GFP-LC3, both WT and ATG5 and U2OS cell lines (kindly given by Prof. Junying Yuan, Harvard Medical School, USA); SH-SY5Y from ATCC (American Type Culture Collection, Manassas, VA, USA); U251 (kindly given by Prof. Nadezda Apostolova, Skopje University, Republic of Macedonia); MEF WT and MEF ATG5 (kindly given by Prof. Mizushima, University of Tokio, Japan) Cell lines were routinely maintained at 37°C, 5% CO<sub>2</sub>, in the following media:

- H4 GFP LC3 (1 L DMEM; 10% FBS; 2 mM L-glutamine; 10 U/mL streptomycin/penicillin; geneticin; 5 ml HEPES)

- SH-SY5Y and U251 (1 L DMEM; 10% FBS; 2 mM L-glutamine; 10 U/mL streptomycin/ penicillin)
- MEF (1 L DMEM; 10% FBS; 2 mM L-glutamine; 10 U/mL streptomycin/ penicillin)

All cell lines were seeded at a density of 100.000 cells/mL.

### 3.8 Treatments

Throughout this work we have used different treatments (**Table 3.2**) to better understand the role of certain signaling pathways or interactions between them.

**Table 3.2** Compounds used to block different signaling pathways.

Drugs	Solvent	[concentration]	Target	Chemical formula	Comercial House
3-MA	DMEM	10mM	PI3K	C <sub>6</sub> H <sub>7</sub> N <sub>5</sub> 149.15 g/mol	Sigma M9281
BFA	DMSO	10µg/mL	Golgi apparatus	C <sub>16</sub> H <sub>24</sub> O <sub>4</sub> 280.36 g/mol	Sigma B7651
CCCP	Ethanol	100 µM	Mitochondria	C <sub>9</sub> H <sub>5</sub> ClN <sub>4</sub> 204.616 g/mol	Sigma C2759
CQ	H <sub>2</sub> O	10 µM	Lysosome	C <sub>18</sub> H <sub>26</sub> ClN <sub>3</sub> · 2H <sub>3</sub> PO <sub>4</sub> 515.86 g/mol	Sigma C6628
CC	DMSO	10 µM	AMPK	C <sub>24</sub> H <sub>25</sub> N <sub>5</sub> O 399.49 g/mol	Sigma P5499
E64d	Ethanol	10 µg/mL	Lysosome	C <sub>17</sub> H <sub>30</sub> N <sub>2</sub> O <sub>5</sub> 342.43 g/mol	Sigma E8640
LA	Ethanol	200µM; 400µM	-	C <sub>18</sub> H <sub>22</sub> Cl <sub>2</sub> O <sub>5</sub> 389.27 g/mol	Sigma L1376
LLOMe	DMSO	250 µM	Lysosome	C <sub>13</sub> H <sub>26</sub> N <sub>2</sub> O <sub>3</sub> 339.27 g/mol	Sigma L7393
PQ <sup>2+</sup>	H <sub>2</sub> O	500 µM	-	C <sub>12</sub> H <sub>14</sub> Cl <sub>2</sub> N <sub>2</sub> 257.16 g/mol	Sigma 36541
Pepstatin	Ethanol	10 µg/mL	Lysosome	C <sub>34</sub> H <sub>63</sub> N <sub>5</sub> O <sub>9</sub> 685.89 g/mol	Sigma P5318
Puromycin	H <sub>2</sub> O	10 µM	-	C <sub>22</sub> H <sub>29</sub> N <sub>7</sub> O <sub>5</sub> · 2HCl 544.43 g/mol	Tocris 4089
Thapsigargin	DMSO	1 µM	Intracellular Ca <sup>2+</sup>	C <sub>34</sub> H <sub>50</sub> O <sub>12</sub> 650.75 g/mol	Sigma T9033
Triclosan	Ethanol	1µg/mL	FASN	C <sub>12</sub> H <sub>7</sub> Cl <sub>3</sub> O <sub>2</sub> 289.54 g/mol	Sigma PHR1338

3-Methyladenine (3-MA) has been widely used as an inhibitor of class III PI3K to block autophagosome formation; however, 10 mM of 3-MA is required to inhibit autophagy. A structural study suggested that 3-MA preferentially inhibits VPS34 in vitro. In vivo, 3-MA can also inhibit class I PI3K, which may explain why it can promote autophagy flux under nutrient-rich conditions (**Wu, Wang et al. 2013**).

Brefeldin A (BFA) inhibits protein transport from the ER to the Golgi apparatus indirectly, by preventing formation of COPI-mediated transport vesicles, causing the disruption of Golgi apparatus.

CCCP is an uncoupling (that is ATP synthesis inhibitor). It is a weak acid liposoluble entering the mitochondria in its protonated form, discharging the proton gradient, and subsequently abandoned in its anionic form, dissipating  $\Delta\Psi_m$  (mitochondrial membrane potential). Negative charge is delocalized over 10 atoms in the form ionized, so that the electric field surrounding the anion is very weak, so that, it can be distributed freely through phospholipid membranes.

CQ is a lysosomal lumen alkalizers that inhibits autophagy by neutralizing the acidic pH, which is required for the activities of lysosomal hydrolases involved in autophagic degradation. Thus, alkylolation of lysosomal vesicles leads to the accumulation of autophagosomes by blocking lysosomal degradation (**Vakifahmetoglu-Norberg, Xia et al. 2015**).

CC is the only available agent that is used as a cell-permeable AMPK inhibitor.

\ Leu-Leu-OMe (LLOMe) is a lysosome-destabilizing agent mediate a third form of programmed necrosis, termed as lysosome-mediated necrosis (LMN) (**Brojatsch, Lima et al. 2014**).

$PQ^{2+}$  have been implicated in autophagy dysregulation in models of neurotoxin-induced dopaminergic cell death.

Puromycin generates protein aggregates.

Triclosan is a FASN inhibitor.

Thapsigargin blocks autophagosomal recruitment of the small GTPase RAB7, which is required for complete autophagic flux. However, disruption of  $Ca^{2+}$  homeostasis by thapsigargin also leads to ER stress, which could induce autophagy (**Mani, Lee et al. 2016**) (**Ganley, Wong et al. 2011**).

### 3.9 Linoleic acid

Linoleic acid (**L1376, SIGMA**) was stored at a concentration of 100 mM. In cell culture, it was used in several proportions, to study its effects. EBSS was used as a positive control of autophagy inducer. Cells were incubated with the components for 4 h.

### 3.10 Western Blot

For detecting the amount of protein in the previously cultured and treated cells, we parted them with trypsin. The cells are centrifuged at 2500 rpm, during 7 minutes at 4°C. We resuspended the pellet, with 1 mL of ice-cold PBS, and the cells are centrifuged again at 6500 rpm, during 5 minutes at 4°C. The pellet lysis is performed by the NP40 buffer (0,5%). Samples with NP40, are incubated on ice for 10-15 minutes and then centrifuged at 13000 rpm during 15 minutes at 4°C. Supernatants were collected and protein concentration is determined using bicinchoninic acid assay (BCA). The BCA assay primarily relies on two reactions:

First, the peptide bonds in protein reduce  $\text{Cu}^{2+}$  ions from the copper (II) sulfate to  $\text{Cu}^+$  (a temperature dependent reaction). The amount of  $\text{Cu}^{2+}$  reduced is proportional to the amount of protein present in the solution. Next, two molecules of bicinchoninic acid chelate with each  $\text{Cu}^+$  ion, forming a purple-colored complex that strongly absorbs light at a wavelength of 562 nm.

The bicinchoninic acid  $\text{Cu}^+$  complex is influenced in protein samples by the presence of cysteine/cystine, tyrosine, and tryptophan side chains.

The plate with the samples and bicinchoninic acid is incubated at 37°C during 30 minutes, to which peptide bonds assisted in the formation of the reaction complex. BSA (bovine serum albumin) was used as reference protein, performing a calibration curve ranging from 0  $\mu\text{g}/\mu\text{L}$  at 2  $\mu\text{g}/\mu\text{L}$  of concentration. The BCA is mixed with 2% copper sulfate. A volume of 200  $\mu\text{L}$  of the mixture will be added to 5  $\mu\text{L}$  of sample in a 96 well plate.

The amount of protein present in a solution is quantified by measuring the absorption spectra (TECAN Sunrise),  $\lambda = 570 \text{ nm}$ , and comparing with protein solutions of known concentration, to construct a standard curve.

According to the quantification, we put 30  $\mu\text{g}$  of protein and PBS and 4  $\mu\text{l}$  of loading buffer (5X). The loading buffer (5X) is made of Tris-HCL, SDS,  $\beta$ -mercaptoetanol, glicerol and blue of bromofenol. The loading buffer favors denaturalization and migration of proteins and allows to equal the charge. The samples are boiled for 10 minutes at 95°C. Samples were separated by an 12% gel SDS-

PAGE. The electrophoresis buffer used was Laemli (TGS 10x, BioRad). Laemli 1X is made of Tris, glycine, SDS and H<sub>2</sub>O. To be transferred, two cassetts are prepared with CAPS solution and the gel is placed close to a PVDF membrane. The transfer runs 90 minutes, at 100V, on cold (4°C). CAPS 1X solution is made of CAPS 10X, methanol and H<sub>2</sub>O.

It's prepared a blocking solution of 10% milk in TTBS 1X, by membrane, and this is incubated for one hour. Then we removed the blocking solution, and wash 3 times with TTBS 1X. So we put the primary antibody, overnight at 4°C. In the next day, the membrane is washed 3 times with TTBS 1X, 5 minutes. The secondary antibody is incubated, one hour at room temperature, together with a new blocking solution. After the membrane is washed again, in the same way, and is added the WB kit ECL (1:1), 5 minutes. Now the membrane can continue to the revelation, on photographic paper (**Gomez-Sanchez, Yakhine-Diop et al. 2016**).

### **3.11 MTT assay**

Cell viability studies provide information on cytotoxic/protective effects of treatments on cells and/or to find doses that reduce the percentage of living cells. To analyze cell viability we have used the technique of MTT (3-(4,5-dimethylthiazol-2-yl)-2,5-diphenyltetrazolium bromide). The MTT assay is a colorimetric test which allows, after treatment, evaluated relatively the number of viable cells through their metabolic activities. MTT is a tetrazolium salt which is reduced in a precipitate of formazan crystals inside living cells. A final concentration (0.45 mg/mL) MTT incubated with cells in culture at 37°C, for 2 h. The precipitate purple formazan is dissolved in 100% isopropanol acid. Its absorbance is read at  $\lambda = 570$  nm with TECAN Sunrise spectrophotometer.

### **3.12 Flow Cytometry**

The propidium iodide (PI) flow cytometric assay is widely used for the evaluation of apoptosis in different experimental models. It is based on the principle that apoptotic cells, among other typical features, are characterized by DNA fragmentation and, consequently, loss of nuclear DNA content. In fact, PI intercalates into double-stranded nucleic acids. It is excluded by viable cells but can penetrate cell membranes of dying or dead cells. PI is excited at 488 nm and emits at a maximum wavelength of 617 nm.

Cells were seeded, treated, in a 6-well plate, and removed with trypsin. We have three wells per condition. Each well was collected in a individually cytometry tube. The samples are centrifuged for 5 min, at 1200 rpm. The pellet obtained is resuspended in tube 200  $\mu$ L of PBS1X. Then 10  $\mu$ L of PI (0,1

mg/mL) are added to each tube. The results are obtained with the flow cytometer where 5,000 events are collected per tube.

### **3.13 Trypan Blue**

Cells were seeded, treated and removed with trypsin. It were centrifuged, at 1200 rpm, for 5 minutes. Then the pellet is resuspended with 1mL of DMEM. Mix 10  $\mu$ L of Trypan Blue, with 10  $\mu$ L of the resuspended pellet. This mixture is placed in the Bio-Rad TC10 <sup>TM</sup> Automated Cell Counter. This machine shows us the cell count, but also the % of live cells. This allows us to know the toxicity of treatments (**Uliasz and Hewett 2000**).

### **3.14 Immunofluorescence**

This technique allows determining the distribution and intensity of endogenous proteins by antigen-antibody reaction visualizing a fluorescent label. Thus, cells are seeded in a 96 well plate at a volume of 100  $\mu$ L/well. After treatment, the medium and cells fixed with paraformaldehyde (PFA) 4% for 20 min at room temperature to preserve all the cellular structures is removed. Then the plate is incubated with a solution of BSA (1mg / mL) in PBS 1X for 1 h at room temperature to block nonspecific reactions. Subsequently, we proceed to the incubation of specific primary antibodies overnight at 4°C. After 3 washes of 5 min each with PBS 1x, the plate was reincubated with the secondary antibody conjugated fluorochrome for 1 h at room temperature. Primary and secondary antibodies are diluted in the BSA solution (1 mg / mL). Between incubations, the plate is washed with PBS 1X three times under stirring to remove excess primary and secondary antibodies and also decrease the background noise from fixation.

#### **3.14.1 Lipid droplets**

We used a hydrophobic fluorochrome, the "Nile red"(Sigma, 19123), that is a LD label. The marking is diluted in acetone at a concentration of 1 mg/mL. From an intermediate dilution of 100  $\mu$ g/mL, we prepare a final concentration of 100 ng / mL in PBS 1X. The fixed cells are incubated with the latter concentration at least 10 min at room temperature, in the dark.

By its hydrophobicity, the "Nile red" is incorporated directly into the heart of lipid vacuoles and binds to TAG, cholesterol etc. The label has a range of excitation and emission very wide and varies

according to the types of lipids. With the Ifdotmeter® program, we measure the number of dots of lipid vacuoles. Images are displayed with inverted microscope (Olympus IX51) equipped with a camera.

### 3.14.2 small interfering RNA (siRNA)

A gene silencing through its mRNA expression level reduces, by 70%. The purpose is to understand the implication of that gene in the development of disease and/or its role in cell signaling pathways. We used a small interfering RNA (siRNA) that prevents protein synthesis causing degradation of the corresponding mRNA. siRNA binds to a specific region of mRNA complementary to cut. The siRNA is anionic, we need a carrier because it can not cross the plasma membrane. Thus, we use a reagent, the Hiperfect (Qiagen, 301704) which is a mixture of cationic and neutral lipids that facilitates the transport and the release of siRNA into cells. The reaction proceeds in a 6-well plate. The mixture (500  $\mu$ L OPTIMEM and 10  $\mu$ M siRNA) is incubated 5 min, at room temperature, to favor complex formation and after is added 5  $\mu$ L of lipofectamine RNAiMAX and it is incubated 15 min, at room temperature, too. Furthermore, it is important to develop with the same mixture for the negative control siRNA (scrambled). In parallel, cells are prepared at a density of 75 000 cells/mL. Subsequently, we mix the complex with the cells and give out on the plate after swirl gently. Cells are maintained in the incubator 24-72 h after being transfected; treatment is included in this period. We used siRNA AMPK $\alpha$  Santa Cruz (sc-45312) and siRNA BECN1 Santa Cruz (sc-29797).

### 3.15 Plasmid transfection

Overexpression of proteins is a powerful way to determine their function or to see if some treatment affects this function. We had used different constructs (**Table 3.3**), all of them at 1  $\mu$ g/ $\mu$ L concentration. We seeded, in a 24-well plate, on coverslips, at 75 000 cells/mL. After 24 h we use 700  $\mu$ L OPTIMEM and added 3,5  $\mu$ g DNA and mixed. After we added 2  $\mu$ L Neuromag (transfection reagent with magnetic nanoparticles) and this mix is incubated for 20 min, at room temperature, to facilitate the formation of Neuromag-DNA complex. We proceed to add the mix to the cell seeded, 50  $\mu$ L/well and put the plate on a magnetic plate, for the plasmid can get into the cells, for 20 min, at 37°C. In the next day, plates are treated and fixed, by PFA 4%, and analysed by immunofluorescence.



**Table 3.3 Plasmids used for overexpression**

<b>Plasmids</b>		<b>Commercial House</b>
<b>ptf-Galectin3</b>	It was a gift from Tamotsu Yoshimoni	Plasmid #64149, AddGene
<b>DsRed-rab7</b>	It was a gift from Richard Pagano	Plasmid #12661, AddGene
<b>LAMP1-mGFP</b>	It was a gift from Esteban Dell'Angelica	Plasmid #34831, AddGene
<b>Calnexin (pCalN-ddGFP-A)</b>	It was a gift from Robert Campbell	Plasmid #40290, AddGene
<b>mCherry-GFP-p62</b>	It was a gift from Dr. Terje Johansen gift	Plasmid #22418, AddGene

### **3.16 Data analysis**

Each experiment was repeated at least three times, with a satisfactory correlation between the results of individual experiments. The data shown are those of a representative experiment. Data were evaluated with the Student's t-test and all comparisons with p value less than 0.05 ( $p < 0.05$ ) were considered statistically significant.  $p < 0.001$ ,  $p < 0.01$  and  $p < 0.05$  are indicated with triple, double or single signs (\*,#), respectively.

## 4. Results

---

### 4.1 *Effect of LA in cell viability*

To determine the effect of LA on cell viability, we performed dose-response experiment in H4 and SH-SY5Y cells using MTT and trypan blue exclusion assays.

Cells were incubated with various concentrations of LA for 2, 4 and 6 h. H<sub>2</sub>O<sub>2</sub> was used as a positive control. The reduction of MTT (a yellow tetrazolium salt) to purple formazan product in living cells is a common method to assess cell viability. Results in **Figure 4.1** indicate that LA reduce the viability of H4 and SH-SY5Y cells in a concentration-dependent manner. 100 or 250 µM of LA have very little effect on cell viability, whereas concentrations higher than 500 µM are extremely toxic. We see also, that 2 h of treatment does not affect much cell viability and 6 h of treatment represents a decrease on it. To confirm these results, we performed trypan blue exclusion assays, a method for the determination of cell death. We treated cells with distinct LA concentrations for 4 h. The trypan blue test (**Figure 4.2**) shows that cell viability decreases from 500 µM. Therefore, we choose 200 and 400 µM concentration to posterior studies for 4 h of treatment

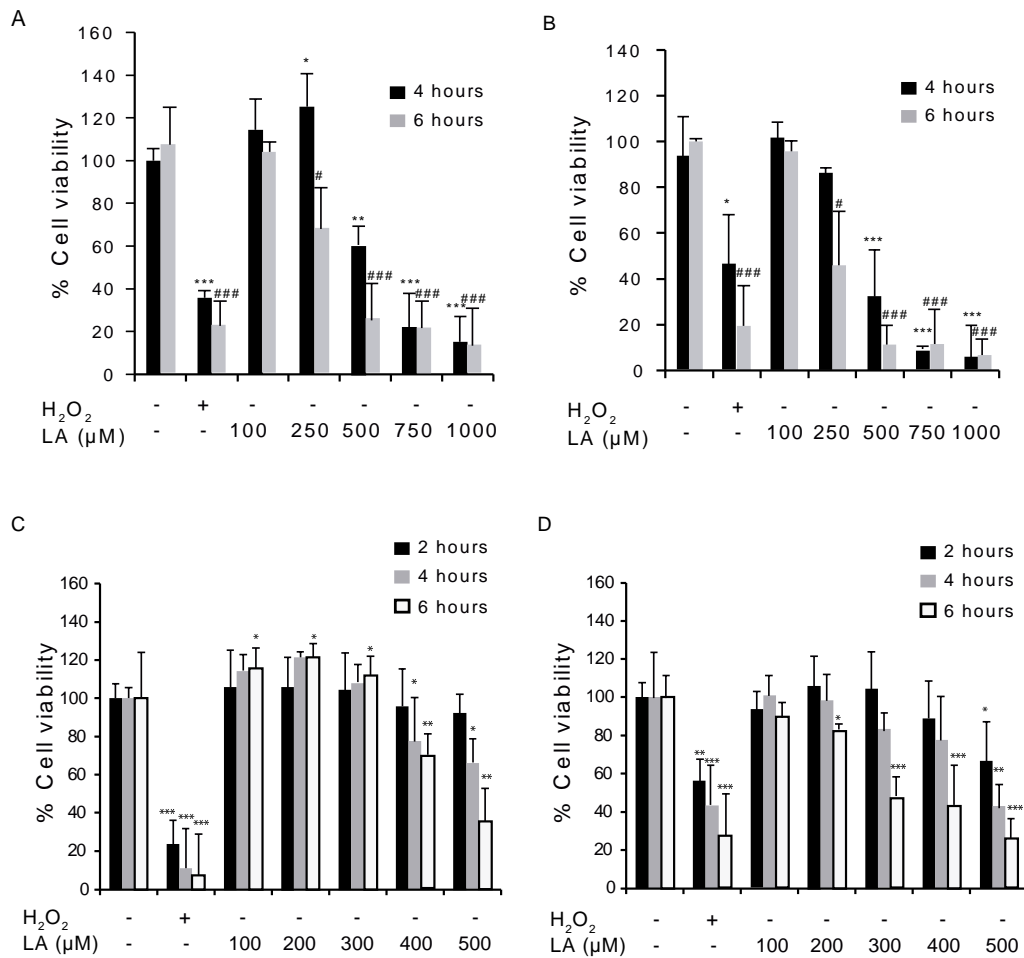


**Figure 4.1 Effect of LA in cell proliferation, by MTT assay.** Cell proliferation screening, with several LA concentrations, by MTT assay. H4 (A) and SH-SY5Y (B) cells were seeded at 100 000 cells/mL density. Cells were treated or not (Co) with different LA concentration (100, 250, 500, 750, 1000 μM), for 4 or 6 h. Data are means ± SEM of at least three independent experiments (\*P < 0.05, \*\*P < 0.01, \*\*\*P < 0.001, for 4 h treatment and #P < 0.05, ##P < 0.01, ###P < 0.001, for 6 h treatment). H4 (C) and SH-SY5Y (D) cells were seeded at 100 000 cells/mL density. Cells were treated with either experimental or control conditions using different LA concentration (100, 200, 300, 400, 500 μM), for 2, 4 or 6 h. Data are means ± SEM of at least three independent experiments (\*P < 0.05, \*\*P < 0.01, \*\*\*P < 0.001, always in relation to the control conditions). In all MTT assays H<sub>2</sub>O<sub>2</sub> was used as positive control. P-value lists the different conditions with control.

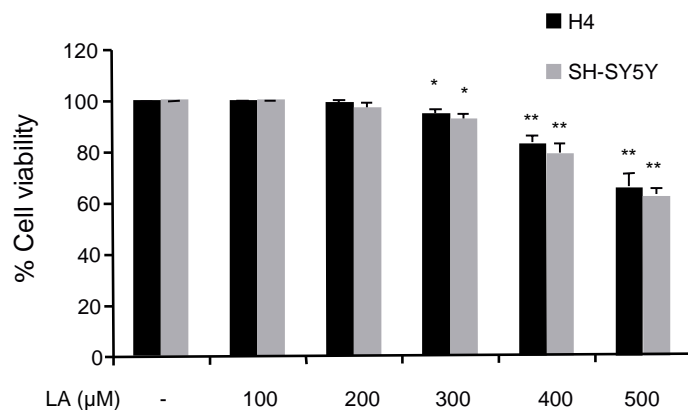
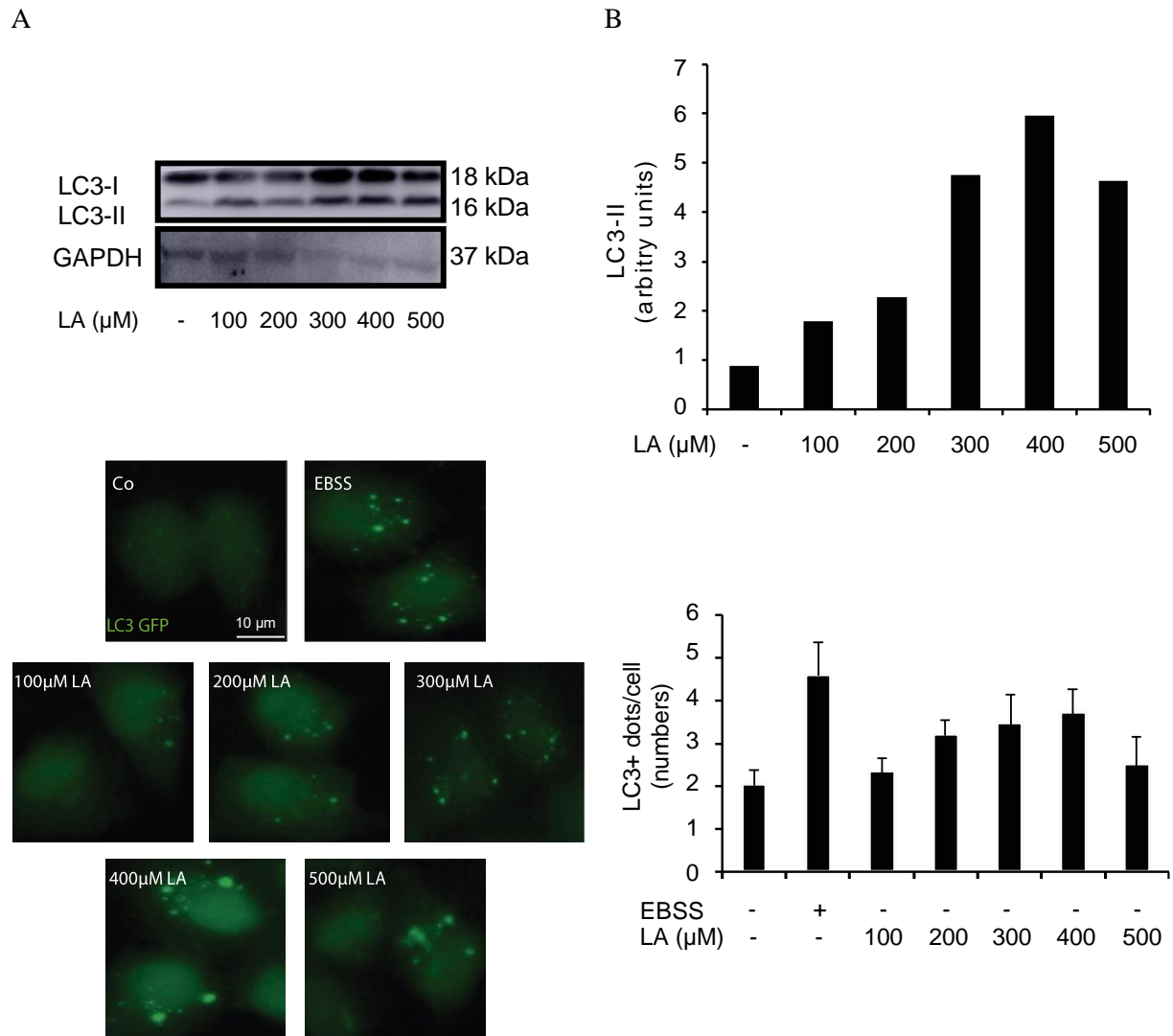


**Figure 4.2 Effect of LA in cell viability.** Cell viability screening, with several LA concentrations, by trypan blue exclusion test. H4 and SH-SY5Y cells were cultured in control conditions (Co) or treated with the indicated LA concentrations (100, 250, 500, 750, 1000 μM) for 4 h, at 100 000 cells/mL density. Data are means ± SEM of at least three independent experiments (\*P < 0.05, \*\*P < 0.01, \*\*\*P < 0.001, in relation to the control conditions). P-value lists the different conditions with control

#### 4.2 LA induces autophagy

Previous studies indicated that LA induces autophagy, in cancer cell lines. We wanted to characterize the effect of linoleic acid in neuronal cell lines. To investigate whether LA induces autophagy, LC3-II levels and LC3 puncta formation was determined by WB and immunofluorescence assays respectively. So, samples were loaded with different concentrations of linoleic acid for 4 h. LC3 is used as a marker for autophagy. As shown in **Figure 4.3**, we observed that LC3 lipidation enhances in a dose-dependent manner. These results were confirmed by fluorescence microscopy using H4 cells with GFP-tagged LC3. Quantitative analysis showed that LA enhances LC3 puncta accumulation. 500  $\mu$ M LA has a lower autophagy than 400  $\mu$ M, because cell viability decreases, a lot.

**Figure 4.3 LA induces autophagy.** LC3 lipidation and LC3 puncta formation was analyzed after treatment with linoleic acid.



H4 GFP-LC3 cells were untreated (Co) or treated with LA at concentrations of 100, 200, 300, 400 or 500 μM, respectively for 4h. EBSS was used as autophagy inducer. (A) Lipidation of LC3 (LC3-II) was determined by WB. GAPDH expression was used as a loading control. Representative blot of at least three independent experiments. (B) Densitometry of each band from the representative blot, expressed in arbitrary units of intensity. Scale bar represents 10 μm.

### 4.3 LA promotes autophagy flux

The determination of autophagosome number is not indicative of autophagy activation. Therefore, we performed autophagy flux assay to monitoring the LC3 turnover in the presence and absence of lysosomal inhibitors. We used CQ (an agent that impairs lysosomal acidification ) (**Figure 4.4 and 4.5 A and B**) and pepstatin /E64D (lysosomal proteases inhibitors) (**Figure 4.5 C and D**). The analysis of LC3 turnover by WB shows that there is an increase of lipidated LC3 in cells treated with CQ. However, the difference in LC3-II levels in the presence and absence of CQ is larger under starvation conditions and LA treatment indicating that autophagy flux is increased during LA treatment (**Figure 4.4**). We confirmed these results by immunofluorescence using CQ and pepstatin/E64D, with the H4 LC3-GFP cell line (**Figure 4.5**).

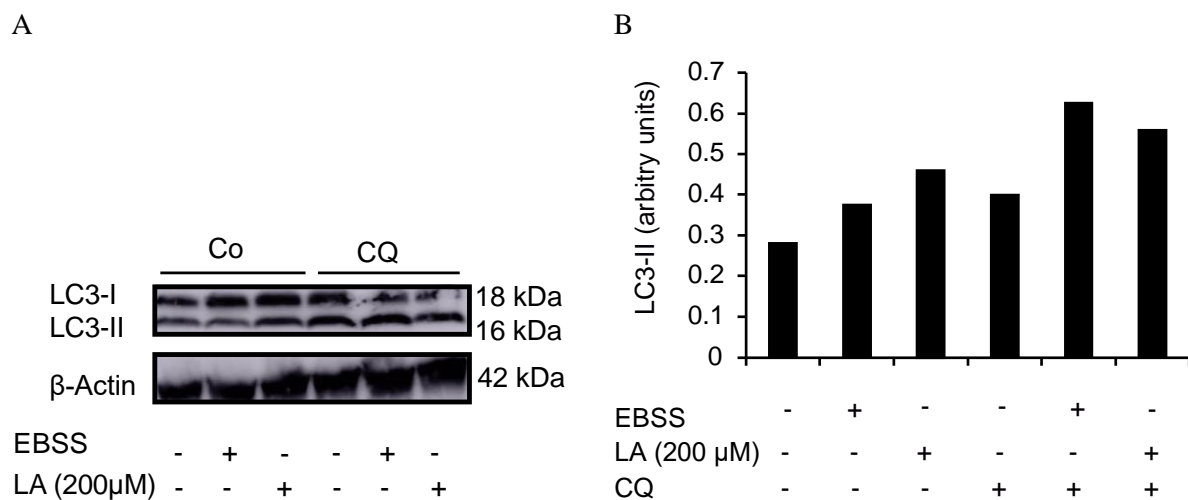


**Figure 4.4 Autophagic flux induced by LA.** (A) H4 cells were seeded at 100 000 cells/mL density and untreated (Co) or pretreated with 10 μM CQ 1 hour before LA or starvation treatments for 4 h. Cell extracts were subjected to western-blotting against the LC3 and β-actin antibodies. (B) Quantification of LC3-II versus β-actin was employed to quantify the abundance of lipidated LC3 (LC3-II). Densitometry of each band from the representative blot, expressed in arbitrary units of intensity.

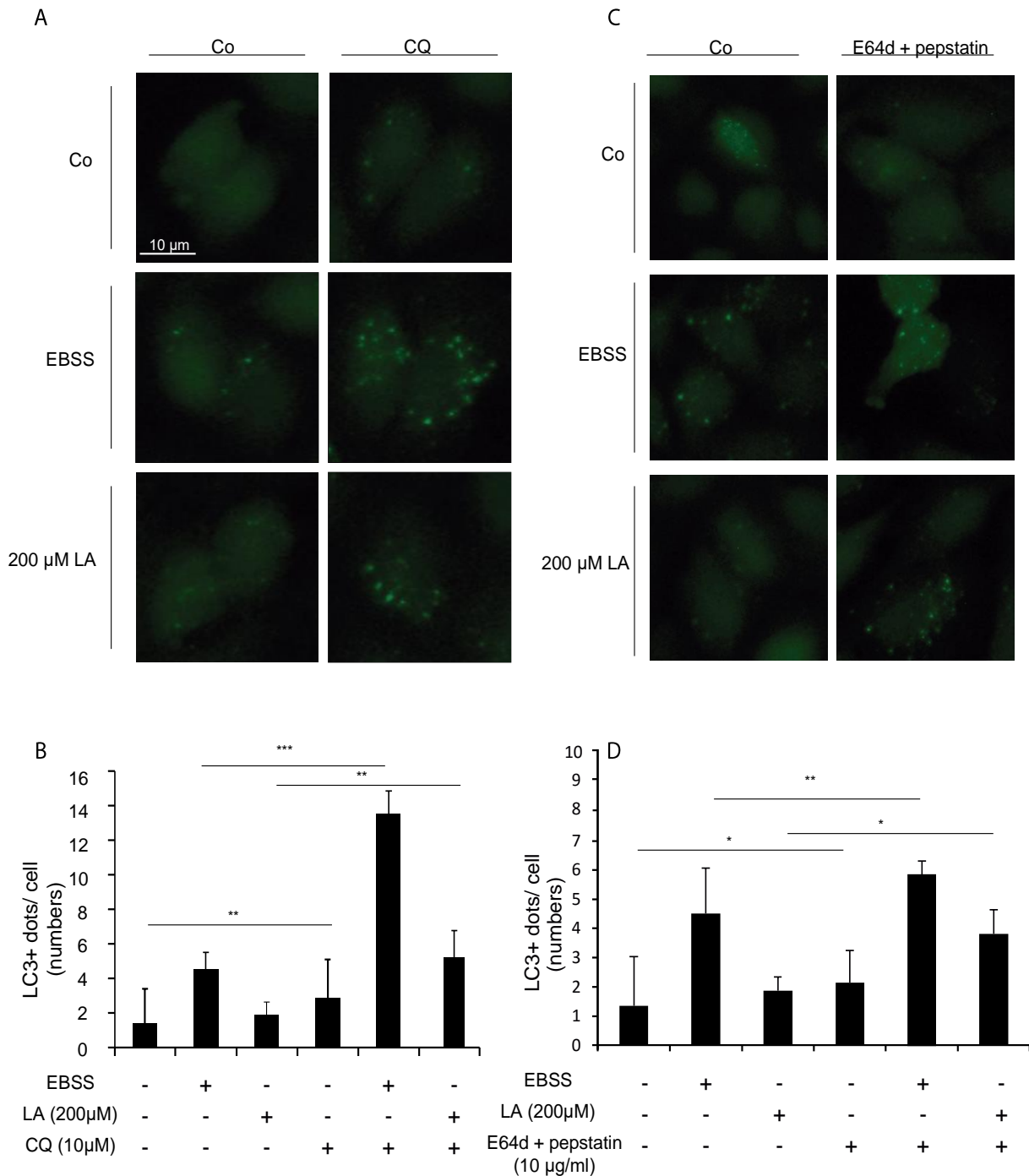
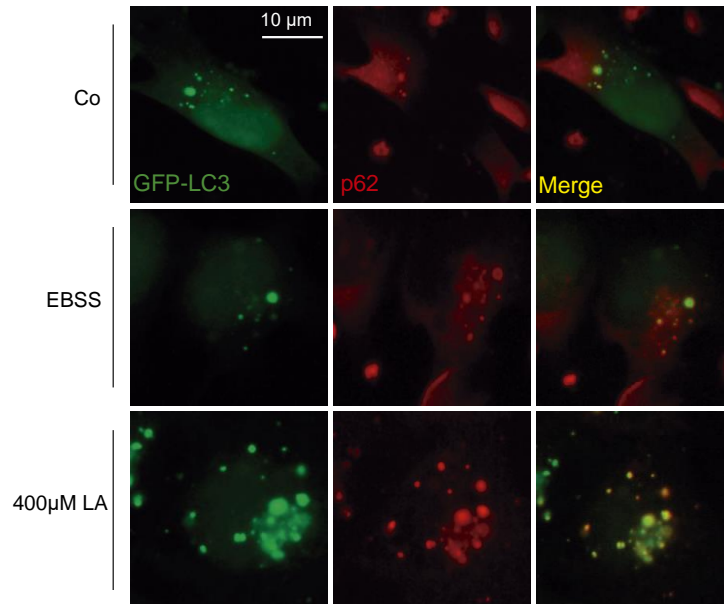


**Figure 4.5 Determination of autophagy flux by fluorescence microscopy.** H4 GFP-LC3 cell line (100 000 cells/mL density) was maintained in control conditions or treated with 200 μM (LA) alone, exposed to starvation conditions or in combination with 10 μM CQ (A) or in combination with E64d+pepstatin (10 μg/ml) (C), for 4 h. Thereafter, the number of cytoplasmic GFP-LC3<sup>+</sup> dots per cell was quantified (B, D). Scale bar represents 10 μm. Data are means ± SEM of at least three independent experiments (\*P < 0.05, \*\*P < 0.01, \*\*\*P < 0.001, in relation to the control conditions).

To confirm that the increase of autophagosomes also reflected the increase of functional autophagic degradation, autophagy flux was analyzed by measuring the levels of the p62, which is a common autophagosome cargo whose degradation reflects the levels of autophagy flux (**Figure 4.6A**). We used a mCherry-GFP double tag strategy to further improve the ability to distinguish neutral p62

inclusion bodies and autophagosomes from acidic amphisomes and autolysosomes. To verify that also p62 is present in acidic vesicles, mCherry-GFP-p62 was expressed in SH-SY5Y cells. As expected, p62 was found in both acidic and neutral structures. Treatment with 10 $\mu$ M CQ strongly increased the number of neutral structures (**Figure 4.6B**).

A



B

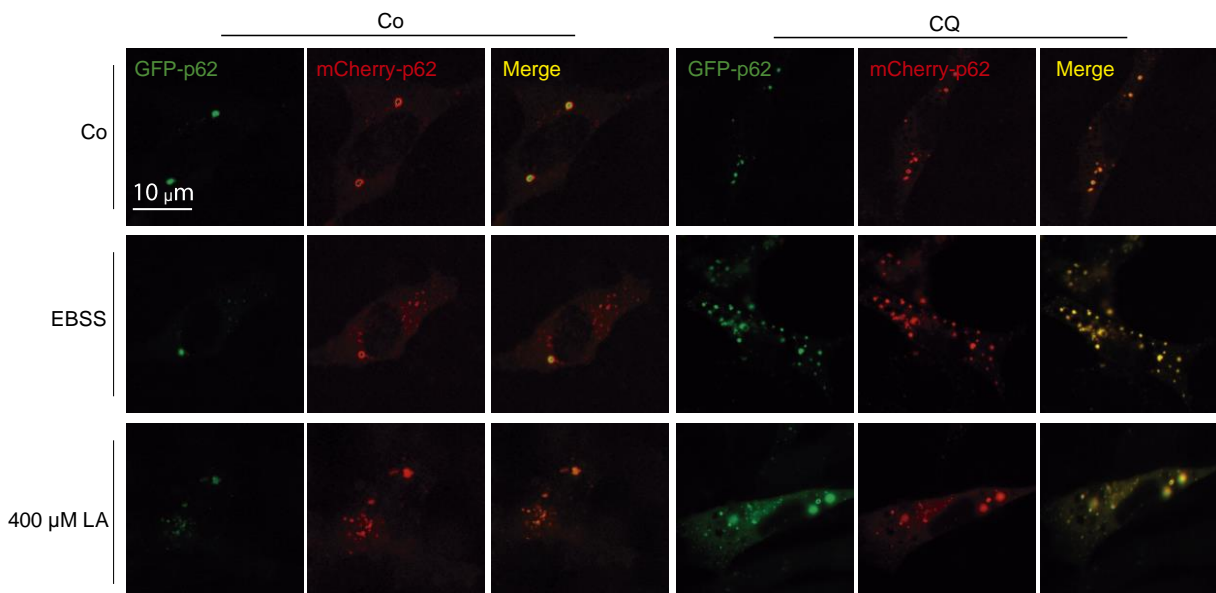


**Figure 4.6 LA promotes autophagy flux.** (A) H4 GFP-LC3 cells (100 000 cells/mL density) were untreated (Co) or treated with 400  $\mu$ M LA or starvation, for 4h, fixed and immunostained for p62 (red). EBSS was used as positive control of autophagy. (B) SH-SY5Y cells were transfected with mCherry-GFP-p62 plasmid for 24 h, and treated with starvation (EBSS), without treatment (Co), or with 400  $\mu$ M LA and 10  $\mu$ M CQ, only or combined, for 4 h, followed by fixation and visualization by fluorescence microscopy. (A) Representative immunofluorescence microphotographs showing GFP-LC3 (green) and p62 (red). (B) Autophagolysosomes and autophagosomes were labeled by red (mCherry-p62) and yellow puncta (mCherry-GFP-p62), respectively. Scale bar represents 10  $\mu$ m.



#### 4.4 LA-induced autophagy is Atg5-dependent

Autophagosome formation is controlled by a set of autophagy-related (ATG) proteins. Autophagy protein 5 is encoded by the *Atg5* gene. It is an E3 ubiquitin ligase which is necessary for autophagy due to its role in autophagosome elongation. This complex is necessary for LC3-I conjugation to PE to form LC3-II. To confirm that LA induced autophagy, we used *Atg5*-deficient cells that have been widely used in autophagy studies. We observed that the depletion of ATG5 abolished the ability of LA to promote the lipidation of LC3 in *Atg5*-knockout MEF and *Atg5*-deficient H4 cells (**Figure 4.7**). Therefore, we conclude that LA-induced autophagy is Atg5-dependent.

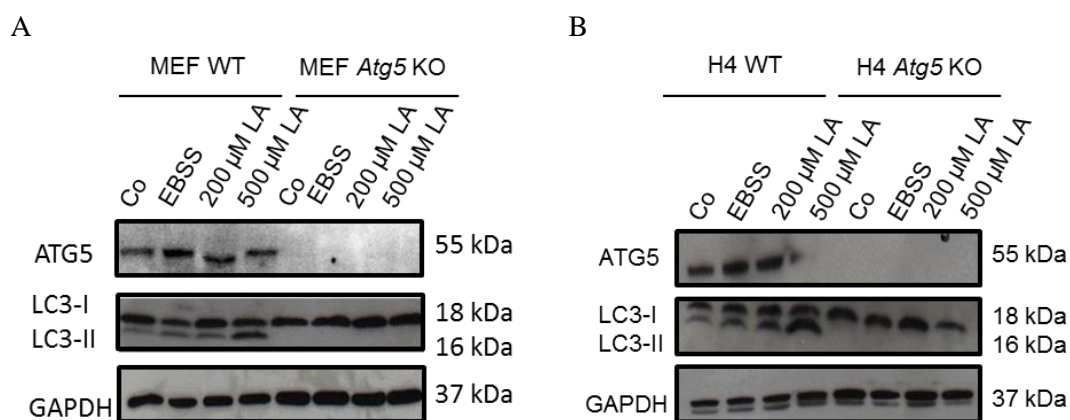


**Figure 4.7 LA-induced autophagy is *Atg5*-dependent.** WT and *Atg5* KO MEFs (A) and H4 cells and *Atg5*-deficient H4 cells (B) were untreated (Co) or treated with EBSS, 200  $\mu$ M or 500  $\mu$ M of LA for 4 h. Cell extracts were subjected to western-blotting against the ATG5, LC3 and GAPDH proteins. GAPDH levels were monitored to ensure equal loading of lanes. Representative blot of at least three independent experiments.

#### 4.5 LA induces mTOR-independent autophagy

Autophagy is controlled by different signaling pathways. The kinase mTOR is a major negative regulator of autophagy induction. Therefore, the inhibition of mTOR pathway by rapamycin or starvation induces autophagy. To analyze the role of mTOR in the autophagy induced by LA, we analyzed the phosphorylation of mTOR and its target S6 ribosomal protein by WB in SH-SY5Y cell line using rapamycin as a specific inhibitor of mTOR pathway. Results in **Figure 4.8** show that starvation treatment reduces the phosphorylation of mTOR and S6K in SH-SY5Y cells. However, cells treated with LA do not affect p-mTOR and p-S6K levels. Rapamycin treatment abolished the phosphorylation of mTOR and S6K. Therefore, These results show that LA induces a mTOR-independent autophagy.

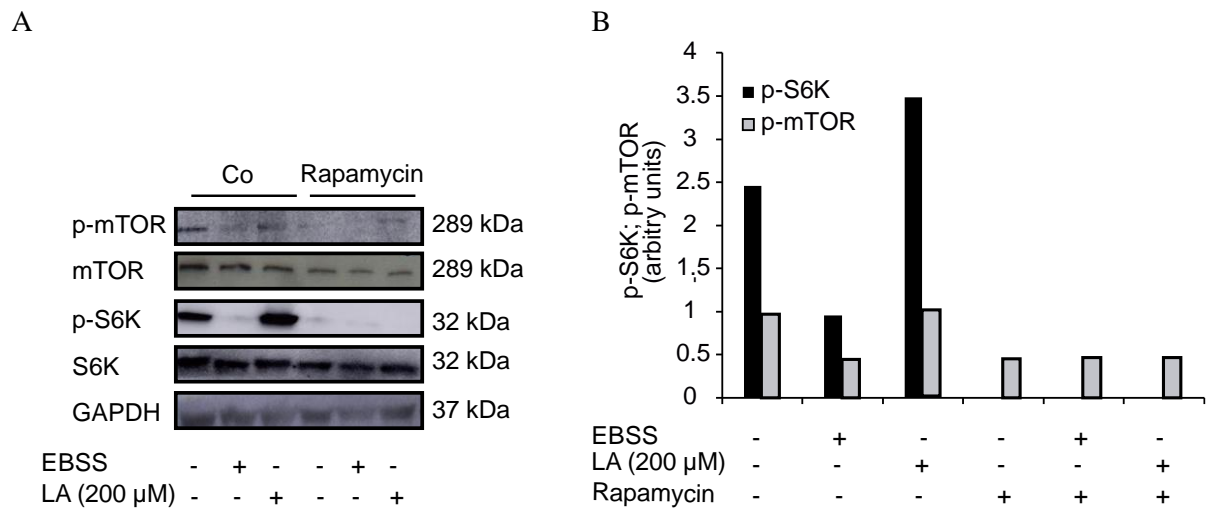


**Figure 4.8 LA-induced autophagy is mTOR-independent.** SH-SY5Y cell line (100 000 cells/mL density) were maintained in control conditions or treated with 200 μM (LA) alone, exposed to starvation (EBSS) conditions, or in combination with rapamycin (10 μM), for 4h. Cell extracts were subjected to western-blotting against the p-mTOR, mTOR, p-S6K, S6K, and GAPDH proteins (A). GAPDH levels were monitored to ensure equal loading of lanes, and densitometry (B) was employed to quantify the abundance of S6K and mTOR. Total mTOR and total S6k levels were monitored to ensure equal loading of lanes, and densitometry was employed to quantify the abundance of mTOR and S6k, respectively. Densitometry of each band from the representative blot, expressed in arbitrary units of intensity. Representative blots of at least three independent experiments.

#### 4.6 LA enhances the phosphorylation of AMPKα

AMP-activated protein kinase (AMPK) plays a key role as a master regulator of cellular energy homeostasis and it is implicated in the induction of autophagy (Liu, Chhipa et al. 2014). AMPK is activated under energy-low conditions, leading to autophagy induction. In addition, AMPK indirectly leads to the induction of autophagy by inhibiting mTOR. Therefore, we analyzed whether AMPK protein is implicated in autophagy induced by LA. Using H4 (Figure 4.9 A) and MEF (Figure 4.9 C) cells, we observed that LA enhanced p-AMPK levels compared to Co. These results show that LA functions as an activator of AMPK signaling pathway. To elucidate the role of AMPK in the autophagy induced by LA, we used CC that is a selective and reversible inhibitor of AMPK. Results in Figure 4.10 show that AMPK inhibition does not block the autophagy induced by LA. Following CC treatment, LC3-II levels were enhanced in cells treated with LA. Similar results were observed by fluorescence microscopy in which CC treatment increased LC3 puncta formation in H4-GFP-LC3 cells.

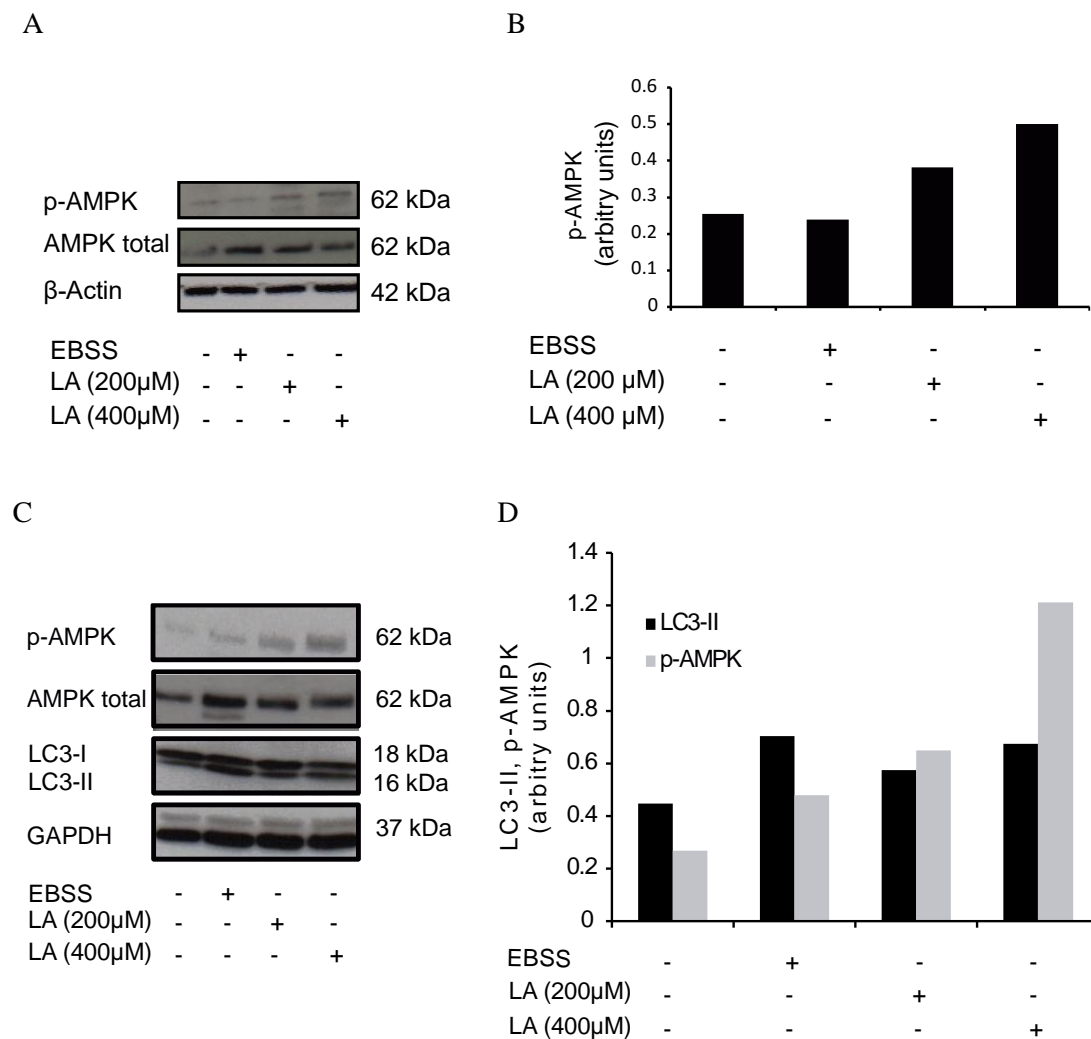


**Figure 4.9 LA enhances the phosphorylation of AMPK $\alpha$ .** (A) H4 cell line (100 000 cells/mL density) were maintained in control conditions or treated with 200  $\mu$ M or 400  $\mu$ M (LA) alone, exposed to nutrient-free (NF) conditions, or in combination, for 4h. Cell extracts were subjected to western-blotting against the p-AMPK, total AMPK, LC3 and  $\beta$ -actin proteins. Total AMPK levels were monitored to ensure equal loading of lanes, and densitometry (B) was employed to quantify the abundance of p-AMPK phosphorylation. (C) MEF WT cell line (100 000 cells/mL density) were maintained in control conditions or treated with 200  $\mu$ M or 400  $\mu$ M (LA) alone, exposed to nutrient-free (NF) conditions, for 4 h. Cell extracts were subjected to western-blotting against the pAMPK, total AMPK, LC3 and GAPDH proteins. GAPDH levels were monitored to ensure equal loading of lanes, and densitometry (D) was employed to quantify the abundance of lipidated LC3 (LC3-II). Total AMPK levels were monitored to ensure equal loading of lanes, and densitometry was employed to quantify the abundance of pAMPK phosphorylation. Densitometry of each band from the representative blot, expressed in arbitrary units of intensity

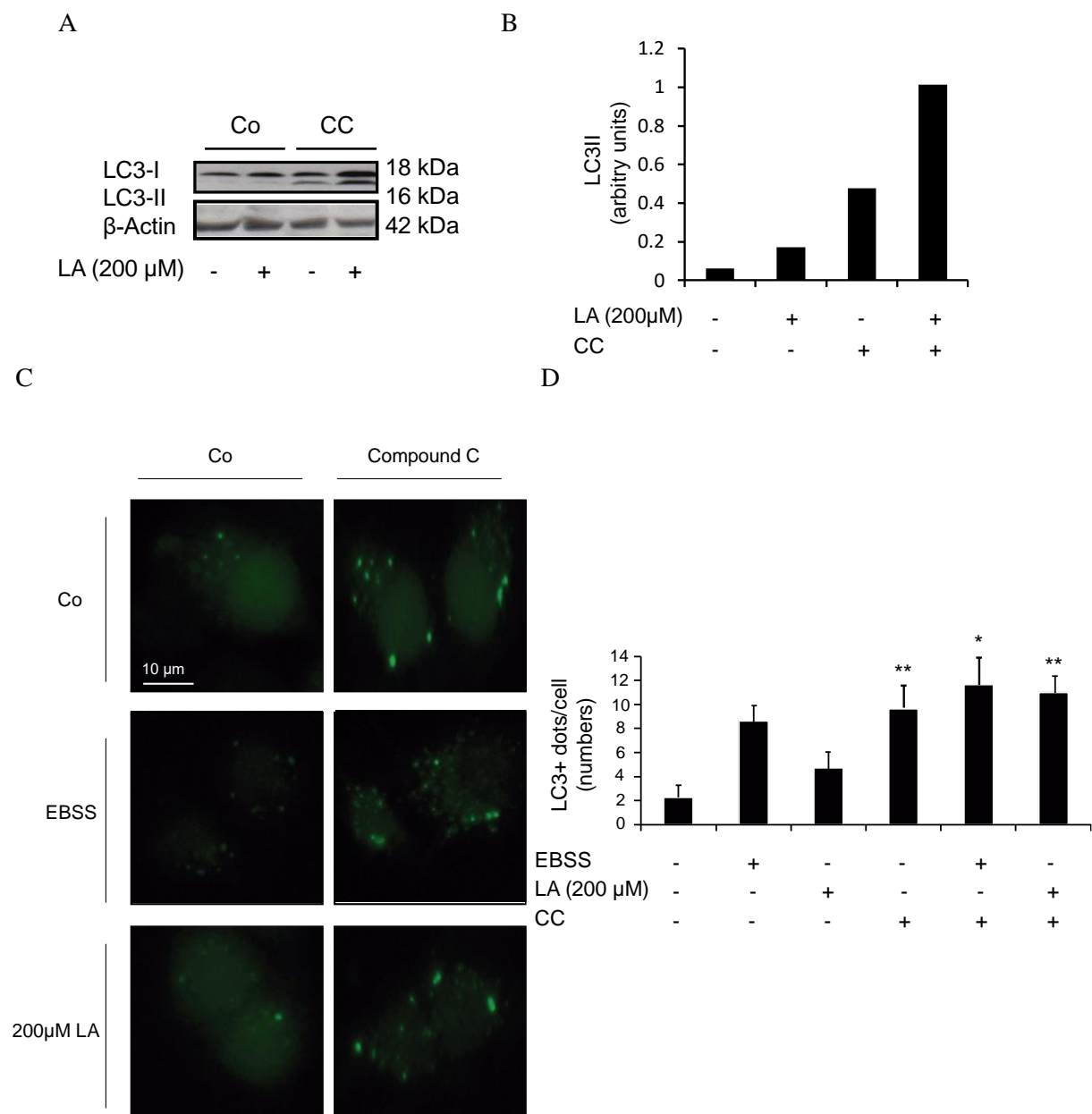


**Figure 4.10 Compound C induces autophagy.** (A) H4 cell line (100 000 cells/mL density) were maintained in control conditions or treated with 200 μM (LA) alone, or in combination with CC (10 μM), for 4h. Cell extracts were subjected to western-blotting against the LC3 and β-actin proteins. β-actin levels were monitored to ensure equal loading of lanes, and densitometry (B) was employed to quantify the abundance of lipidated LC3 (LC3-II). Densitometry of each band from the representative blot, expressed in arbitrary units of intensity. (C) H4 GFP-LC3 cell line (100 000 cells/mL density) was maintained in control conditions or treated with 200 μM (LA) alone, exposed to nutrient-free (NF) conditions or in combination with 10 μM CC, for 4h and the quantification of the number of cytoplasmic GFP-LC3<sup>+</sup> dots per cell, respectively (D). (A) Representative blots of at least three independent experiments. (C) Representative immunofluorescence microphotographs of GFP-LC3 puncta formation. P-value lists Co with Co+CC; EBSS with EBSS+CC and LA with LA+CC). Scale bar represents 10 μm.

Since it has previously been reported that the effects of CC on autophagy might be dose- cell type- and/or context-dependent, we evaluated the effect of AMPK knockdown on autophagy using small interfering RNA (siRNA) of AMPK. To do so, we analyzed AMPK knockdown by WB and we found

that the downregulation of AMPK reduced LC3 lipidation in cells treated with LA and starvation (**Figure 4.11**). Our results suggest that LA induces autophagy through AMPK activation. ,

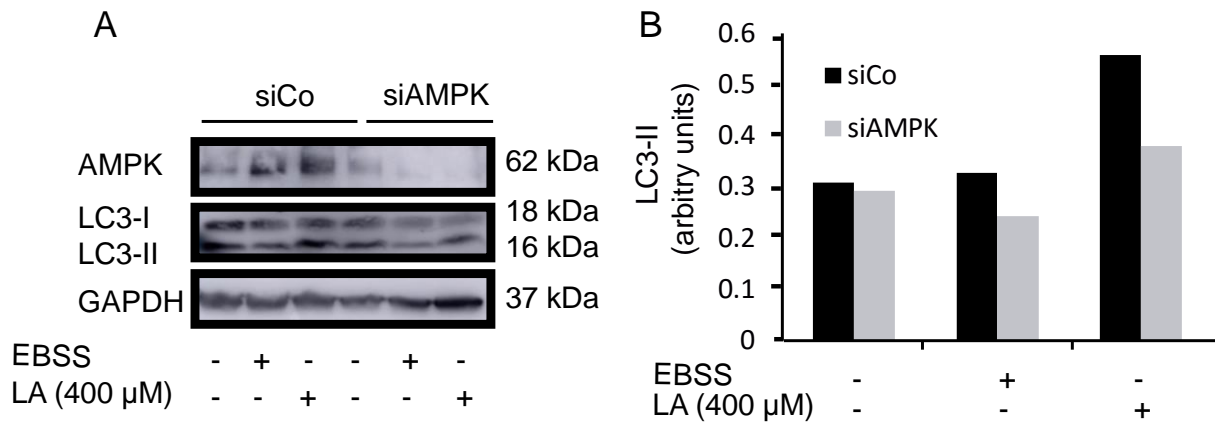


**Figure 4.11 LA-induced autophagy is AMPK-dependent.** (A) H4 cells (75 000 cells/mL density) were transfected with a control siRNA (siUNR) or with siRNA targeting AMPK for 48 h and either untreated (Co) or treated with starvation or LA 400 μM. Cell extracts were subjected to western-blotting against LC3 and GAPDH proteins. GAPDH levels were monitored to ensure equal loading of lanes. Representative blots of at least three independent experiments. (B) Densitometry of each band from the representative blot, expressed in arbitrary units of intensity

#### 4.7 LA-induced autophagy is BECN1-independent

Class III PI3K complex, containing hVps34, BECN1 (a mammalian homolog of yeast Atg6), p150 (a mammalian homolog of yeast Vps15), and Atg14-like protein (Atg14L or Barkor) or ultraviolet irradiation resistance-associated gene (UVRAG), is required for the induction of autophagy. To analyze the implication of PI3K/BECN1 pathway in the autophagy induced by LA, we used H4 cell line that were untreated (Co) or treated with EBSS and LA for 4h. Starvation was used as BECN1 dependent autophagy inducer (**Figure 4.12**). WB analysis using BECN1 antibody showed that LA do not modulate the level of BECN1 protein compared to Co. However, EBSS treatment enhances BECN1 levels. Next, we investigated whether PI3K/BECN1 pathway has a role in the autophagy induced by LA, we used 3-MA that is an inhibitor of Class III PI3K (**Figure 4.13**). We know that 3-MA inhibits the lipidation of LC3 in cells treated with EBSS, however the inhibition of BECN1 by 3-MA does not affect LC3-II levels of LA-induced autophagy. This is further proof that not active LA this route.

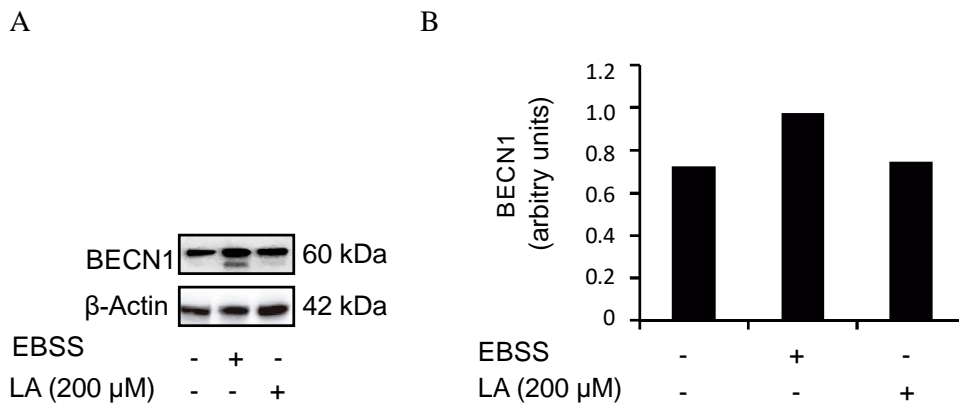


**Figure 4.12 Autophagy induced by LA is BECN1-independent.** H4 cells (100 000 cells/mL density) were maintained in control conditions or exposed to starvation (EBSS) or treated with 200  $\mu$ M linoleic acid (LA), for 4 h. Cell extracts were subjected to western-blotting against the BECN1 and  $\beta$ -actin proteins.  $\beta$ -actin levels were monitored to ensure equal loading of lanes. Representative blots of at least three independent experiments. (B) Densitometry of each band from the representative blot, expressed in arbitrary units of intensity

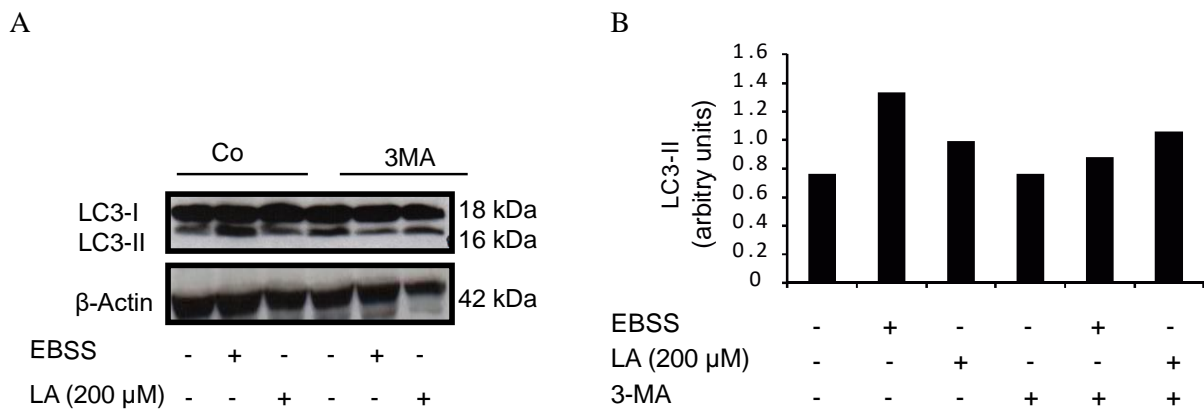


**Figure 4.13 3-MA does not inhibit the autophagy induced by LA.** H4 GFP-LC3 cells (100 000 cells/mL density) were maintained in control or nutrient-free (NF) conditions or treated with 200  $\mu$ M linoleic acid (LA), alone or combined with 10 mM 3MA, for 4 h. Cell extracts were subjected to western-blotting against LC3 and  $\beta$ -actin proteins.  $\beta$ -actin levels were monitored to ensure equal loading of lanes. (B) Densitometry of each band from the representative blot, expressed in arbitrary units of intensity.

To confirm that LA induce autophagy in a BECN1 independent manner, we induced autophagy inhibition with BECN1 siRNA. These experiment were realized on H4 GFP-LC3 cells (150 000 cells/siRNA) by WB and fluorescence microscopy. EBSS was used as positive control. As we can see, BECN1 silencing reduced starvation-induced LC3 lipidation. By contrast, the silencing of beclin-1 does not affect the lipidation of LC3 induced by LA (**Figure 4.14**). Similar results were observed by fluorescence microscopy. The number of GFP-LC3 structures decrease with starvation treatment, but we didn't observe a decrease of GFP-LC3 puncta formation in cells treated with LA (**Figure 4.15**). Therefore, we can conclude that LA-induced autophagy is BECN1-independent.

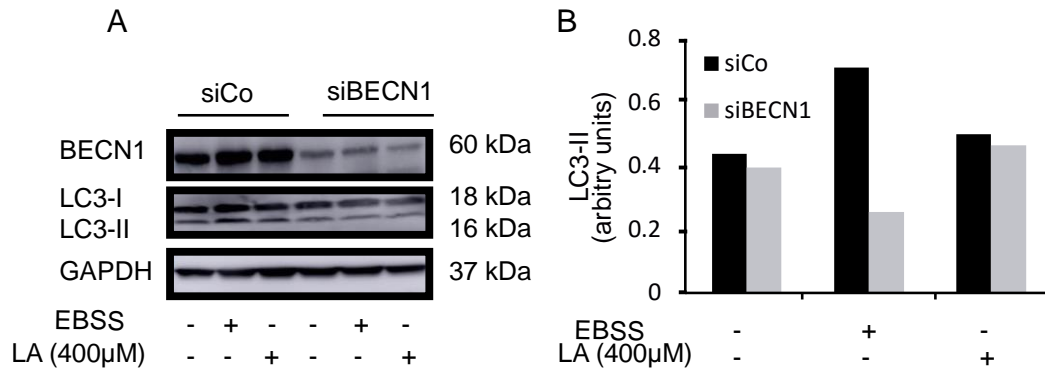


**Figure 4.14 LA-induced autophagy is BECN1-independent.** (A) H4 cells (75 000 cells/mL density), alone or combined with 10 µM siBECN1, for 24 h, with an no antibiotic medium. Next day medium was changed for DMEM. After 24 h cells were maintained in control or starvation (EBSS) conditions or treated with 400 µM linoleic acid (LA). Cell extracts were subjected to western-blotting against LC3 and GAPDH proteins. GAPDH levels were monitored to ensure equal loading of lanes and densitometry (B) was employed to quantify the abundance of LC3 (LC3-II). Densitometry of each band from the representative blot, expressed in arbitrary units of intensity. Representative blots of at least three independent experiments

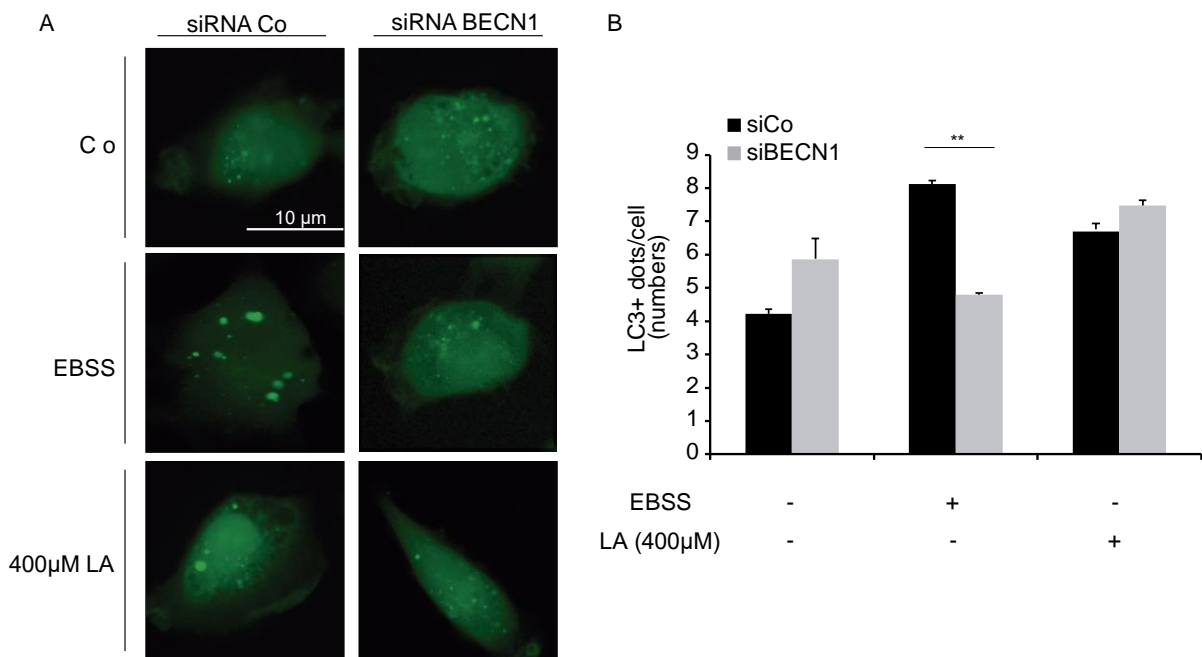


**Figure 4.15 Implication of BECN1 in LA-induced autophagy.** (A) GFP-LC3-expressing H4 cells were transfected (75 000 cells/mL) with a control siRNA (siCo) or with siRNA targeting BECN1 (siBECN1) for 48 h and either maintained in control conditions (Co) or treated with 400 µM linoleic acid (LA), for 4 h. (A) Representative immunofluorescence microphotographs of GFP-LC3 puncta formation and quantification of GFP-LC3<sup>+</sup> dots (B). Scale bar represents 10 µm.

## 4.8 Effect of LA in different organelles

### 4.8.1 LA does not alter organelle structures

We have analyzed the autophagic signaling pathways activated by LA. We next wanted to determine the effect of LA in different organelles and its role in neuronal cell viability. To this purpose, cells were transfected with several plasmids using classic transfection technologies. These technologies have initially been developed for introducing plasmid DNA into cells, and plasmid DNA still remains the most common vector for transfection. DNA plasmids containing recombinant genes and regulatory elements can be transfected into cells to study gene function and regulation, mutational analysis and biochemical characterization of gene products, effects of gene expression on the health and life cycle of cells, as well as for large scale production of proteins for purification and downstream applications.

We used as plasmids mCherry-GFP-p62, ptf-Galectin3, DsRed-rab7, Calnexin (pCalN-ddGFP-A) and LAMP1-Mgfp (all used at 1µg/µL concentration).

Galectins are a large family with relatively broad specificity. Thus, they have a broad variety of functions including mediation of cell–cell interactions, cell–matrix adhesion and transmembrane signalling. Galectin-3 is a marker of damaged endomembranes (**Paz et al, 2010**). tfGal3 is a mRFP-GFP-tandem-tagged Gal3. GFP and mRFP are differentially sensitive to acidic environments. GFP fluorescence is rapidly quenched and it is degraded by lysosomal hydrolases. mRFP fluorescence is more stable. Therefore, to monitor the pH change in damaged lysosomes, cells were transfected with tfGal3 and we used the lysomotropic compound L-Leucyl-L-leucine methyl ester (LLOMe) to disrupt the lysosomal membrane. Thus, as shown in **Figure 4.16**, we observed GFP and RFP puncta in cells untreated (Co) and treated with LA whereas mRFP-GFP puncta decrease in cells treated with LLOMe. Therefore, LA treatment does not damage lysosomes. We confirmed this result using GFP-Lamp1 plasmid. The LAMP-1 glycoprotein is a type I transmembrane protein which is expressed at high or medium levels in at least 76 different normal tissue cell types. It resides primarily across lysosomal membranes, and functions to provide selectins with carbohydrate ligands. As we can see in figure 4.16, LA does not affect lysosomes compared to LLOMe treatment.



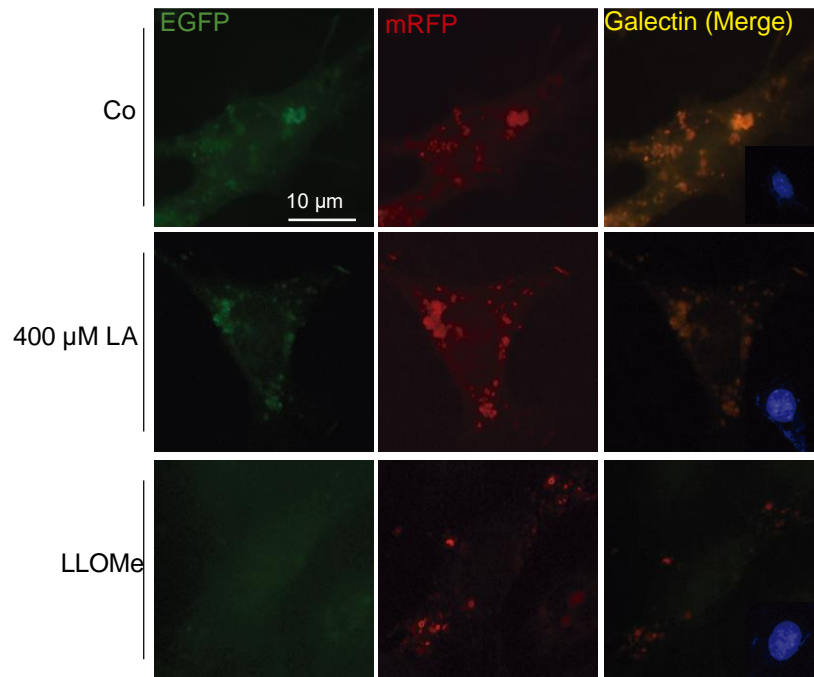


**Figure 4.16 LA does not impair lysosomes.** Fluorescence microscopy in SH-SY5Y cells (75 000 cells/mL density) overexpressing tfGal3. SH-SY5Y cells were seeded on coverslips, in 24-well plates, and transfected with tfGal3 using Neuromag protocol. Next day, cells were untreated (Co) or treated with 400 μM LA or LLOMe, for 4 h, followed by fixation and visualization by fluorescence microscopy. Representative immunofluorescence microphotographs show tfGal3 (green and red fluorescence) and Hoechst 33342 stain (blue fluorescence). Scale bar represents 10 μm.

Rab7 has been localized to late endosomes and shown to be important in the late endocytic pathway. ER is another organelle that has an important role in endocytic pathway. Calnexin is a 67 kDa integral protein of the ER. It is a chaperone characterized by assisting protein folding and quality control, ensuring that only properly folded and assembled proteins proceed further along the secretory pathway. To disrupt the endocytic pathway, cells were treated with BFA. In **Figure 4.17**, SH-SY5Y cells expressing fluorescently tagged Rab7 and Calnexin untreated (Co) and treated with LA show perinuclear punctate structures. However, BFA alters endocytic pathway, and BFA-treated cells do not show punctate structure. Finally, we analyze the effect of LA in mitochondria. To do this, we performed cytochrome c immunostaining. Cyt C is located in the mitochondrial intermembrane space. During the early stages of apoptosis, the mitochondria is damaged and Cyt C is often released from mitochondria to the cytosol. To impair the mitochondria, we used the herbicide  $PQ^{2+}$ . As shown in **Figure 4.17**, Cyt C is located in the mitochondria when cells are treated with LA compared to PQ.

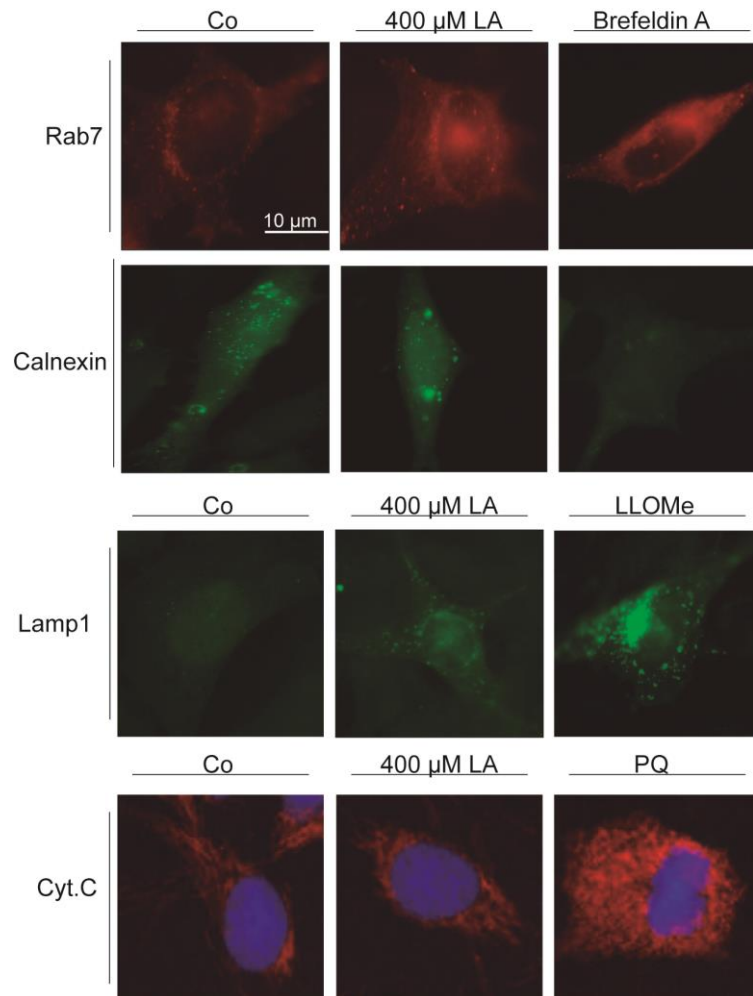


**Figure 4.17 Effect of LA treatment in organelle structures.** Fluorescence microscopy in SH-SY5Y cells (75 000 cells/mL density) overexpressing Rab7, Calnexin and Lamp1. SH-SY5Y cells were seeded on coverslips, in 24-well plates, and transfected, after 24 h, with 2 μl Neuromag and plate was colocated on a magnetic plate. Next day, DMEM is changed, for an additional 24 h. Cells were then treated with serum-free DMEM supplemented, without treatment (Co) or with 400 μM LA and BFA or LLOMe, for 4 h, followed by fixation and visualization by fluorescence microscopy. For the PQ treatment, SH-SY5Y cells (75 000 cells/mL density) were seeded, in 96-well plates, untreated (Co) or treated with 400 μM LA or 500 μM PQ, for 24 hours. Next day, it were fixed (PFA 4% and Hoechst 33342) and incubated with anti-Cyt C (red label), for visualization by fluorescence microscopy. Scale bar represents 10 μm.

As we can see LA seems always like Co conditions, what means, that not affects mitochondria, ER, lysosomes or cell membrane.

#### 4.8.2 LA induces autophagy even with lysosome and mitochondria damage.

To evaluate the role of different organelles in autophagy induced by LA, organelles were damaged with various specific compounds and we analyzed whether autophagy is affected by immunofluorescence microscopy. We used LLOMe to damage the lysosome membranes, CCCP to impair the mitochondria (**Figure 4.18**) and BFA to alter endocytic pathway (**Figure 4.19**) and thapsigargin (**Figure 4.20**) that causes stress on the ER. To perform these experiments by immunofluorescence, we used H4-GFP-LC3 cells.

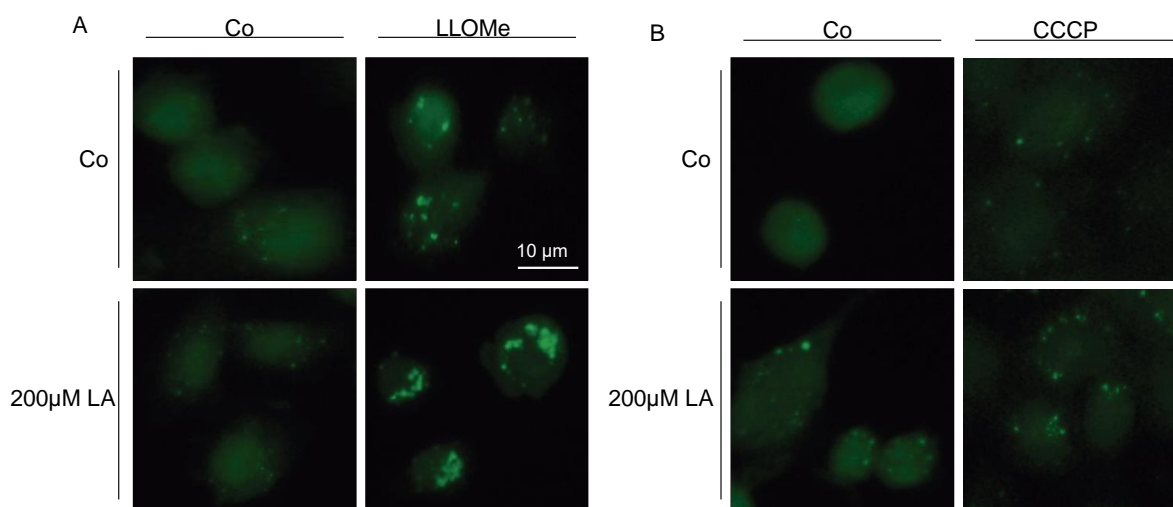


**Figure 4.18** Effect of LA treatment in organelle structures. H4-GFP-LC3 cells (100 000 cells/mL density) were maintained in control conditions (Co) or treated with 200 μM (LA) alone, or in combination with 250 μM LLOMe (A) or 100 μM CCCP (B). Representative immunofluorescence microphotographs show LC3 puncta (green). Scale bar represents 10 μm.

We observed that the number of GFP-LC3 structure is similar in cells treated with LLOMe or CCCP when compared to LA alone. And they further increase with the combined treatment (LA+CCCP or LA+LLOMe). These results show that damaged lysosomes and mitochondria do not reduce the autophagy induced by LA (**Figure 4.18**). Similar results were obtained when cells were treated with thapsigargin and BFA (**Figures 4.19** and **4.20**). Therefore, LA-induced autophagy is organelles-independent.

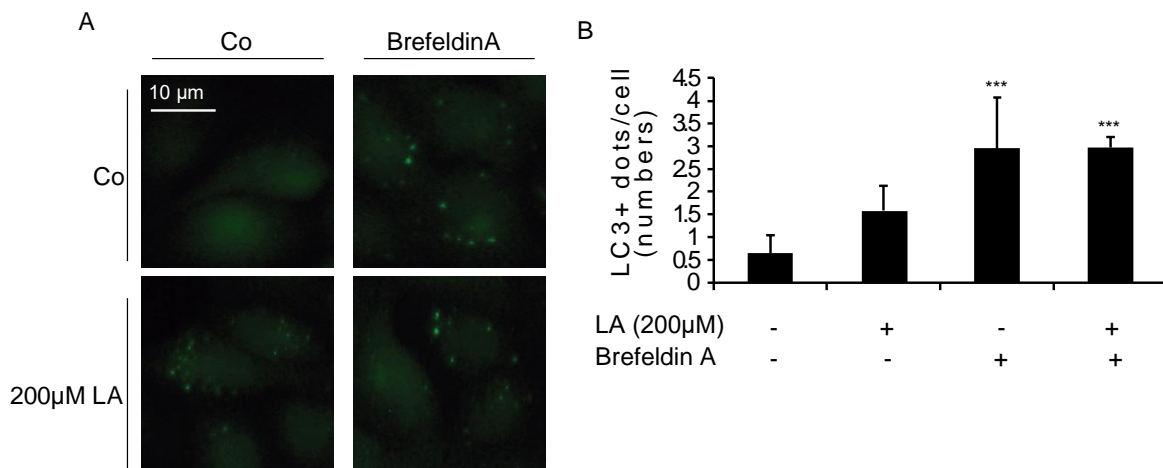


**Figure 4.19 LA-induced autophagy is Golgi-apparatus-independent.** H4 GFP-LC3 cells (100 000 cells/mL density) were maintained in control conditions (Co) or treated with 200 µM (LA) alone, or in combination with 10 µg/mL BFA, for 4 h, and the quantification of the number of cytoplasmic GFP-LC3+ dots per cell (B). P-value lists the different conditions with control. Scale bar represents 10 µm.

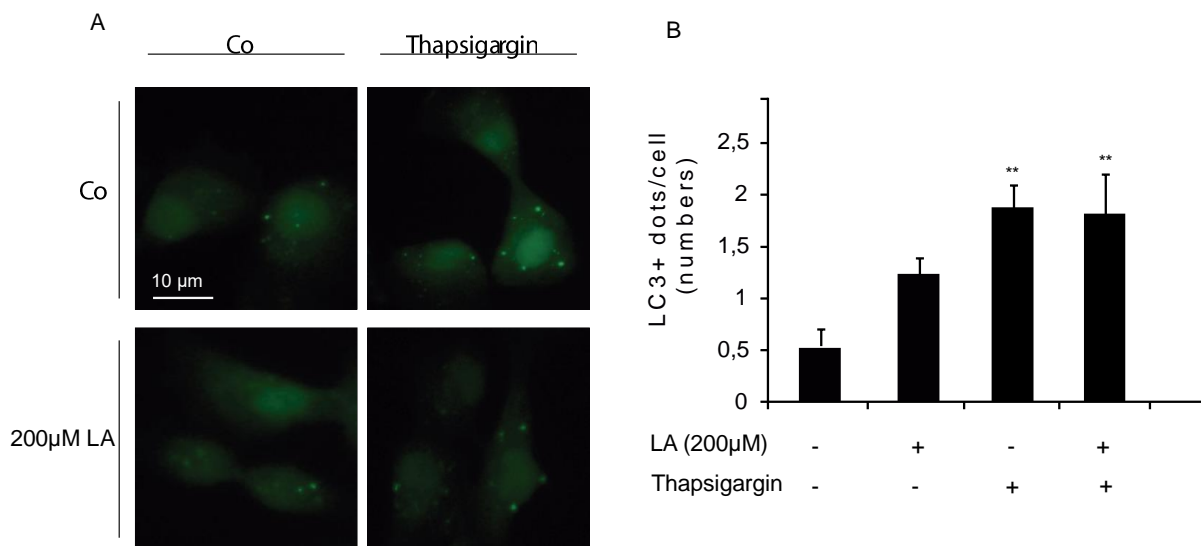


**Figure 4.20 LA-induced autophagy is ER-independent.** H4 GFP-LC3 cells (100 000 cells/mL density) were maintained in control conditions (Co) or treated with 200 µM (LA) alone, or in combination with 1 µM Thapsigargin, for 4 h, and the quantification of the number of cytoplasmic GFP-LC3+ dots per cell (B). P-value lists the different conditions with control. Scale bar represents 10 µm.

Using branding Nile Red (when in a lipid-rich environment can be intensely fluorescent, with varying colours from deep red to strong yellow-gold emission) and treatment with Triclosan (FASN inhibitor), we can observe the increase of LDs with LA alone (**Figure 4.21**). When cells are treated with triclosan more LA, we remark a diminution of LDs. Biogenesis of LD and its lipolysis by specific lipases are important for autophagosome biogenesis.

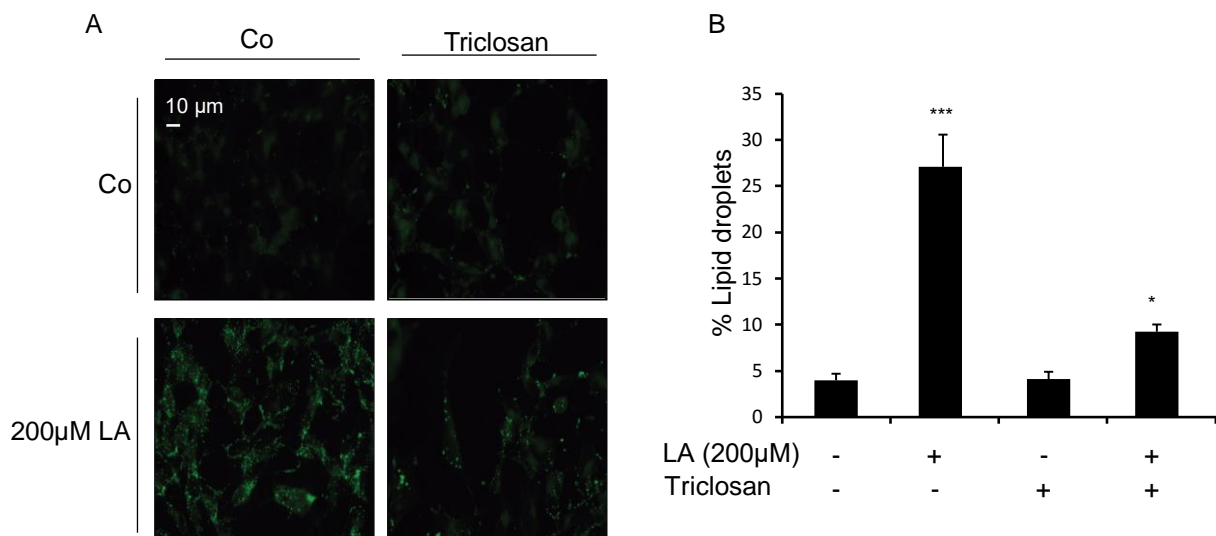


**Figure 4.21** LA induces lipid droplets biogenesis. SH-SY5Y cells (100 000 cells/mL density) treated with 10 μM triclosan and/or 200 μM LA, for 4h. EBSS was used as positive control. Cells were labelled with Nile Red (that marks LD) and visualized by fluorescence microscopy. (A) Representative microphotographs of Nile Red stain. The quantification of the percentage of LD is shown in (B). P-value lists the different conditions with control. Scale bar represents 10 μm.

## 4.9 LA has neuroprotector role in neuronal cell lines

### 4.9.1 LA does not protect neurons against cell death

We wanted to evaluate whether LA protects against  $PQ^{2+}$ -induced cytotoxicity through autophagy. To this purpose, we performed cell viability assays by flow cytometry and trypan blue assay. We treated H4 cell line (100 000 cells/mL density) with 400 μM LA and 500 μM PQ, combined or not, for 4 h and after we replaced the culture medium, for 24 h. As mentioned above, PQ induces apoptosis through mitochondrial oxidative stress. As seen in **Figure 4.22**, LA does not protect cells against the toxicity induced by  $PQ^{2+}$  using trypan blue test. Next, we proceed to measure cell viability by flow cytometry analyzing the percentage of apoptotic cells (propidium iodide positive cells). Results in **Figure 4.23** show that PQ alone and in combination with LA caused 60 % of  $PI^+$  cells. Therefore, LA does not protect from PQ-induced cell death.

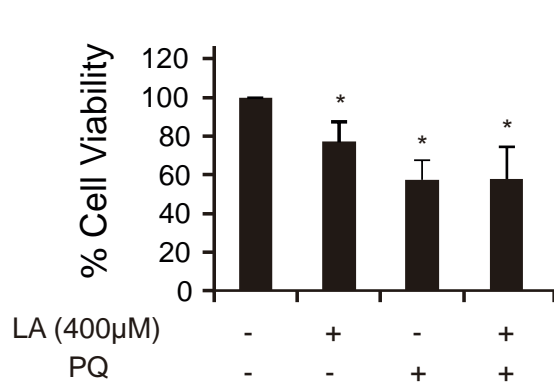


**Figure 4.22 LA does not protect cells against cell death induced by PQ.** Cell viability screening, by trypan blue exclusion test. H4 cells were cultured in control conditions (Co) or treated with 400 µM LA and/or 500 µM PQ, for 4 h.. After 4h treatment, medium was changed by DMEM for 24 h. Data are means  $\pm$  SEM of at least three independent experiments (\*P < 0.05). P-value lists the different conditions with control.

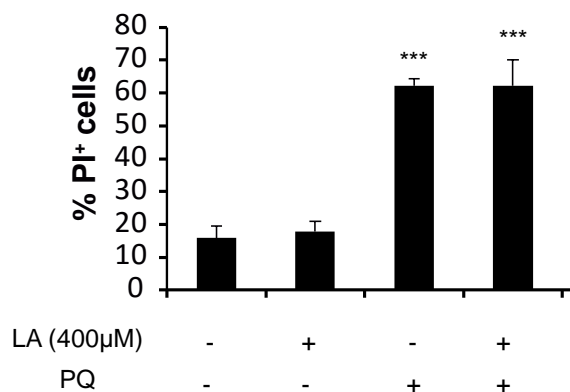


**Figure 4.23 LA does not reduce %PI+ cells induced by PQ.** Cells were analyzed for cell viability by flow cytometry using propidium iodide (PI) and we previously know that only living cells are PI negative. Cells were untreated (Co) or treated with 400 µM LA and 500 µM PQ<sup>2+</sup>, only or combined. After 4 h treatment, the medium was changed to a medium without treatment through 24 hours. Data are means  $\pm$  SEM of at least three independent experiments (\*\*\*P<0.001). P-value lists the different conditions with control.

#### 4.9.2 LA protects neurons from protein aggregates

The accumulation of protein aggregates is a common pathological hallmark of PD. Autophagy contributes to the removal protein aggregates in neurodegenerative diseases. Therefore, LA may protect cells against the accumulation of proteins aggregates through autophagy activation. To confirm this hypothesis, we treated cells with puromycin (that causes intracellular accumulation of polyubiquitinated aggregates) for 4 h. After treatment, the medium was changed and 24 h later cell viability was analyzed by trypan blue and flow cytometry assays.

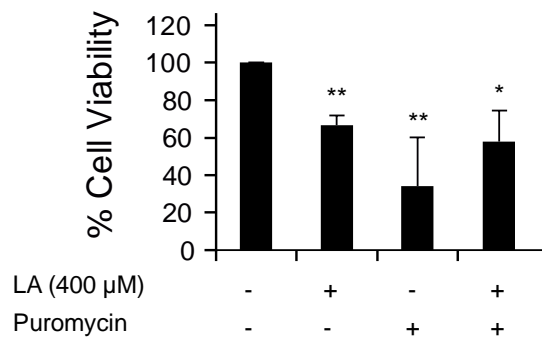


**Figure 4.24** LA protect cells against cell death induces by puromycin. Cell viability screening by trypan blue exclusion test. H4 cells were cultured in control conditions (Co) or treated with 400  $\mu$ M LA and/or 10  $\mu$ M puromycin, for 4 h. After treatment, the medium was changed and cell viability was analyzed 24 h later. Data are means  $\pm$  SEM of at least three independent experiments (\*P < 0.05, \*\*P < 0.01). P-value lists the different conditions with control

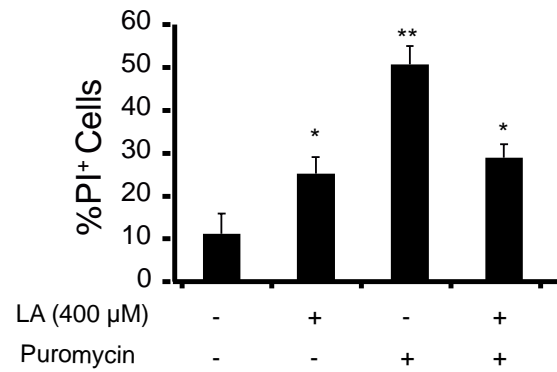


**Figure 4.25** LA reduce %PI+ cells, with puromycin. Cells were analyzed for cell viability by flow cytometry using propidium iodide (PI) and we previously know that only living cells are PI negative. It was a 4 hours treatment with Co (control), 400  $\mu$ M LA and with puromycin at 10  $\mu$ M, only or combined. After treatment, the medium was changed and cell viability was analyzed 24 h later. Data are means  $\pm$  SEM of at least three independent experiments (\*P < 0.05, \*\*P < 0.01). P-value lists the different conditions with control

The trypan blue analysis show that puromycin significantly reduces the percentage of cell viability compare to control. However, the combination of both LA and puromycin treatment enhances cell viability compare to puromycin alone (**Figure 4.24**). Similar results were obtained by flow cytometry. Pretreatment with LA 1h prior to puromycin incubation reduces the percentage of PI<sup>+</sup> cells compare to puromycin alone (**Figure 4.25**). These results suggest that LA protects cells against apoptosis induced by puromycin through autophagy activation (**Figure 4.26**).

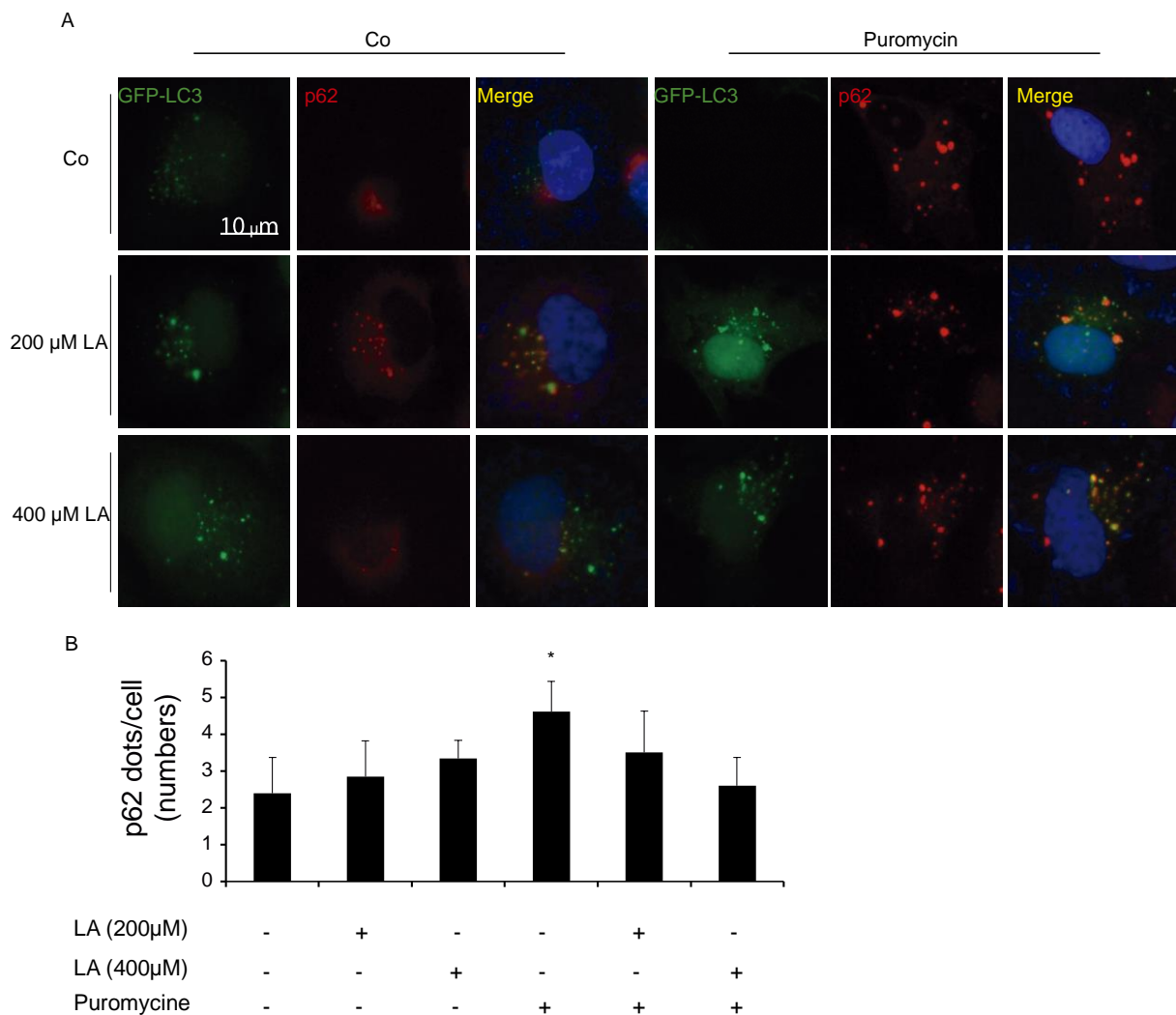


**Figure 4.26 LA enhances p62 degradation.** H4 GFP-LC3 cells (100 000 cells/mL density) were maintained in control conditions (Co) or treated with 200  $\mu$ M (LA) alone, or in combination with 10  $\mu$ M puromycin, for 4 h, and the quantification of the number of cytoplasmic p62 dots per cell. Nuclei were marked with Hoechst 33342. Data are means  $\pm$  SEM of at least three independent experiments (\* $P < 0.05$ ). P-value lists the different conditions with control. Scale bar represents 10  $\mu$ m.

It has been shown that puromycin induces p62 positive aggregates (Nicot, Lo Verso et al. 2014), We propose that LA induces autophagy and promote the degradation of this p62 positive aggregates. Therefore, we measure p62<sup>+</sup> dots by immunofluorescence and we observed that the treatment with LA 400  $\mu$ M prior to puromycin incubation reduce the number of p62 dots compared to puromycin alone. This result confirmed that puromycin- induced protein aggregates are degraded by LA-induced autophagy.







## 5. Discussion

---

Parkinson's disease (PD) is a paradigmatic example of neurodegenerative disorder with a critical role of oxidative stress in its etiopathogenesis (**Kalia, 2015**). Genetic susceptibility factors of PD, such as mutations in Parkin, PINK1, and DJ-1 as well as the exposure to pesticides and heavy metals, both contribute to altered redox balance and degeneration of dopaminergic neurons in the substantia nigra (**Gan-Or, 2015**). Dysregulation of autophagy, a lysosomal-driven process of self degradation of cellular organelles and protein aggregates, is also implicated in PD and PD-related mutations, and environmental toxins deregulate autophagy (**Son, 2012**). However, experimental evidence suggests a complex and ambiguous role of autophagy in PD since either impaired or abnormally upregulated autophagic flux has been shown to cause neuronal loss. Finally, it is generally believed that oxidative stress is a strong proautophagic stimulus. However, some evidences, coming from neurobiology, indicate an inhibitory role of reactive oxygen species and reactive nitrogen species on the autophagic machinery (**Lynch-Day, 2012**).

Interestingly, it was found a role for macroautophagy (non-specific bulk autophagy) in the shuttling of fatty acids in starved MEFs. LD grew in size and number in wild-type but not macroautophagy-deficient cells. By labelling and monitoring phosphatidylcholine (a major constituent of cell membranes) the authors were able to conclude that cellular membranes are shuttled to lysosomes by macroautophagy, where they are broken down to release fatty acids that can associate with LD; this ensures a sufficient supply of LD during starvation (**Wrighton, 2015**).

Autophagy plays a major role in the differentiation and function of adipocytes, in the mobilization of LD within hepatocytes (a process that has been dubbed "lipophagy"), as well as in the oxidation of fatty acids (FAs), underscoring its significant impact on lipid metabolism. Conversely, several saturated FAs (SFAs) and unsaturated FAs (UFAs) appear to modulate autophagy. Moreover, neutral LD have recently been shown to contribute to autophagic responses by providing substrates for the formation of autophagosomes (**Shpilka, 2015**).

Autophagy regulates lipid content because: inhibition of autophagy increased TGs and LDs in vitro and in vivo; loss of autophagy decreased TG breakdown; TGs and LD structural proteins co-localized with autophagic compartments; and LC3 associated with LDs. Moreover, a reverse relationship exists in which an abnormal increase in intracellular lipid impairs autophagic clearance as shown by decreased LD/LAMP1 co-localization and the absence of autophagic upregulation in hepatocytes cultured with lipids, as well as reduced association of autophagic vacuoles with LDs in response to starvation in HFD-fed mice (**Shpilka, 2015**).

Since several studies have shown the importance of fatty acids in the induction of autophagy, we choose linoleic acid as a substance to be studied. This compound choice was based, first because it is a compound very present in our diet (MeDi). Therefore, if LA was a potential neuroprotective would be low cost and easy access. Second, this compound was not never studied as autophagy inducer. It was just mentioned as an example of PUFAs, in an article that correlates PUFAs-induced autophagy, by with a higher longevity of life (**O'Rourke, 2013**).

Therefore, our study describes for the first time that LA is an autophagy inducer in neuronal cell lines using several techniques such as WB and immunofluorescence.

The molecular mechanism of autophagy involves several conserved autophagy-related genes (Atg) and these genes have multiple functions in various physiological contexts. Among these genes, Atg5 protein in a conjugated form with Atg12 and Atg8 (LC3) are involved in the early stages of autophagosome formation. Our study shows that LA-induced autophagy is Atg5-dependent using atg5 knockout cell lines. Moreover, we analyzed several autophagy signaling pathways. We studied the implication of mTOR kinase, Beclin1/PI3K and AMPK protein. mTOR is a major regulator of the autophagic process and it is regulated by starvation, growth factors and cellular stressors. Upstream of mTOR the survival PI3K/AKT pathway modulates mTOR activity that is also altered in neurodegenerative diseases such as Alzheimer and Parkinson disease. In conditions where nutrients are scarce, AMPK acts as a metabolic checkpoint inhibiting cellular growth. The most thoroughly described mechanism by which AMPK regulates cell growth is through suppression of the mTORC1 pathway.

According to Niso-Santano and coworkers (**Niso-Santano, Bravo-San Pedro et al. 2015**), the UFAs induce a non-canonical autophagy, in cancer models. In our study, we characterized the autophagy induced by LA in neuronal and glial models. Analysis of mTOR and BECN1 pathways show similar results to Niso-Santano study. We demonstrate that the inhibition of BECN1 using 3-MA or the downregulation of BECN1 do not inhibit the LA-induced autophagy. Moreover, we show by WB and fluorescence microscopy that the autophagy induced by LA is mTOR-independent. Similar results were obtained with n-6 PUFA. In this study, n-6 PUFA-triggered activation of autophagy seems to be additive to treatment of HeLa cells with rapamycin, suggesting that n-6 fatty acids would activate autophagy through a mTOR-independent mechanism (**O'Rourke, 2013**).

However, our study shows that AMPK plays a key role in the autophagy induced by LA. For a better characterization of the AMPK pathway, it was used the inhibitor CC, however in our model we see an increase of LC3II levels, instead of a reduction. This fact is referred in several bibliography, that says, that depending on cell model, it can exist a protective autophagy induction, once upon CC is cytotoxic (**Liu, 2014**). However, the downregulation of AMPK partly inhibited autophagy by reducing LC3 lipidation. Niso-Santano and coworkers shows that the downregulation of AMPK does not inhibit the autophagy induced by unsaturated fatty acid. Another study, using the docosahexaenoic acid, shows

that autophagy induced by this n-3 PUFA is also AMPK-dependent (**Kim, Jeong et al. 2015**). To do this, Kim and coworkers used AMPK knockout models.

We also studied the effect of LA treatment in the structure of different organelles and we analyzed whether these organelles are important in the autophagy induced by LA. In the article (**Niso-Santano, 2015**), it is found that the induction of autophagy by oleate is dependent of a functional Golgi Apparatus. Using specific markers for lysosomes, endosomes, ER and mitochondria, we demonstrated that LA does not damage these organelles. Moreover, the combination of LA and compounds that alter the endocytic pathway, lysosome membranes, E, mitochondria and Golgi Apparatus does not reduce LC3 puncta formation. These results show that the autophagy induced by LA does not require any intact organelle.

Autophagy is a basic cellular process that maintains homeostasis and is crucial for postmitotic neurons. Thus, impaired autophagic processes in neurons lead to improper homeostasis and neurodegeneration. Recent studies have suggested that impairments of the autophagic process are associated with several neurodegenerative diseases. In recent years, environmental toxins and drugs, including MPP<sup>+</sup>, rotenone, PQ, and metamphetamine, have been implicated in autophagy dysregulation in models of neurotoxin-induced dopaminergic cell death. Data from neuroblastoma cell lines, primary neuronal cultures and, in some cases, from animal models suggest that oxidative stress induces an excessive levels of autophagy leading to apoptotic or nonapoptotic cell death. However, the accumulation of  $\alpha$ -synuclein-rich protein inclusions similar to LB reported in in vivo models of pesticide-induced parkinsonism (e.g., following exposure to rotenone and PQ) is compatible with an autophagy block, rather than with its excessive stimulation.

To the study of LA as neuroprotective or neurotoxic, we conducted trials with PQ and puromycin. PQ induces cell death, while the use of puromycin elicits protein aggregates. The combination of PQ and LA have a slight improvement in cell viability, but are not meaningful results. However, pretreatment with LA prior puromycin incubation show a significant increase in cell viability. This fact makes us believe that the activation of autophagy mediated by LA protect cells against stress-induced protein aggregates.

We also observed by immunofluorescence that LA reduces the accumulation of p62 induced by puromycin. The protective ability of PUFAs in the presence of protein aggregates had already previously been described, although whether the studies have been made with n-3 PUFA. Docosahexaenoic acid (PUFA n-3) partially rescued the cell proliferation following a puromycin challenge. These results indicate that under conditions where p62 is induced, there is also an improved tolerance for misfolded proteins formed in response to puromycin. (**Johansson, 2015**). With LA there is an autophagy induction, that probably destroys the protein aggregates and degrades the p62, being the reason for a decrease of p62 levels.

In the Rotterdam Study, a prospective population-based cohort study of people ages 55, the association between intake of unsaturated fatty acids and the risk of incident PD was evaluated among 5,289 subjects who were free of dementia and parkinsonism and underwent complete dietary assessment at baseline, shows that, of the n-6-PUFAs, only linoleic acid seemed protective to PD. (**de Lau, 2005**). However there are some in vitro studies that clearly demonstrated the links between the pro-inflammatory properties of linoleic acid and metabolic diseases (**Choque, 2014**).

In summary, our findings demonstrated that LA can induce non-canonical autophagy, that is BECN1-independent, through a conserved mechanism that can require an intact Golgi apparatus and/or ER. LA-induced autophagy is mTOR-independent and AMPK-dependent. We see, also, that LA exerts a cytoprotection on cells with protein aggregates, by induction of autophagy.

## 6. Conclusions

---

Regarding the initial aims of this Master thesis, we believe that we have successfully addressed most of the questions we set out to answer.

The data presented and discussed herein allowed us to conclude that:

- LA induces autophagy, with concentrations between 200 $\mu$ M and 500 $\mu$ M
- LA-induced autophagy is PI3K/Beclin1 independent; is AMPK-dependent and mTOR-independent;
- LA-induced autophagy is organelles-independent
- LA-induced autophagy protects from protein aggregates.

In conclusion, this study contributed to clarify the role of LA, in the autophagy process, on PD. Moreover, it showed how a natural product, very present on our diet, can modulate, at least, one of the regulation system, we have, the autophagy. This work presented the active autophagy pathways, by LA and demonstrated the existence of a neuroprotection, in some cases.

This work reinforced the importance of PUFA, in neurodegenerative disorders, as always described. The studies of several componentes can help to development of new efficier drugs, to the PD patients.





## 7. References

---

- Agim, Z. S. and J. R. Cannon (2015). "Dietary factors in the etiology of Parkinson's disease." Biomed Res Int **2015**: 672838.
- Albarracin, S. L., B. Stab, Z. Casas, J. J. Sutachan, I. Samudio, J. Gonzalez, L. Gonzalo, F. Capani, L. Morales and G. E. Barreto (2012). "Effects of natural antioxidants in neurodegenerative disease." Nutr Neurosci **15**(1): 1-9.
- Alcalay, R. N., Y. Gu, H. Mejia-Santana, L. Cote, K. S. Marder and N. Scarmeas (2012). "The association between Mediterranean diet adherence and Parkinson's disease." Mov Disord **27**(6): 771-774.
- Appukuttan, T. A., N. Ali, M. Varghese, A. Singh, D. Tripathy, M. Padmakumar, P. K. Gangopadhyay and K. P. Mohanakumar (2013). "Parkinson's disease cybrids, differentiated or undifferentiated, maintain morphological and biochemical phenotypes different from those of control cybrids." J Neurosci Res **91**(7): 963-970.
- Aranda, A., L. Sequedo, L. Tolosa, G. Quintas, E. Burello, J. V. Castell and L. Gombau (2013). "Dichloro-dihydro-fluorescein diacetate (DCFH-DA) assay: a quantitative method for oxidative stress assessment of nanoparticle-treated cells." Toxicol In Vitro **27**(2): 954-963.
- Bang, Y., B. Y. Kang and H. J. Choi (2014). "Preconditioning stimulus of proteasome inhibitor enhances aggresome formation and autophagy in differentiated SH-SY5Y cells." Neurosci Lett **566**: 263-268.
- Bankaitis, V. A. (2015). "Unsaturated fatty acid-induced non-canonical autophagy: unusual? Or unappreciated?" EMBO J **34**(8): 978-980.
- Brenner, C., L. Galluzzi, O. Kepp and G. Kroemer (2013). "Decoding cell death signals in liver inflammation." J Hepatol **59**(3): 583-594.
- Brojatsch, J., H. Lima, A. K. Kar, L. S. Jacobson, S. M. Muehlbauer, K. Chandran and F. Diaz-Griffero (2014). "A proteolytic cascade controls lysosome rupture and necrotic cell death mediated by lysosome-destabilizing adjuvants." PLoS One **9**(6): e95032.
- Cetrullo, S., B. Tantini, F. Flamigni, C. Pazzini, A. Facchini, C. Stefanelli, C. M. Caldarera and C. Pignatti (2012). "Antiapoptotic and antiautophagic effects of eicosapentaenoic acid in cardiac myoblasts exposed to palmitic acid." Nutrients **4**(2): 78-90.
- Chen, X., B. Khambu, H. Zhang, W. Gao, M. Li, X. Chen, T. Yoshimori and X. M. Yin (2014). "Autophagy induced by calcium phosphate precipitates targets damaged endosomes." J Biol Chem **289**(16): 11162-11174.
- Chen, Z., Y. Zhang, C. Jia, Y. Wang, P. Lai, X. Zhou, Y. Wang, Q. Song, J. Lin, Z. Ren, Q. Gao, Z. Zhao, H. Zheng, Z. Wan, T. Gao, A. Zhao, Y. Dai and X. Bai (2014). "mTORC1/2 targeted by n-3 polyunsaturated fatty acids in the prevention of mammary tumorigenesis and tumor progression." Oncogene **33**(37): 4548-4557.
- Chen, Z. T., W. Zhao, S. Qu, L. Li, X. D. Lu, F. Su, Z. G. Liang, S. Y. Guo and X. D. Zhu (2015). "PARP-1 promotes autophagy via the AMPK/mTOR pathway in CNE-2 human nasopharyngeal carcinoma cells following ionizing radiation, while inhibition of autophagy contributes to the radiation sensitization of CNE-2 cells." Mol Med Rep **12**(2): 1868-1876.
- Cheng, Y., X. Ren, W. N. Hait and J. M. Yang (2013). "Therapeutic targeting of autophagy in disease: biology and pharmacology." Pharmacol Rev **65**(4): 1162-1197.

- Choque, B., D. Catheline, V. Rioux and P. Legrand (2014). "Linoleic acid: between doubts and certainties." Biochimie **96**: 14-21.
- Choudhury, Y., Z. Yang, I. Ahmad, C. Nixon, I. P. Salt and H. Y. Leung (2014). "AMP-activated protein kinase (AMPK) as a potential therapeutic target independent of PI3K/Akt signaling in prostate cancer." Oncoscience **1**(6): 446-456.
- de Lau, L. M., M. Bornebroek, J. C. Witteman, A. Hofman, P. J. Koudstaal and M. M. Breteler (2005). "Dietary fatty acids and the risk of Parkinson disease: the Rotterdam study." Neurology **64**(12): 2040-2045.
- Delattre, A. M., B. Carabelli, M. A. Mori, P. G. Kempe, L. E. Rizzo de Souza, S. M. Zanata, R. B. Machado, D. Suchecki, B. L. Andrade da Costa, M. M. Lima and A. C. Ferraz (2016). "Maternal Omega-3 Supplement Improves Dopaminergic System in Pre- and Postnatal Inflammation-Induced Neurotoxicity in Parkinson's Disease Model." Mol Neurobiol.
- Dong, J., J. D. Beard, D. M. Umbach, Y. Park, X. Huang, A. Blair, F. Kamel and H. Chen (2014). "Dietary fat intake and risk for Parkinson's disease." Mov Disord **29**(13): 1623-1630.
- Egan, D. F., D. B. Shackelford, M. M. Mihaylova, S. Gelino, R. A. Kohnz, W. Mair, D. S. Vasquez, A. Joshi, D. M. Gwinn, R. Taylor, J. M. Asara, J. Fitzpatrick, A. Dillin, B. Viollet, M. Kundu, M. Hansen and R. J. Shaw (2011). "Phosphorylation of ULK1 (hATG1) by AMP-activated protein kinase connects energy sensing to mitophagy." Science **331**(6016): 456-461.
- Enot, D. P., M. Niso-Santano, S. Durand, A. Chery, F. Pietrocola, E. Vacchelli, F. Madeo, L. Galluzzi and G. Kroemer (2015). "Metabolomic analyses reveal that anti-aging metabolites are depleted by palmitate but increased by oleate in vivo." Cell Cycle **14**(15): 2399-2407.
- Filograna, R., V. K. Godena, A. Sanchez-Martinez, E. Ferrari, L. Casella, M. Beltramini, L. Bubacco, A. J. Whitworth and M. Bisaglia (2016). "Superoxide Dismutase (SOD)-mimetic M40403 Is Protective in Cell and Fly Models of Paraquat Toxicity: IMPLICATIONS FOR PARKINSON DISEASE." J Biol Chem **291**(17): 9257-9267.
- Finkbeiner, S., A. M. Cuervo, R. I. Morimoto and P. J. Muchowski (2006). "Disease-modifying pathways in neurodegeneration." J Neurosci **26**(41): 10349-10357.
- Gan-Or, Z., P. A. Dion and G. A. Rouleau (2015). "Genetic perspective on the role of the autophagy-lysosome pathway in Parkinson disease." Autophagy **11**(9): 1443-1457.
- Ganley, I. G., P. M. Wong, N. Gammoh and X. Jiang (2011). "Distinct autophagosomal-lysosomal fusion mechanism revealed by thapsigargin-induced autophagy arrest." Mol Cell **42**(6): 731-743.
- Ge, L. and R. Schekman (2014). "The ER-Golgi intermediate compartment feeds the phagophore membrane." Autophagy **10**(1): 170-172.
- Giuliano, S., Y. Cormerais, M. Dufies, R. Grepin, P. Colosetti, A. Belaid, J. Parola, A. Martin, S. Lacas-Gervais, N. M. Mazure, R. Benhida, P. Auberger, B. Mograbi and G. Pages (2015). "Resistance to sunitinib in renal clear cell carcinoma results from sequestration in lysosomes and inhibition of the autophagic flux." Autophagy **11**(10): 1891-1904.
- Glick, D., S. Barth and K. F. Macleod (2010). "Autophagy: cellular and molecular mechanisms." J Pathol **221**(1): 3-12.
- Gomez-Sanchez, R., S. M. Yakhine-Diop, M. Rodriguez-Arribas, J. M. Bravo-San Pedro, G. Martinez-Chacon, E. Uribe-Carretero, D. C. Pinheiro de Castro, E. Pizarro-Estrella, J. M. Fuentes and R. A. Gonzalez-Polo (2016). "mRNA and protein dataset of autophagy markers (LC3 and p62) in several cell lines." Data Brief **7**: 641-647.

- Gonzalez-Polo, R. A., J. M. Fuentes, M. Niso-Santano and L. Alvarez-Erviti (2013). "Implication of autophagy in Parkinson's disease." Parkinsons Dis **2013**: 436481.
- Grotmeier, A., S. Alers, S. G. Pfisterer, F. Paasch, M. Daubrawa, A. Dieterle, B. Viollet, S. Wesselborg, T. Proikas-Cezanne and B. Stork (2010). "AMPK-independent induction of autophagy by cytosolic Ca<sup>2+</sup> increase." Cell Signal **22**(6): 914-925.
- Grube, S., P. Dunisch, D. Freitag, M. Klausnitzer, Y. Sakr, J. Walter, R. Kalff and C. Ewald (2014). "Overexpression of fatty acid synthase in human gliomas correlates with the WHO tumor grade and inhibition with Orlistat reduces cell viability and triggers apoptosis." J Neurooncol **118**(2): 277-287.
- Gwinn, D. M., D. B. Shackelford, D. F. Egan, M. M. Mihaylova, A. Mery, D. S. Vasquez, B. E. Turk and R. J. Shaw (2008). "AMPK phosphorylation of raptor mediates a metabolic checkpoint." Mol Cell **30**(2): 214-226.
- Hoyer-Hansen, M., L. Bastholm, P. Szyniarowski, M. Campanella, G. Szabadkai, T. Farkas, K. Bianchi, N. Fehrenbacher, F. Elling, R. Rizzuto, I. S. Mathiasen and M. Jaattela (2007). "Control of macroautophagy by calcium, calmodulin-dependent kinase kinase-beta, and Bcl-2." Mol Cell **25**(2): 193-205.
- Hu, X., F. Zhang, R. K. Leak, W. Zhang, M. Iwai, R. A. Stetler, Y. Dai, A. Zhao, Y. Gao and J. Chen (2013). "Transgenic overproduction of omega-3 polyunsaturated fatty acids provides neuroprotection and enhances endogenous neurogenesis after stroke." Curr Mol Med **13**(9): 1465-1473.
- Ichimura, Y. and M. Komatsu (2010). "Selective degradation of p62 by autophagy." Semin Immunopathol **32**(4): 431-436.
- Igarashi, M., H. W. Kim, L. Chang, K. Ma and S. I. Rapoport (2012). "Dietary n-6 polyunsaturated fatty acid deprivation increases docosahexaenoic acid metabolism in rat brain." J Neurochem **120**(6): 985-997.
- Janda, E., C. Isidoro, C. Carresi and V. Mollace (2012). "Defective autophagy in Parkinson's disease: role of oxidative stress." Mol Neurobiol **46**(3): 639-661.
- Janda, E., A. Lascalea, C. Carresi, M. Parafati, S. Aprigliano, V. Russo, C. Savoia, E. Ziviani, V. Musolino, F. Morani, C. Isidoro and V. Mollace (2015). "Parkinsonian toxin-induced oxidative stress inhibits basal autophagy in astrocytes via NQO2/quinone oxidoreductase 2: Implications for neuroprotection." Autophagy **11**(7): 1063-1080.
- Jiang, P. and N. Mizushima (2015). "LC3- and p62-based biochemical methods for the analysis of autophagy progression in mammalian cells." Methods **75**: 13-18.
- Johansson, I., V. T. Monsen, K. Pettersen, J. Mildnerberger, K. Misund, K. Kaarniranta, S. Schonberg and G. Bjorkoy (2015). "The marine n-3 PUFA DHA evokes cytoprotection against oxidative stress and protein misfolding by inducing autophagy and NFE2L2 in human retinal pigment epithelial cells." Autophagy **11**(9): 1636-1651.
- Kalia, L. V. and A. E. Lang (2015). "Parkinson's disease." Lancet **386**(9996): 896-912.
- Kang, R., H. J. Zeh, M. T. Lotze and D. Tang (2011). "The Beclin 1 network regulates autophagy and apoptosis." Cell Death Differ **18**(4): 571-580.
- Kim, J., M. Kundu, B. Viollet and K. L. Guan (2011). "AMPK and mTOR regulate autophagy through direct phosphorylation of Ulk1." Nat Cell Biol **13**(2): 132-141.
- Kim, N., S. Jeong, K. Jing, S. Shin, S. Kim, J. Y. Heo, G. R. Kweon, S. K. Park, T. Wu, J. I. Park and K. Lim (2015). "Docosahexaenoic Acid Induces Cell Death in Human Non-Small Cell Lung Cancer

Cells by Repressing mTOR via AMPK Activation and PI3K/Akt Inhibition." Biomed Res Int **2015**: 239764.

Le, W. (2014). "Role of iron in UPS impairment model of Parkinson's disease." Parkinsonism Relat Disord **20 Suppl 1**: S158-161.

Liu, X., R. R. Chhipa, I. Nakano and B. Dasgupta (2014). "The AMPK inhibitor compound C is a potent AMPK-independent antiglioma agent." Mol Cancer Ther **13**(3): 596-605.

Lopez-Vicario, C., J. Alcaraz-Quiles, V. Garcia-Alonso, B. Rius, S. H. Hwang, E. Titos, A. Lopategi, B. D. Hammock, V. Arroyo and J. Claria (2015). "Inhibition of soluble epoxide hydrolase modulates inflammation and autophagy in obese adipose tissue and liver: role for omega-3 epoxides." Proc Natl Acad Sci U S A **112**(2): 536-541.

Luo, Y., A. Hoffer, B. Hoffer and X. Qi (2015). "Mitochondria: A Therapeutic Target for Parkinson's Disease?" Int J Mol Sci **16**(9): 20704-20730.

Lynch-Day, M. A., K. Mao, K. Wang, M. Zhao and D. J. Klionsky (2012). "The role of autophagy in Parkinson's disease." Cold Spring Harb Perspect Med **2**(4): a009357.

Mani, M., U. H. Lee, N. A. Yoon, H. J. Kim, M. S. Ko, W. Seol, Y. Joe, H. T. Chung, B. J. Lee, C. H. Moon, W. J. Cho and J. W. Park (2016). "Developmentally regulated GTP-binding protein 2 coordinates Rab5 activity and transferrin recycling." Mol Biol Cell **27**(2): 334-348.

Marlin, M. C. and G. Li (2015). "Differential effects of overexpression of Rab5 and Rab22 on autophagy in PC12 cells with or without NGF." Methods Mol Biol **1298**: 295-304.

McKinnon, C. and S. J. Tabrizi (2014). "The ubiquitin-proteasome system in neurodegeneration." Antioxid Redox Signal **21**(17): 2302-2321.

Mihaylova, M. M. and R. J. Shaw (2011). "The AMPK signalling pathway coordinates cell growth, autophagy and metabolism." Nat Cell Biol **13**(9): 1016-1023.

Mizushima, N., T. Yoshimori and B. Levine (2010). "Methods in mammalian autophagy research." Cell **140**(3): 313-326.

Moreno, C., A. Macias, A. Prieto, A. de la Cruz, T. Gonzalez and C. Valenzuela (2012). "Effects of n-3 Polyunsaturated Fatty Acids on Cardiac Ion Channels." Front Physiol **3**: 245.

Nicot, A. S., F. Lo Verso, F. Ratti, F. Pilot-Storck, N. Streichenberger, M. Sandri, L. Schaeffer and E. Goillot (2014). "Phosphorylation of NBR1 by GSK3 modulates protein aggregation." Autophagy **10**(6): 1036-1053.

Niso-Santano, M., J. M. Bravo-San Pedro, M. C. Maiuri, N. Tavernarakis, F. Cecconi, F. Madeo, P. Codogno, L. Galluzzi and G. Kroemer (2015). "Novel inducers of BECN1-independent autophagy: cis-unsaturated fatty acids." Autophagy **11**(3): 575-577.

Niso-Santano, M., S. A. Malik, F. Pietrocola, J. M. Bravo-San Pedro, G. Marino, V. Cianfanelli, A. Ben-Younes, R. Troncoso, M. Markaki, V. Sica, V. Izzo, K. Chaba, C. Bauvy, N. Dupont, O. Kepp, P. Rockenfeller, H. Wolinski, F. Madeo, S. Lavandro, P. Codogno, F. Harper, G. Pierron, N. Tavernarakis, F. Cecconi, M. C. Maiuri, L. Galluzzi and G. Kroemer (2015). "Unsaturated fatty acids induce non-canonical autophagy." EMBO J **34**(8): 1025-1041.

Padman, B. S., M. Bach, G. Lucarelli, M. Prescott and G. Ramm (2013). "The protonophore CCCP interferes with lysosomal degradation of autophagic cargo in yeast and mammalian cells." Autophagy **9**(11): 1862-1875.

- Pimentel-Muinos, F. X. and E. Boada-Romero (2014). "Selective autophagy against membranous compartments: Canonical and unconventional purposes and mechanisms." Autophagy **10**(3): 397-407.
- Rajan, V. R. and W. E. Mitch (2008). "Muscle wasting in chronic kidney disease: the role of the ubiquitin proteasome system and its clinical impact." Pediatr Nephrol **23**(4): 527-535.
- Rappold, P. M. and K. Tieu (2010). "Astrocytes and therapeutics for Parkinson's disease." Neurotherapeutics **7**(4): 413-423.
- Rodriguez, M., C. Rodriguez-Sabate, I. Morales, A. Sanchez and M. Sabate (2015). "Parkinson's disease as a result of aging." Aging Cell **14**(3): 293-308.
- Rovito, D., C. Giordano, D. Vizza, P. Plastina, I. Barone, I. Casaburi, M. Lanzino, F. De Amicis, D. Sisci, L. Mauro, S. Aquila, S. Catalano, D. Bonofiglio and S. Ando (2013). "Omega-3 PUFA ethanalamides DHEA and EPEA induce autophagy through PPARgamma activation in MCF-7 breast cancer cells." J Cell Physiol **228**(6): 1314-1322.
- Rubinsztein, D. C., P. Codogno and B. Levine (2012). "Autophagy modulation as a potential therapeutic target for diverse diseases." Nat Rev Drug Discov **11**(9): 709-730.
- Russell, R. C., H. X. Yuan and K. L. Guan (2014). "Autophagy regulation by nutrient signaling." Cell Res **24**(1): 42-57.
- Sadowski, M. C., R. H. Pouwer, J. H. Gunter, A. A. Lubik, R. J. Quinn and C. C. Nelson (2014). "The fatty acid synthase inhibitor triclosan: repurposing an anti-microbial agent for targeting prostate cancer." Oncotarget **5**(19): 9362-9381.
- Sanchez-Guajardo, V., N. Tentillier and M. Romero-Ramos (2015). "The relation between alpha-synuclein and microglia in Parkinson's disease: Recent developments." Neuroscience **302**: 47-58.
- Schapira, A. H. and A. Schrag (2011). "Parkinson disease: Parkinson disease clinical subtypes and their implications." Nat Rev Neurol **7**(5): 247-248.
- Segura-Aguilar, J., I. Paris, P. Munoz, E. Ferrari, L. Zecca and F. A. Zucca (2014). "Protective and toxic roles of dopamine in Parkinson's disease." J Neurochem **129**(6): 898-915.
- Shen, Y. F., Y. Tang, X. J. Zhang, K. X. Huang and W. D. Le (2013). "Adaptive changes in autophagy after UPS impairment in Parkinson's disease." Acta Pharmacol Sin **34**(5): 667-673.
- Shpilka, T. and Z. Elazar (2015). "Lipid droplets regulate autophagosome biogenesis." Autophagy **11**(11): 2130-2131.
- Shpilka, T., E. Welter, N. Borovsky, N. Amar, M. Mari, F. Reggiori and Z. Elazar (2015). "Lipid droplets and their component triglycerides and steryl esters regulate autophagosome biogenesis." EMBO J **34**(16): 2117-2131.
- Son, J. H., J. H. Shim, K. H. Kim, J. Y. Ha and J. Y. Han (2012). "Neuronal autophagy and neurodegenerative diseases." Exp Mol Med **44**(2): 89-98.
- Su, P., J. Zhang, D. Wang, F. Zhao, Z. Cao, M. Aschner and W. Luo (2016). "The role of autophagy in modulation of neuroinflammation in microglia." Neuroscience **319**: 155-167.
- Svenning, S. and T. Johansen (2013). "Selective autophagy." Essays Biochem **55**: 79-92.
- Tao, B. B., H. He, X. H. Shi, C. L. Wang, W. Q. Li, B. Li, Y. Dong, G. H. Hu, L. J. Hou, C. Luo, J. X. Chen, H. R. Chen, Y. H. Yu, Q. F. Sun and Y. C. Lu (2013). "Up-regulation of USP2a and FASN in gliomas correlates strongly with glioma grade." J Clin Neurosci **20**(5): 717-720.

- Tavakkoli, M., R. Miri, A. R. Jassbi, N. Erfani, M. Asadollahi, M. Ghasemi, L. Saso and O. Firuzi (2014). "Carthamus, Salvia and Stachys species protect neuronal cells against oxidative stress-induced apoptosis." Pharm Biol **52**(12): 1550-1557.
- Tsakiri, E. N. and I. P. Trougakos (2015). "The amazing ubiquitin-proteasome system: structural components and implication in aging." Int Rev Cell Mol Biol **314**: 171-237.
- Uliasz, T. F. and S. J. Hewett (2000). "A microtiter trypan blue absorbance assay for the quantitative determination of excitotoxic neuronal injury in cell culture." J Neurosci Methods **100**(1-2): 157-163.
- Vakifahmetoglu-Norberg, H., H. G. Xia and J. Yuan (2015). "Pharmacologic agents targeting autophagy." J Clin Invest **125**(1): 5-13.
- Wager, K. and C. Russell (2013). "Mitophagy and neurodegeneration: the zebrafish model system." Autophagy **9**(11): 1693-1709.
- Wang, C., J. Ma, N. Zhang, Q. Yang, Y. Jin and Y. Wang (2015). "The acetyl-CoA carboxylase enzyme: a target for cancer therapy?" Expert Rev Anticancer Ther **15**(6): 667-676.
- Wirdefeldt, K., H. O. Adami, P. Cole, D. Trichopoulos and J. Mandel (2011). "Epidemiology and etiology of Parkinson's disease: a review of the evidence." Eur J Epidemiol **26 Suppl 1**: S1-58.
- Wrighton, K. H. (2015). "Lipid metabolism: fatty acids on the move." Nat Rev Mol Cell Biol **16**(4): 204.
- Wu, Y., X. Wang, H. Guo, B. Zhang, X. B. Zhang, Z. J. Shi and L. Yu (2013). "Synthesis and screening of 3-MA derivatives for autophagy inhibitors." Autophagy **9**(4): 595-603.